UNIVERSIDADE ESTADUAL DE CAMPINAS
INSTITUTO DE BIOLOGIA

LUCAS PEREIRA LOPES DE SOUZA

POTENCIAL TERAPÊUTICO DE VIDROS BIOATIVOS CONTENDO NIÓBIO OU GÁLIO NO TRATAMENTO DE DESORDENS ÓSSEAS: ESTUDO EXPERIMENTAL *IN VITRO E IN VIVO*

THERAPEUTIC POTENTIAL OF NIOBIUM- OR GALLIUM-DOPED BIOACTIVE GLASSES FOR TREATMENT OF BONE DISORDERS: AN *IN VITRO* AND *IN VIVO* EXPERIMENTAL STUDY

CAMPINAS
2018

LUCAS PEREIRA LOPES DE SOUZA

THERAPEUTIC POTENTIAL OF NIOBIUM- OR GALLIUM-DOPED BIOACTIVE GLASSES FOR TREATMENT OF BONE DISORDERS: AN IN VITRO AND IN VIVO EXPERIMENTAL STUDY

POTENCIAL TERAPÊUTICO DE VIDROS BIOATIVOS CONTENDO NIÓBIO OU GÁLIO NO TRATAMENTO DE DESORDENS ÓSSEAS: ESTUDO EXPERIMENTAL IN VITRO E IN VIVO

Thesis presented to the Institute of Biology of the University of Campinas in partial fulfillment of the requirements for the degree of doctor of structural and cellular biology in the field of Anatomy

Tese apresentada ao Instituto de Biologia da Universidade Estadual de Campinas como parte dos requisitos exigidos para a obtenção do título de doutor em biologia celular e estrutural na área de anatomia

ESTE ARQUIVO DIGITAL CORRESPONDE À VERSÃO FINAL DA TESE DEFENDIDA PELO ALUNO LUCAS PEREIRA LOPES DE SOUZA E ORIENTADA PELO PROFESSOR JOSÉ ANGELO CAMILLI

Orientador: JOSÉ ANGELO CAMILLI

CAMPINAS
2018

Agência(s) de fomento e nº(s) de processo(s): CNPq, 141210/2017-6

Ficha catalográfica
Universidade Estadual de Campinas
Biblioteca do Instituto de Biologia
Mara Janaina de Oliveira - CRB 8/6972

So89t

Souza, Lucas Pereira Lopes de, 1989-
Therapeutic potential of niobium- or gallium-doped bioactive glasses for treatment of bone disorders : an *in vitro* and *in vivo* experimental study / Lucas Pereira Lopes de Souza. – Campinas, SP : [s.n.], 2018.

Orientador: José Angelo Camilli.
Tese (doutorado) – Universidade Estadual de Campinas, Instituto de Biologia.

1. Nióbio. 2. Gálio. 3. Estudos *in vivo*. 4. Técnicas *in vitro*. 5. Fraturas – Tratamento. I. Camilli, José Angelo, 1963-. II. Universidade Estadual de Campinas. Instituto de Biologia. III. Título.

Informações para Biblioteca Digital

Título em outro idioma: Potencial terapêutico de vidros bioativos contendo nióbio ou gálio no tratamento de desordens ósseas : estudo experimental *in vitro* e *in vivo*
Palavras-chave em inglês:
Niobium
Gallium
In vivo studies
In vitro techniques
Fractures - Treatment
Área de concentração: Anatomia
Titulação: Doutor em Biologia Celular e Estrutural
Banca examinadora:
José Angelo Camilli [Orientador]
Paulo Henrique Ferreira Caria
Larissa Akemi Kido de Barros
Adriana Fogagnolo Mauricio
Renato Ferretti
Data de defesa: 31-07-2018
Programa de Pós-Graduação: Biologia Celular e Estrutural

Campinas, 31 de Julho de 2018.

COMISSÃO EXAMINADORA

Prof. Dr. José Angelo Camilli

Prof. Dr. Paulo Henrique Ferreira Caria

Prof. Dr. Renato Ferretti

Profa. Dra. Larissa Akemi Kido de Barros

Profa. Dra. Adriana Fogagnolo Mauricio

Os membros da Comissão Examinadora acima assinaram a Ata de defesa, que se encontra no processo de vida acadêmica do aluno.

DEDICATÓRIA

Dedico essa tese aos meus pais Herbert e Clarice e a minhas irmãs Anna Clara e Camila

AGRADECIMENTOS

Agradeço ao meu orientador José Angelo Camilli por todos os anos de amizade, paciência e orientação. O agradeço principalmente por me incentivar a sonhar alto e fazer o possível e até mesmo o impossível para conquistar meus sonhos. A ele eu devo todo conhecimento sobre docência que adquiri ao longo desses anos juntos, com diversos estágios em ensino e diversos cursos de anatomia. A ele eu devo meu estágio no exterior e todas as parcerias de pesquisa colecionadas ao longo dessa caminhada.

Agradeço ao professor Celso Aparecido Bertran pela incrível colaboração feita com nosso grupo de pesquisa produzindo e nos disponibilizando os materiais que viabilizaram a realização dessa pesquisa. Além disso, o agradeço por toda atenção que me deu ao longo desse período, sempre me esclarecendo dúvidas e me auxiliando em tudo que era possível.

Agradeço ao agora professor do Instituto Tecnológico da Aeronáutica (ITA) doutor João Henrique Lopes por ser o meu principal parceiro de pesquisa e um grande amigo que tive o prazer de conhecer e trabalhar junto durante esses seis anos de UNICAMP (2 de mestrado e 4 de doutorado). Apenas com a ajuda dele foi possível desenvolver esse trabalho tão interdisciplinar.

Agradeço ao professor Alexandre Leite Rodrigues de Oliveira por disponibilizar o seu laboratório para realização de vários experimentos descritos nessa tese.

Agradeço ao professor Sergiy Kyrylenko por me ensinar a cultivar células-tronco embrionárias e pela amizade que se mantém até hoje (mesmo estando de volta ao seu país de origem, a Ulcrânia).

Agradeço a professora Valéria Helena Alves Cagnon Quitete por me disponibilizar acesso ao seu laboratório para a realização de vários experimentos descritos nesse texto.

Agradeço a professora Elaine Minatel também por colaborar com minha pesquisa permitindo meu acesso ao seu laboratório de cultura de células.

Agradeço ao professor Wagner José Fávaro por abrir as portas do seu laboratório para mim ao longo desses anos e também por uma série de conselhos e orientações que me deu sobre ensino e pesquisa. Tive a sorte de o meu orientador dividir a sala com ele e assim poder me beneficiar da sua experiência, do seu conhecimento e da sua amizade.

Agradeço a Catharina Nucci Martins, minha companheira de laboratório por todos os ensinamentos acerca do trato com os animais. Eu tenho certeza que aprendi com a melhor que já vi sobre como lhe dar com animais de pesquisa de forma ética e correta.

Agradeço as futuras cientistas Bruna Bighetto Cain e Júlia Camilli pela amizade e parceria durante esses anos dividindo laboratório. Tenho certeza que as duas se tornarão grandes profissionais independentemente da área que escolham trabalhar, pois o foco e profissionalismo delas são inspiradores.

Agradeço aos meus amigos doutores Renato Rissi, George Azevedo Lemos e Marcos Maciel Junior pela amizade de anos dividindo o mesmo ambiente de trabalho e a mesma casa. A amizade deles foi essencial para manutenção da minha sanidade mental durante esses anos.

Agradeço a doutora Flávia Pires Rodrigues por me propiciar a oportunidade de realizar meu doutorado sanduíche na Inglaterra e pela linda amizade formada durante esses anos.

Agradeço ao professor Richard Alan Martin por me receber na Aston University em Birmingham na Inglaterra para realização do meu doutorado sanduíche e por ter se tornado um grande amigo e parceiro de pesquisa desde lá.

Agradeço a todos os meus familiares, especialmente a meus pais e minhas irmãs, por todo o apoio que me deram durante esses anos e pela compreensão por toda minha ausência em momentos importantes das vidas deles devido as minhas obrigações relacionadas ao doutorado.

Agradeço ao Conselho Nacional de Desenvolvimento Científico e Tecnológico (CNPq) pela bolsa de doutorado (141210/2017-6) que me possibilitou a realização desse trabalho.

RESUMO

Desordens musculoesqueléticas estão entre os acometimentos mais comuns a saúde humana com as fraturas ósseas se destacando como uma das mais debilitantes. Fraturas comprometem a qualidade de vida das pessoas e impõem significativa sobrecarga econômica a sociedade. O câncer ósseo, por sua vez, ocorre mais frequentemente em crianças e adultos jovens entre 5 e 20 anos de idade. Por ano cerca de 1000 novos casos de osteosarcoma (câncer ósseo) são diagnosticados só nos Estados Unidos. Por ano cerca de 1000 novos casos de osteosarcoma (câncer ósseo) são diagnosticados só nos Estados Unidos. Objetivando melhorar a qualidade do tratamento para essas condições nós alteramos a composição do vidro bioativo Bioglass®45S5 adicionando Dióxido de Nióbio (Nb2O5) ou Gálio (Ga). Nós buscamos dois diferentes objetivos principais: (1) aumentar a bioatividade do Bioglass®45S5 por meio da adição do Nb2O5 o que alteraria a estrutura interna do vidro, aumentando sua taxa de dissolução e consequentemente a formação da camada de hidroxiapatita sobre sua superfície a fim de ser usado para a regeneração de grandes fraturas; (2) produzir vidros bioativos capazes de liberar Gálio localmente, de uma forma controlada, para que este atue na regeneração de defeitos ósseos pós- osteotomia enquanto mata células cancerígenas remanescentes no local da lesão. Para alcançar esses objetivos nós conduzimos duas séries diferentes de estudos que estão apresentados nessa tese em duas partes. A parte um descreve três investigações que mostram que a adição do Nb2O5 a rede do Bioglass®45S5 produziu um vidros biocompatíveis, não genotóxicos e com bioatividade aumentada estimulando maior formação de osso subperiostal e a diferenciação de Células Tronco Embrionárias humanas (CTEs) e Células Mesenquimais derivadas da medula óssea. Além disso, esses vidros sofram capaz de proporcionar a regeneração de um defeito ósseo de 5 mm de diâmetro na calvária de ratos em 8 semanas. A segunda parte dessa tese mostra um estudo no qual nós investigamos o potencial da incorporação de Gálio em vidros bioativos biodegradáveis projetados especificamente para aplicações em câncer ósseo. Nós observamos que adição de 3% de Gálio promoveu a morte de mais de 50% das células de osteosarcoma (SAOS2 cells) sem afetar os osteoblastos saudáveis. Os vidros bioativos contendo gálio fornecem uma entrega controlada e local de íons gálio no sítio da fratura e tem potencial considerável em aplicações clínicas para o tratamento de câncer ósseo. Nós acreditamos que através do desenvolvimento de novos biomateriais para substituição óssea nosso estudo irá contribuir para a redução da morbidade e melhorar o prognóstico de milhões de vítimas de fraturas. Além disso, o conhecimento gerado pelo presente trabalho vem a aumentar a compreensão acerca da interação entre substitutos

ósseos sintéticos e o tecido ósseo lesado, esclarecendo as respostas do corpo a presença de vidros bioativos contendo Nióbio ou Gálio. Assim, o presente estudo fomenta a literatura com informação relevante para prática clínica e futuras investigações.

ABSTRACT

Musculoskeletal disorders are the most widespread human health issue with bone fractures standing among the most debilitating ones. Bone fractures compromises the quality of life of people and cause significant economic burden to society. On the other hand, bone cancer occurs most frequently in children and young adults between the age of 5 and 20 years, but may also grow in the elderly. Each year, about 1,000 new cases of osteosarcoma are diagnosed in the United States alone.Aiming to improve the quality of the treatment for these conditions we altered the composition of the Bioglass®45S5 adding Niobium Dioxide (Nb_2O_5) or Gallium (Ga). We targeted two different main goals: (1) increase the bioactivity of the Bioglass®45S5 by means of doping it with Nb_2O_5 which would alter the glass' internal structure, enhancing its dissolution rate and consequently the formation of a hydroxyapatite-like layer on its surface in order to use it for the regeneration of large fractures; (2) to produce a Ga-doped bioactive glass that can locally release gallium in a controlled manner to regenerate post-osteotomy defects whilst killing any remainder cancer cell. To meet these goals we conducted two different series of studies that are displayed in this thesis in two parts. Part one describes three investigations that show that the addition of Nb_2O_5 into Bioglass®45S5 produced biocompatible, non-genotoxic glasses which stimulated greater subperiosteal bone formation and the differentiation of Embryonic Stem Cells (ESCs) and bone marrow- derived Mesenchymal Stem Cells (BM-MSCs). Furthermore one composition of Nb-doped glass was able to regenerate a 5-mm size calvarial defect in rats after 8 weeks. The second part of this thesis shows a study in which we investigated the potential of incorporating gallium into bio-degradable bioactive glasses specifically targeted towards bone cancer applications. We observed that adding 3% of gallium killed more than 50% of the osteosarcoma cells (SAOS2) whilst it did not affect healthy human osteoblasts. The gallium doped bioactive glasses provide a localised controlled delivery of gallium ions at the surgical site of interest and has considerable potential clinical applications for bone cancer treatment. We believe that developing novel biomaterials for bone replacement our study will reduce the morbidity and to improve the prognostic of millions of victims of fractures. Nonetheless, the knowledge generated by the present work comes to improve the comprehension about the interaction between the synthetic bone substitutes and the injured bone tissue, clarifying the responses of the body in the presence of the Nb or Ga- doped bioactive glasses. Thus, the present study foments the literature with relevant information for clinic practise and further investigations.

Summary

INTRODUCTION

Nb-doped bioactive glasses to treat bone fractures

Throughout the history of humankind, several advancements in healthcare and infrastructure have provided humans with tools to slow down the process of natural selection. Nowadays, diseases that used to kill non-adapted individuals preventing their reproduction can be treated with a single pill[1]. As a result of this progress, the last century has witnessed a significant increase in life expectancy, whereby a human can be expected to live for 60-83 years on average[2]. The downside of these advancements was the emergence of a new category of diseases, known as 'mismatch diseases'. As the name suggests, these disorders are caused by a mismatch between our genetic code (which is still quite similar to that of the Palaeolithic men) and the environment we are now living in. Examples of these disorders include type 2 diabetes, stroke, atherosclerosis, cavities, osteoporosis, and some types of cancers[1].

Being one of the mismatch diseases that affect bones, osteoporosis is just the final step of a natural event that takes place in all human beings, called osteopenia. It is the process in which our bones progressively lose density due to the natural aging of our bone cells[3]. It did not seem to be a problem thousands of years ago because people did not use to live longer than 30-40 years. These days though, with many people reaching their seventies this progressive bone loss has been dramatically affecting the quality of life of millions of people around the world. Worldwide, osteoporosis is estimated to cause around 8.9 million fractures per year, which results in one fracture every 3 seconds[4]. In fact, the International Osteoporosis Foundation (IOF) estimated that, worldwide, 1 in 3 women over age 50 will suffer osteoporotic fractures, as will 1 in 5 men aged over 50[2].

The burden brought about by fractures is physical and psychological which consequently turns it into economical. In 2010 the total cost of fractures in the United Kingdom alone was about £4,3 billion[5]. Of course osteoporosis is not the only origin of fractures, but, it is certainly the one that is not likely to be reducing in the future decades as life expectancy and global population are only expected to increase.

The continuing increase in the number of fractures has concerned governments and researchers igniting the search for new effective treatments that could accelerate

patient recovery and reduce the risk of morbidity and mortality following a fracture. These investigations culminated with several improvements in fracture healing and management[6]. An outstanding advancement was the development of inorganic materials that could be used to replace damaged bones and joints[7,8]. Due to the capacity of these materials to be implanted into the body without stimulating a significant immune reaction, they were named 'Biomaterials'[9]. The first generation of biomaterials was composed of low-reactive materials, such as some low-reactive metals and polymers. Their main characteristic was their compatibility with living cells, behaving as a nearly inert matter when inside the human body. Many 'inert materials' were produced based on metals such as aluminum, zirconia and titanium, and are still used in orthopaedics for manufacturing prosthesis, plates, nails, screws, etc. Polymers, on the other hand, have been used for drug delivery, extracellular matrix mimickers, and cartilage repair[8–11].

The problem with these nearly inert materials is the nature of their fixation with the living tissue. Basically, a nearly inert implant attaches to a living tissue morphologically. This means that they have indentations or grooves on their surface that are meant to be filled with new-forming bone[12]. The fulfilment of these grooves with new bone creates a morphological attachment that sticks both material and bone together. Nevertheless, micro movements that occur at the material-bone interface might compromise their fixation by stimulating bone resorption which consequently comes to reduce the stability of the implant. Moreover, metallic implants still show some level of rejection by the body that responds with some degree of encapsulation and a mild inflammatory response, which consequently also comes to cause instability[9]. These drawbacks limit the lifespan of these materials to 10 to 20 years[12]. With the increase in life expectancy, many patients began to outlive their implants. This constituted a serious problem for orthopaedic surgeons, as in order to replace a loose implant, the patient, often frail and elderly, would have to undergo further surgery.

Interestingly, it was a war that ignited a revolution in the quality of bone implants. In 1969, a ceramic engineer named Larry Hench was attending a conference of the US Army Force to present his work on coatings for satellites. On his way to the conference he bumped into an army colonel. After an exciting talk explaining all the advantages of his satellite coatings, Hench was surprised by the following question, asked by the colonel: 'If you can make materials that can resist solar radiation, can you create a material that is able to resist the human body?' This question instigated the

research that culminated with the development of the first bioactive material, the Bioglass® 45S5. It is a glass belonging to the system SiO2 – CaO – Na2O (45 wt% SiO2, 24.5 wt% CaO and 6 wt% P2O5)[8,13].

The main innovation brought about by this material was the fact that it was not only biocompatible; it was also formed bounds with hard and soft tissues[14]. Bioglass®45S5 when in contact with the body fluid, undergoes a series of inorganic reactions by means of ion exchange that result in the formation of a hydroxyapatite-like layer on its surface[8,13]. The formation of this layer is a crucial step for bioactivity once proteins and pluripotent cells attach to it and carry out a biological response. This response promotes osteogenic differentiation of the pluripotent cells and the formation and mineralization of a bone matrix[11]. This neo-formed mineralized bone matrix is so interconnected with the hydroxyapatite-like layer that Hench described this material-bone interface as being even more resistant than both material and bone alone, which provided great stability for implants, solving the previous problems of instability and rejection[8].

By definition a bioactive material for use in bone replacement has to be biocompatible, osteoconductive (allow bone to grow onto its surface), osteostimulative (stimulate osteoblasts that are not in direct contact with its surface to proliferate and maturate), and osteoinductive (stimulate pluripotent cells to differentiate into osteoblasts)[11]. Bioglass® 45S5 was the first material to fulfil all of these requirements and started to be commercialized in the middle of the 1980's[15]. The original Bioglass®45S5 has been used in orthopaedics to repair bone defects of the jaw in more than one million patients. However, considering its potential, perhaps this figure is not as big as it should be. The composition still lacks bioactivity to repair large defects, so its use is limited to dental applications and the repair of facial bone fractures[15].

The biological properties of a material are directly related to its chemical composition. The great advantage of glasses is that one can easily manipulate their chemical structure to achieve different biological responses[10,11]. It was observed that the different ions that come from the dissolution of the glass, such as Si, Ca, and Na can influence cell response in different manners[16]. With that in mind, many researchers developed dozens of variations of the original Bioglass 45S5, some of which showed high bioactivity, e.g. 58S, S53P4, 70S30C[15,17].

Recent works reported the ability of niobium ions to enhance differentiation and mineralization of osteogenic cells in *in vitro* assessment[18,19]. Niobium has been used in titanium alloys for endosseous implants, aiming to increase the biocompatibility, corrosion resistance and superior fatigue resistance[20]. Similar behaviors for phosphate bioactive glass were observed by adding Nb_2O_5[21,22]. Apparently, the most effective glass compositions for biomedical purpose are derived from silicate systems[17,23]. Niobo-silicate bioglass compositions were first explored by our previous work[24].

In this study, we exhaustively investigated the structure of two series of bioglass (derived from 45S5 Bioglass) with varying niobium oxide contents using multinuclear ^{29}Si, ^{31}P, and ^{23}Na solid-state MAS NMR and Raman spectroscopies combined with some physical properties of the glasses. The first series (I) was a substitution of P_2O_5 for Nb_2O_5, while the second series (II) was a substitution of SiO_2 for Nb_2O_5, keeping the Na_2O:CaO ratio fixed in both series. The results revealed that Nb_2O_5 participates of silicate network in different ways for both of the studied bioglass series. For Series I, Nb_2O_5 acts by breaking the Si-O-Si bonds to form structures such as -Si-O-Nb-O-Si- chains, while for the series II, it acts as crosslinker, forming crosslinks between the several oxygens of the silicate chains. The alterations observed in series I (mainly up to 1.3% wt of N2O5), significantly increased the glass dissolution rate and magnitude, which is related to a greater bioactivity[24].

Even though Nb2O5-doped silicate glass appears to possess interesting bioactive properties, its effect over pluripotent cells and bone regeneration has not been investigated yet. In view of this, the objective of the investigations described in part one of this thesis was to evaluate the *in vitro* and *in vivo* effects of different compositions of these glasses on important issues for osteointegration of medical materials for bone replacement, such as, cytotoxicity, osteoinduction, osteoconduction, and osteostimulation.

Ga-Doped bioactive glasses for bone cancer applications

Bone cancer occurs most frequently in children and young adults between the age of 5 and 20 years, but may also grow in the elderly. Each year, about 1,000 new cases of osteosarcoma (one type of bone cancer) are diagnosed in the United States

alone. Approximately 450 of these are in children and teenagers[25]. The mutations might be acquired during one's lifetime after repetitive exposure to carcinogenic agents such as radiation, as when patients that are undergoing repetitive radiotherapy to treat another prior cancer end up developing osteosarcoma. However, the majority of the cases seem to have a hereditary cause because other hereditary conditions that affect bones such as Li–Fraumeni syndrome (LFS), hereditary retinoblastoma (RB), Rothmund–Thomson syndrome (RTS), RAPADILINO syndrome (RAPA), Werner syndrome (WS), Bloom syndrome (BS), Diamond–Blackfan anemia (DBA), and Paget's disease of bone (PDB) seem to facilitate the development of bone tumors. The 5-year-survival rate of non-metastatic disease is about 70% whereas metastatic disease is associated with survival rates of 15-30% [25–27].

The standard treatment of osteosarcoma consists of surgical resection of the tumor, chemotherapy and, in some cases, radiotherapy. Nevertheless, despite advances in surgery and multi-agent chemotherapy, there has been no significant improvement in the survival of patients over the last four decades[25,27]. In order to improve the clinical outcome, safe and effective therapeutic materials are required. The minimum key requirements for an effective biomaterial targeted towards osteosarcoma therapy are (1) to successfully eradicate any residual tumour not excised during the surgery without being cytotoxic to the surrounding tissue and (2) to provide a suitable platform for the regeneration of new bone. A potential solution to this problem is to engineer materials capable of replacing damaged tissue whilst simultaneously preventing reoccurrence and/or metastases of tumours following surgery. The development of synthetic alternatives that help regenerate bone by acting as active temporary scaffolds has been nurturing considerable research activity. However there have been very few reports of synergistic scaffolds which can help manage cancer and simultaneously promote wound healing. Aiming to solve this problem we considered creating bioactive glasses that could be used for such purpose. The addition of Gallium (Ga) into the glass's network seems to be promising once Ga has successfully been used as a complementary agent in the treatment of some types of cancers[27,28].

Gallium is the second metal ion, after platinum, to be used in cancer treatment. Ga binds to the blood protein transferrin preventing its attachment to Fe^{+3} [27] . The complex Ga-transferrin is internalized into cells by binding to transferrin receptors. Once inside the cells Ga is transferred to cellular ferritin, as is iron itself. It acts

inhibiting DNA synthesis and modifying the three-dimensional structure of the DNA, modulating protein synthesis, inhibiting H+ - dependent ATPase, among other functions. In sum, trivalent Ga acts as an antagonist to several divalent ions including Mg2+, Fe2+, Zn2+ and Ca2+, it promotes a decrease in cell proliferation and maturation and triggers cellular apoptosis[28]. It is well known that cancer cells possess more transferrin receptor than normal cells which highlights Gallium as a possible treatment for bone cancers.

Based upon its clinical efficacy, gallium nitrate (Ganite™) is used as a treatment for cancer-associated hypercalcaemia[28]. The recommended mode of administration for gallium nitrate is via a continuous intravenous infusion for 5–7 days. However, this treatment is very inconvenient since patients receive this drug either intravenously in hospital or as an outpatient via a pump device. A scaffold that can provide a site specific controlled delivery of gallium would therefore be highly advantageous. Gallium ions have previously been incorporated into phosphate based glasses to deliver a controlled antimicrobial effect[29,30]. Wren *et al.* and Towler *et al.* incorporated Ga into bioactive glasses for bone cement applications and for antimicrobial functionality[31]. More recently, Frachini *et al*. and Lusvardi *et al.* have incorporated gallium oxide into bioactive glasses for antimicrobial applications[32,33]. However there have been no studies undertaken on osteosarcoma cells. The investigation described in part two of this thesis aimed to verify the potential of incorporating gallium into bio-degradable bioactive glasses specifically targeted towards bone cancer applications.

PART ONE: DOPING BIOGLASS® WITH NIOBIUM DIOXIDE (Nb2O5) PROMOTES SUPERIOR BIOACTIVITY AND STIMULATES DIFFERENTIATION OF BOTH HUMAN EMBRIONIC STEM CELLS (hESCs) AND BONE-MARROW-DERIVED MESENCHYMAL STEM CELLS

Objectives of these studies:

This set of experiments aimed to determine the effect of the addition of Nb2O5 into Bioglass®45S5 over its structure and physicochemical properties as well as to verify the biocompatibility and the potential of these glasses to stimulate osteogenic differentiation of both Human Embryonic Stem Cells (hESCs) and Mesenchymal Stem Cells derived from the bone marrow (BM-MSCs). We also investigated whether Nb-containing bioactive glass is able to stimulate bone regeneration in long and flat bones. The methods and results of these studies are described in the following scientific papers:

Article 1: ***Comprehensive in vitro and in vivo studies of novel melt-derived nb-substituted 45S5 bioglass reveal its enhanced bioactive properties for bone healing.*** ***(*****Accepted for publication by the journal Scientific Reports)**

Article 2: ***Systematic evaluation of the osteogenic capacity of novel melt-derived nb-substituted 45S5 bioglass: in vitro and in vivo studies***

Article 3: ***Biocompatibility and osteostimulative properties of nb- containing bioactive glass: an experimental in vitro and in vivo study***

ARTICLE 1: Comprehensive *in vitro* and *in vivo* studies of novel melt-derived Nb-substituted 45S5 bioglass reveal its enhanced bioactive properties for bone healing

***Lucas Pereira Lopes De Souza*[1,‡], *João Henrique Lopes*[2,‡,*], *Davi Encarnação*[2], *Italo Odone Mazali*[3], *Richard Alan Martin*[4] , *José Angelo Camilli*[1], *Celso Aparecido Bertran*[2]**

AUTHOR INFORMATION

L. P. L. De Souza

[1]Department of Structural and Functional Biology, Institute of Biology, University of Campinas – UNICAMP, 13083-862, Campinas, SP, Brazil.

E-mail: (lpls2002@hotmail.com)

J. H. Lopes (Corresponding Author)

[2]Department of Physical Chemistry, Institute of Chemistry, University of Campinas – UNICAMP, P.O. Box 6154, 13083-970, Campinas, SP, Brazil.

E-mail: (henriquelopez@gmail.com)

D. Encarnação

[2]Department of Physical Chemistry, Institute of Chemistry, University of Campinas – UNICAMP, P.O. Box 6154, 13083-970, Campinas, SP, Brazil.

E-mail: (davi.encarnacao1@gmail.com)

I. O. Mazali

[3]Department of Inorganic Chemistry, Institute of Chemistry, University of Campinas – UNICAMP, P.O. Box 6154, 13083-970, Campinas, SP, Brazil.

E-mail: (mazali@iqm.unicamp.br)

R. A. Martin

[4]School of Engineering & Aston Research Centre for Healthy Ageing, Aston University, B47ET Birmingham, United Kingdom.

E-mail: (r.a.martin@aston.ac.uk)

J. A. Camilli

[1]Department of Structural and Functional Biology, Institute of Biology, University of Campinas – UNICAMP, 13083-862, Campinas, SP, Brazil.

E-mail: (jcamilli@unicamp.br)

C. A. Bertran

[2]Department of Physical Chemistry, Institute of Chemistry, University of Campinas – UNICAMP, P.O. Box 6154, 13083-970, Campinas, SP, Brazil.

E-mail: (bertran@iqm.unicamp.br)

**Correspondence to henriquelopez@gmail.com*

‡ *These authors contributed equally.*

ABSTRACT

The present work presents and discusses the results of a comprehensive study on the bioactive properties of Nb-substituted silicate glass derived from 45S5 bioglass. *In vitro* and *in vivo* experiments were performed. We undertook three different types of *in vitro* analyses: (i) investigation of the kinetics of chemical reactivity and the bioactivity of Nb-substituted glass in simulated body fluid (SBF) by ^{31}P MASNMR spectroscopy, (ii) determination of ionic leaching profiles in buffered solution by inductively coupled plasma optical emission spectrometry (ICP-OES), and (iii) assessment of the compatibility and osteogenic differentiation of human embryonic stem cells (hESCs) treated with dissolution products of different compositions of Nb-substituted glass. The results revealed that Nb-substituted glass is not toxic to hESCs. Moreover, adding up to 1.3 mol% of Nb_2O_5 to 45S5 bioglass significantly enhanced its osteogenic capacity. For the *in vivo* experiments, trial glass rods were implanted into circular defects in rat tibia in order to evaluate their biocompatibility and bioactivity. Results showed all Nb-containing glass was biocompatible and that the addition of 1.3 mol% of Nb_2O_5, replacing phosphorous, increases the osteostimulation of bioglass. Therefore, these results support the assertion that Nb-substituted glass is suitable for biomedical applications.

INTRODUCTION

Fractures, bone tumours, periodontal diseases, and degenerative cartilage disorders disrupt daily activities of people. Therapeutic approaches to these pathologic conditions prompted the development of materials that could replace bone and joint tissues[1-3]. Many materials were produced based on metals, such as aluminium, zirconia and titanium, and were used in orthopaedics for manufacturing prosthesis, plates, nails, screws, and other such components. However, as these materials in general have a lifespan of around 10-20 years and human life expectancy has increased, these implants frequently deteriorate prior the patient's death[6-8].

At the beginning of the 1970s, the researcher Larry. L. Hench and his colleagues developed the first bioactive material, the 45S5 bioglass (Bioglass®). This biomaterial not only induced no inflammatory response in the body, but also formed strong bonds with bone and soft tissues, optimizing stability of the implant and extending its durability[8-10]. This material is a bioactive glass belonging to the system SiO_2-CaO-Na_2O-P_2O_5 (46.1 mol% SiO_2, 26.9 mol% CaO, 24.4 mol% Na_2O, and 2.6 mol% P_2O_5) [11]. The strong interface between biomaterial and tissue is established through chemical reactions that occur on the surface of the bioglass, concomitant with biological events leading to the formation of a nanocrystalline calcium phosphate hybrid composite permeated by biological molecules[9,10].

Several articles have been published, reviewing the literature discussing the effect of 45S5 bioglass composition on bioactivity, angiogenesis, osteostimulation, osteoconduction, and other important properties for bone regeneration[12-16]. As the chemical composition of glass dictates its effects on living tissues, many other variations of the original Bioglass® have been manufactured and investigated for use as biomaterial; some of them showed high bioactivity, for example 58S, S53P4, and 70S30C[2,17-21].

Furthermore, several types of transition metal-doped soda lime silica glass have been prepared, and their bioactivity has been evaluated for biomedical applications[22,23]. Among the various vitreous compositions investigated, glass containing niobium oxide have received special attention, since the presence of niobium species has been associated with improvements in bioactive and mechanical properties[24-28]. Moreover, recent works have reported the ability of niobium ions to enhance differentiation and

mineralization of osteogenic cells *in vitro*[26,27]. Metallic niobium has been used in titanium alloys for endosseous implants, aiming to increase the biocompatibility and corrosion resistance, with superior fatigue resistance[29]. Similar behaviour of phosphate bioactive glass was observed on adding Nb_2O_5[25,28]. It is noteworthy, however, that the Nb_2O_5 is an effective nucleating agent and generally leads to the development of glass-ceramic in silica-poor compositions (inverted glass), such as 45S5[30].

In our previous study, the structures of two series of bioglass (derived from 45S5 Bioglass® composition) with varying niobium oxide contents were exhaustively investigated by multinuclear ^{29}Si, ^{31}P, and ^{23}Na solid-state MAS NMR and Raman spectroscopy, and some physical properties of the glass were also studied[31]. The structural investigation of bioglass resulting from the substitution of P_2O_5 by Nb_2O_5 revealed that Nb_2O_5 participates in the silicate network by breaking the Si-O-Si bonds to form structures, such as -Si-O-Nb-O-Si- chains. These alterations significantly changed the glass dissolution rate and magnitude, which is of interest for understanding its higher bioactivity[31,32].

Even though Nb-substituted silicate glass appears to possess interesting bioactive properties, its effect over pluripotent cells and bone regeneration has not been investigated till date. In view of this, the objective of this study was to evaluate the *in vitro* and *in vivo* effects of different compositions of Nb-substituted bioglass on properties, namely, cytotoxicity, osteoinduction, osteoconduction, and osteostimulation, that are essential for osteointegration of medical materials for bone replacement. The *in vitro* approach consisted of treating human embryonic stem cells (hESCs) with the dissolution products from the glass and verifying cell viability and osteogenic differentiation. For the *in vivo* assay, glass rods were implanted into circular defects in rat tibia and bone formation was quantified. In addition, the leaching profile of Si, Ca, Na, P, and Nb species from the bioglass, and the kinetics of structural transformations of different compositions of Nb-substituted silicate glass were investigated.

Results and Discussion

Dissolution studies. The leaching rate of Na, Ca, Si, and P ions from bioglass in the earliest stages of the bioreactivity is of utmost importance since the results of the leaching processes will control the subsequent biomineralization. To examine leaching rates, two promising compositions of Nb_2O_5-containing bioactive glass were studied. The 45S5 bioglass composition is also presented for the purpose of comparison. The nomenclature and chemical composition of all samples studied in this work are shown in **Table 1**.

Table 1 - Glass compositions of BG45S5 and Nb-substituted 45S5 bioglass.

Glass	SiO_2	CaO	Na_2O	P_2O_5	Nb_2O_5
BG45S5	*46,1*	*26,9*	*24,4*	*2,6*	-
BGPN2.6	*46,1*	*26,9*	*24,4*	-	*2,6*
BGPN1.3	*46,1*	*26,9*	*24,4*	*1,3*	*1,3*

The effect of Nb_2O_5-content on the glass solubility was studied by time-dependence of species release from bioglass particles dispersed in 50.69 mM HEPES buffered solution (pH = 7.4). The leaching curves for Na, Ca, Si, P (**Figure 1**) and Nb (**Figure 2**) species were determined by using inductively coupled plasma optical emission spectrometry (ICP-OES).

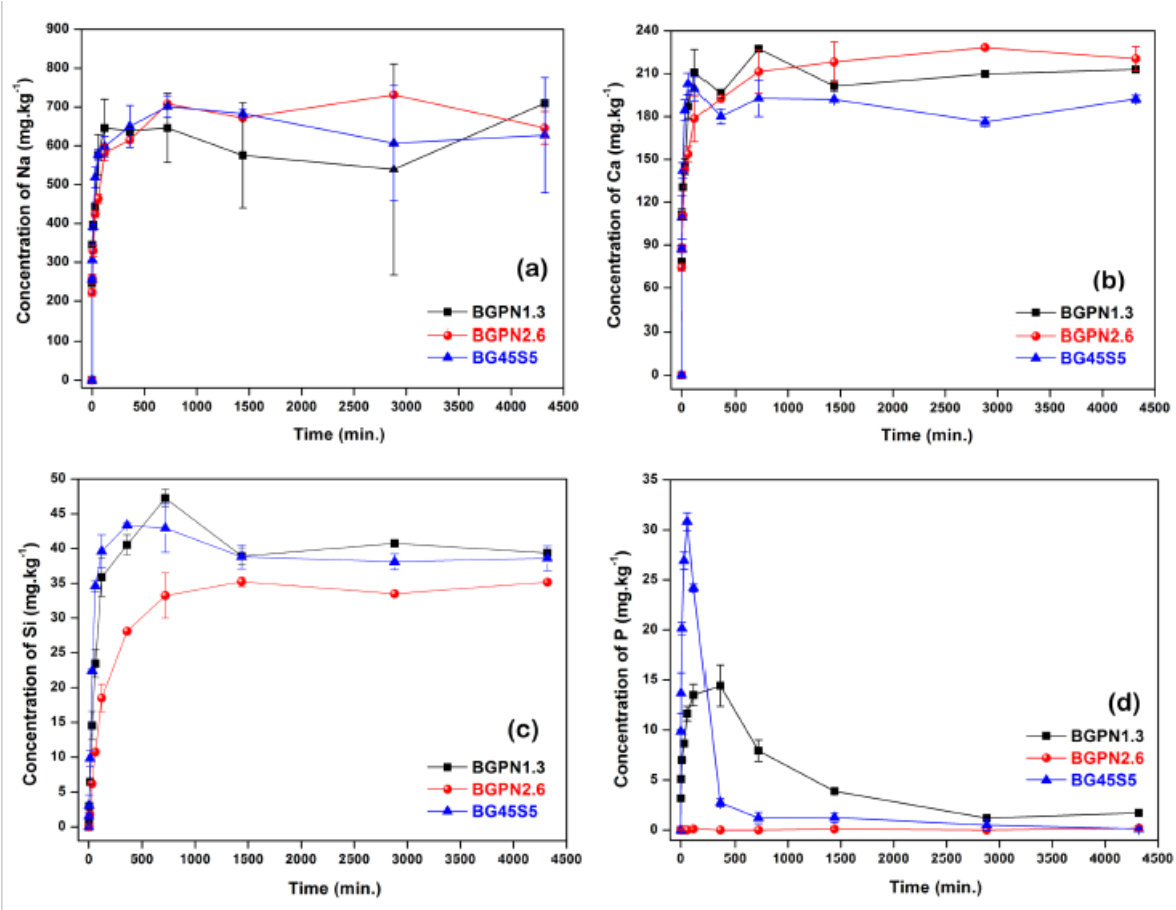

Figure 1. ICP data: ion release vs. time in 50.69 mM HEPES solution at pH 7.40 for BG45S5 and Nb- substituted bioactive glass. The data displayed in (a), (b), (c) and (d) are related to leached Na, Ca, Si, and P species from glass derived from substitution of P2O5 for Nb2O5.

We found that the initial elemental concentrations of sodium, calcium, silicon, and phosphorus, up to about 120 min for all compositions, are a linear function of the square root of time, which indicates a diffusion-controlled process (**Supplementary Information - Figure SI3 a-d**)[10]. The shape of the curves is consistent with Hench's mechanism, which describes all events on bioglass surface in contact with body fluid in five steps: (i) rapid exchange of Na^+/Ca^{2+} from glass network with H_3O^+ from solution, (ii) loss of soluble silica/ formation of silanol groups at the glass solution interface, (iii) condensation and repolymerization of a SiO_2-rich layer, (iv) growth of the amorphous $CaO\text{-}P_2O_5$-rich film by incorporation of soluble calcium and phosphates from solution, (v) crystallization of the amorphous $CaO\text{-}P_2O_5$ film by incorporation of OH^- and CO_3^{2-} anions from solution [5,6,9,33].

The leaching profiles of network modifier ions, Na^+ and Ca^+, for BG45S5 and Nb_2O_5-substituted bioglass showed an abrupt increase, reaching a maximum concentration value for these species at around 2 hours and remaining constant for longer times (**Figure 1a-b)**. The release curves showed that the amount and rate at which Na and Ca ions are leached from the glass networks were similar to each other, in particular, within the first hours after dipping. This result is of extreme importance because it shows that the replacement of P_2O_5 by the Nb_2O_5 in the 45S5 composition did not alter the onset of the cascade of events, which includes ion exchange between Na^+ and Ca^{2+} ions and H_3O^+, as described by the Hench mechanism for biomineralization[9,33,34]. In addition, recognizing that sodium niobate and/or calcium niobate are highly water insoluble species close to the neutral pH, these results corroborate with those previously reported on structural data for these glassy compositions[31], suggesting that niobium (NbO_6) would be behaving as a network former by establishing chemical bonds with silicon tetrahedral (Si-O-Nb-O-Si) in the glass backbone (chain of alternating Si and O atoms).

Conversely, the leaching curves for the species of silicon and phosphorus showed peculiar behaviours for each bioglass composition (**Figure 1c-d**). The amounts of soluble silicon species determined after the first hour of immersion were similar, except for the BGPN2.6 sample, which exhibited a reduced concentration of silicon. This result indicates the presence of Si-O-Nb bonds, where the NbO_6 octahedra replaces part of the SiO_2 tetrahedra in the glass network. Evidently, an increase in niobium content in the composition must result in a greater number of Nb-O-Si bonds, so that such structures may act as traps for the silicon species in the glass matrix, preventing and delaying their leaching. The release profile of phosphorus suggests a maximum concentration (approximately the solubility limit), from which there is a dramatic reduction, possibly associated with the removal of some of the soluble phosphate species to form the calcium phosphate layer on the bioglass surface (**Figure 1d**). Although the rate at which species of phosphorus are released into solution is similar to BG45S5 and BGPN1.3 samples, the removal of phosphorus from solution is slower for the BGPN1.3, which can be attributed to its lower P_2O_5 concentration (phosphorus concentration was not high enough to reach the limit solubility of calcium phosphate). As expected, no appreciable amount of phosphate species was observed for BGPN2.6.

The leaching curves for the species of niobium exhibit similar profiles to those observed for phosphorus species (**Figure 2**).

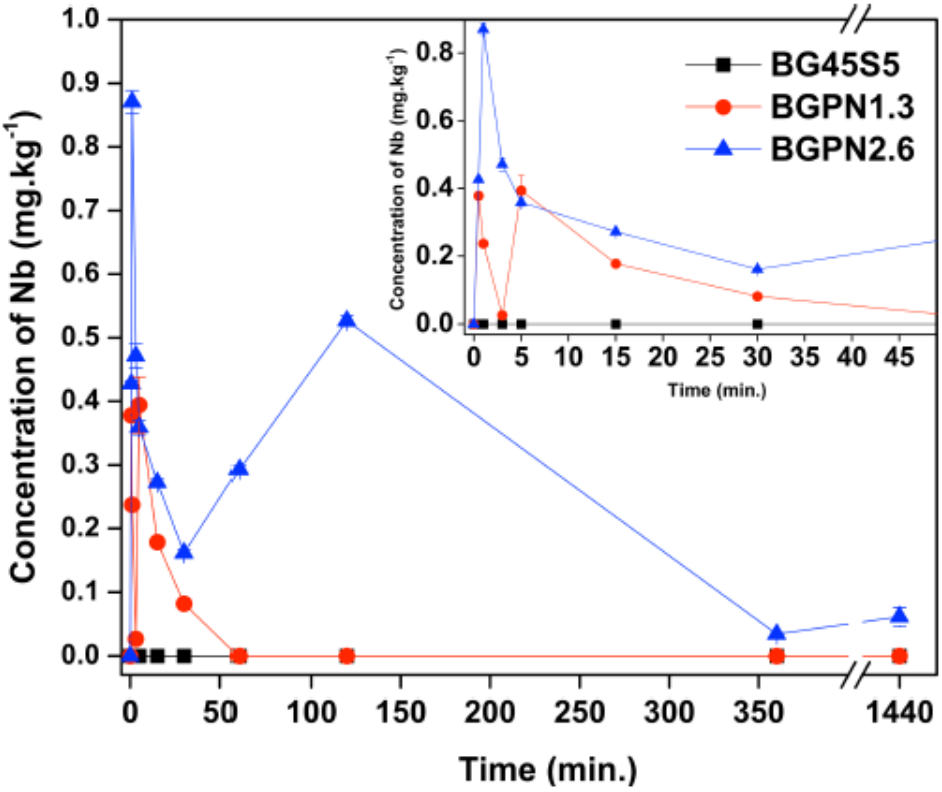

Figure 2. ICP data: Nb ion release vs. time in 50.69 mM HEPES solution at pH 7.40 for BG45S5 and Nb-substituted bioactive glass. The amounts of niobium determined by ICP-OES is consistent with the niobium content in each sample, i.e. BGPN2.6 exhibits a higher peak of niobium concentration compared to the BGPN1.3 bioglass. As expected, no niobium was detected for BG45S5.

At early soaking times, it is possible to observe an abrupt increase in the niobium concentration in the medium, reaching a maximum value, followed by a dramatic reduction of concentration value. This initial burst can be credited for the leaching of niobium species near surface and/or release of isolated NbO_6 units isolated niobium octahedral in the vitreous matrix, which are more labile since their release does not require extra energy to break bonds. The maximum niobium species concentration determined for samples BGPN1.3 and BGPN2.6 was 0.4 ppm after 30s and 0.9 ppm after 1 minute, respectively. The drastic decrease in niobium content observed for samples BGPN1.3 and BGPN2.6 is closely related to the very low solubility of niobium species at pH 7.4 in aqueous medium. The presence of a second peak of Nb

concentration was observed for the BGPN1.3 and BGPN2.6 bioglass of 0.4 ppm after 5 minutes and 0.5 ppm after 120 minutes, respectively. This second event is directly related to the leaching of isolated niobium species in the bulk and/or Nb species that were more firmly trapped in the vitreous network. Again, the abrupt decrease in niobium concentration is due to the fact that the product solubility is small for niobium species. In fact, the concentration of niobium after each release peak tends to go to zero, confirming that the residence time of the Nb species in the solution body is short. Consequently, almost all niobium, if not all, may be retained in aggregates in the solution (removed during the filtration step) or in silica gel formed at the bioglass/solution interface.

Generally, it is common to use chelating agents such as citrates and oxalates to increase the solubility of niobium species[35,36]. It is noteworthy that all the studies of leaching presented in this report were carried out using a medium containing HEPES, which is an often-used agent in studies, among several other reasons because it does not chelate with metals. Obata et al[27] investigated a glass series belonging to 60CaO-30P_2O_5-(10-x)Na_2O-xNb_2O_5 - system (mol%, x = 0-10) and quantified the content of niobium in the leachate by ICP-OES after a few hours of immersion. However, in this study, the dissolution of the glass was carried out in a complex culture medium (minimal medium culture + bovine serum) containing various chelating ligands, which may explain the presence of niobium in the solution. It is also worth noting that these phosphate glasses studied by Obata and co-workers can dissolve completely in aqueous solution giving ionic species, which may form precipitates upon reaching the maximum solubility (solubility product constant - K_{sp}). Moreover, another important point deserving attention in the work of Obata is that the culture medium has not apparently been filtered, consequently, the undissolved vitreous particles and the possibly formed ionic-molecular agglomerates, both containing niobium, remain in the medium. Hence, not only the niobium species chelated in the medium, but also those present in the glass particles or aggregates are released into the solution during the oxidation step of the organic material (commonly under acidic conditions) required for ICP-OES analysis were quantified[27]. Thus, the low solubility of the species of niobium in solution together with the filtration step using membranes of 0.22 μm, and the absence of chelating agents in the present study suggests that the Si-O-Nb bond undergoes hydrolysis, but only small amount of niobium goes into the solution, while the leached niobium tends to

form complex structures (niobium-silica gel layer), which is retained on the glass surface.

Apatite layer formation ability by ^{31}P MAS NMR spectroscopy. The development of an apatite layer on the bioglass surface in the physiological environment (even under simulated conditions) is a common feature among all the bioactive vitreous compositions described in the literature[9,10,18,37]. Therefore, the time required for this layer to be established has been an initial parameter for assessing and ranking the different vitreous compositions in the bioactivity domain, since apatite is a cell-friendly environment[10,20]. In contrast to other analysis methods, MAS NMR spectroscopy is a powerful, univocal and sensitive tool for studying changes in the chemical environment of phosphorus, capable of identifying subtle changes in local structural arrangement of phosphorus even for early soaking times. The partial dissolution and apatite formation on the bioglass surface in simulated body fluid (SBF) has been verified by ^{31}P MAS NMR (**Figure 3 (a-c)).**

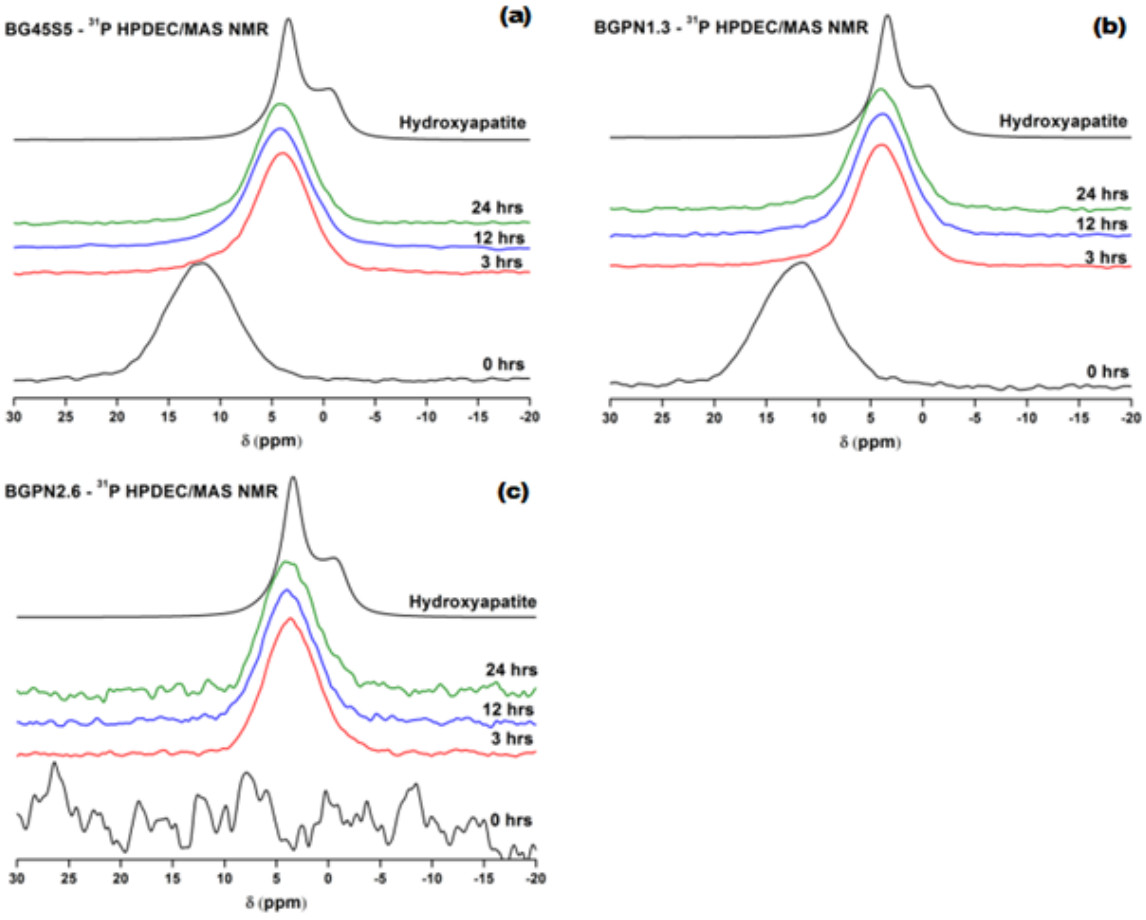

Figure 3. 31P MAS-NMR spectra for the different glass compositions, recorded at a magnetic field strength of 9.4 T and a spinning speed of 10 kHz: (a) BG45S5, (b) BGPN1.3, and (c) BGPN2.6. The chemical environmental for 31P shifts progressively evolves to lower values of δ, reaching a peak position similar to the 31P spectrum observed in the hydroxyapatite control. The absence of phosphorus in BGPN2.6 did not prevent the calcium phosphate layer formation on its surface.

The ^{31}P MAS NMR spectrum of BG45S5 consists of one broad resonance with linewidth of 7.9 ppm and peak maximum at 9.0 ppm assigned to isolated orthophosphate units, which coordinate modifier cations (Na^+ and Ca^{2+}), subtracting them from the silicate network[31,32]. The ^{31}P resonance spectra for the glass compositions containing Nb_2O_5 illustrate a similar spectrum to BG45S5 with one broad resonance and asymmetric peak with a chemical shift ranging from 18 to -3 ppm with an approximate linewidth of 8 ppm.

^{31}P MAS NMR peak positions and full width half maximums (FWHM) for BG45S5 and Nb-substituted glass, unreacted and after 3, 12, and 24 hours of immersion in SBF are listed **Table 2**. ^{31}P MAS NMR spectrum of commercial hydroxyapatite was added as a reference for the phase of calcium phosphate formed**.**

Table 2 - ^{31}P MAS NMR peak positions and full width half maxima (FWHM) for BG45S5, Nb-substituted 45S5 bioglass and commercial hydroxyapatite.

Glass	^{31}P MAS NMR							
	Immersion time in SBF (hours)							
	0		3		12		24	
	Peak (ppm)	FWHM (ppm)	Peak (ppm)	FWHM (ppm)	Peak (ppm)	FWHM (ppm)	Peak (ppm)	FWHM (ppm)
BG45S5	*11.9*	*7.9*	*4.0*	*6.2*	*4.3*	*6.6*	*4.0*	*6.1*
BGPN1.3	*11.6*	*7.9*	*3.9*	*6.0*	*3.9*	*5.9*	*4.0*	*6.0*
BGPN2.6	--	--	*3.5*	*5.9*	*3.8*	*5.9*	*3.7*	*5.8*
Reference								
Hydroxyapatite	*3.4*	*2.7*	--	--	--	--	--	--

In general, ^{31}P MAS NMR spectra for all glass exhibit the same trends, which can be summarised by the chemical shift to lower frequencies and a decrease in FWHM values. Such spectral changes are intimately related to partial degradation of glass and precipitation of amorphous calcium phosphate and its progressive crystallization[32].

^{31}P MAS NMR spectra for BG45S5 **(Figure 3a)** and BGPN1.3 **(Figure 3b)** after 3 hours of incubation in SBF showed a main peak at ~4 ppm with slight asymmetry on the left-hand side of the peak owing to the residual glass fraction. This subtle spectral feature was not observed for BGPN2.6 **(Figure 3c)**, which exhibited a single and symmetrical peak at 3.6 ppm, confirming that the presence of P_2O_5 in the glass bulk is not mandatory for precipitation of calcium phosphate layer. Although subtle, the changes observed in the spectra in the range of 3-24 hours are related mainly to the gradual increase in the crystallinity of calcium phosphate (increase of long-range order). The ^{31}P MAS NMR spectra after 24 hours in SBF for all the glass compositions show chemical shifts and bandwidths similar to those observed for commercial hydroxyapatite (top spectrum in **Figure 3c**). These results indicate that glass containing niobium leads to the formation of a calcium phosphate with a higher degree of crystallinity compared to BG45S5, with similar

soaking time in SBF. In fact, it has been reported that Nb-OH groups in the amorphous phase of sol-gel-derived niobium oxide gels are very effective for apatite nucleation, which is a friendly environment for cells[38].

Biocompatibility assessment. The first step when developing a new biomaterial to be used for tissue replacement is to ensure that it cannot represent a risk when implanted into the body. Therefore, we carried out *in vitro* and *in vivo* experiments to test the biocompatibility of Nb-containing glass. In the *in vitro* approach we treated human embryonic stem cells (hESCs), CCTL12, with the dissolution products of Nb-containing glass (BGPN1.3 and BGPN2.6) and the control glass (BG45S5) for 14 days and performed a resazurin assay. This assay revealed that none of the glass compositions were cytotoxic (**Figure 4**).

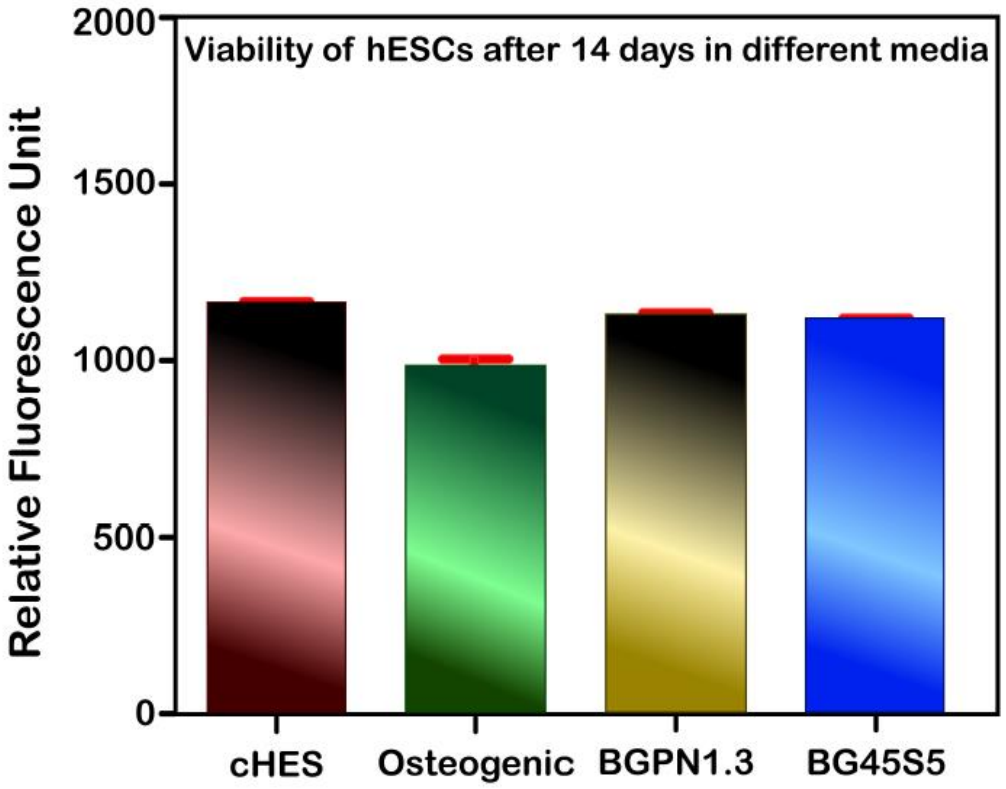

Figure 4. Relative fluorescence of hESCs stained with 5 µM of resazurin after 14 days of treatment with different culture media. There was no significant difference between the groups, which shows that none of the media were cytotoxic for this cell line. This study was carried out only for the BG45S5 and BGPN1.3 samples. cHES: conditioned human embryonic stem cells medium.

Both, BG45S5 and BGPN1.3 glass showed similar fluorescence relative to that of the control group (cHES medium) after 14 days of treatment ($P > 0.05$). This result corroborates with those from some other reports[24,27,39] that have studied the cytocompatibility of bioactive glass containing niobium; these studies concluded that the addition of this metal does not impair the compatibility of the biomaterial. One of these reports showed that when osteoblast-like cells are in direct contact with the surface of calcium phosphate invert glasses (PIGs) containing Nb_2O_5 they attach and spread after 6 hours on all different concentrations of soluble niobium species[27]. The same authors performed experiments with dissolution products of niobium-doped PIGs and revealed that they are not harmful for osteoblast-like cells (MC3T3-E1), and instead they stimulated some positive biological responses[27].

Similar results were found by another study using a different cell line and a different formulation[26]. In this study, human mesenchymal stem cells (hMSCs) were cultured on niobium-doped fluorapatite glass-ceramics, and the results showed that after 3 hours, the hMSCs attached on niobium glass as well as they did on the control surface; the report also shows the scanning electron microscopy (SEM) micrographs of cells attached to the glass surface after 2-4 days[26].

Testing cytocompatibility is not enough to ensure the safety of implants. Inorganic material may intoxicate some high-metabolic-rate organs that participate in the metabolism and excretion of the material, for example the liver and kidneys, which may lead to morphological alterations in these organs. Because of that, we calculated the relative weights of the livers and kidneys of rats that had undergone implantation of glass rods at circular defects in their tibia, and compared the mean values with a control group of rats. We observed no difference between the groups neither after 14 nor 28 post-operative days, proving that no alterations in these organs were caused by the presence of the inorganic implants (**Table 3**).

Table 3 - Relative weight of liver and kidneys of rats treated with different bioactive glasses for 14 and 28 days.

Time	Groups	Liver (g)	Kidneys (g)	Body Weight (g)
14 days	Control	11.4 ± 0.2	5.17 ± 0.07	366.0
	BG45S5	11.4 ± 0.2	5.28 ± 0.06	381.0
	BGPN1.3	11.4 ± 0.1	5.10 ± 0.09	376.0
	BGPN2.6	11.2 ± 0.1	5.22 ± 0.07	373.0
	Sham	11. 5 ± 0.2	5.29 ± 0.08	387.0
28 days	Control	10.8 ± 0.1	5.0 ± 0.1	474.0
	BG45S5	10.8 ± 0.2	5.00 ± 0.07	466.0
	BGPN1.3	10.74 ± 0.08	4.99 ± 0.05	434.0
	BGPN2.6	10.9 ± 0.1	5.05 ± 0.07	421.0
	Sham	10.6 ± 0.2	5.02 ± 0.04	443.0

Average values of 6 animals. represented by mean ± SEM. Considering $p<0.05$ no significant difference was detected. One-way ANOVA followed by Student Newman-Keuls test. Sham = no bone defect was created.

Taken together, these results suggest that regardless of the biological model and material formulation used, Nb-substituted bioglass is biocompatible, and such bioglass have proved to be excellent candidates for biomedical applications.

Osteogenic potential of Nb-containing bioglass. Several studies have shown that by transplanting adequate numbers of competent osteoprogenitor cells on biomaterial scaffolds, cell-based bone tissue engineering strategies may promote functional reconstruction of skeletal defects[40-42]. We chose to work with human embryonic stem cells (hESCs) because we believe these cells show some important advantages compared to other more commonly used multipotent cell types like mesenchymal stem cells (MSCs). We understand that MSCs may represent a reliable source of multipotent stem cells for bone cell transplantation. However, the fact that the numbers of adult MSCs are limited, and decline with age[43], and because they are present at different stages of differentiation at the time of harvest[44], their use is not without problems. Human ESCs, on the other hand, possess unlimited growth and differentiation potential, accessibility, and do not require a donor site[45], facilitating the

acquisition of a large amount of cells to be used with biomaterial scaffolds for bone regeneration.

The capacity of niobium to stimulate osteogenic differentiation of hESCs was tested by the analysis of matrix mineralization, carried out after 21 days of treatment. This assay revealed the formation of large calcified nodules on the cells treated with BGPN1.3, which suggests cells differentiated into osteoblasts that formed a mineralized bone matrix. These nodules were larger than those observed in the cells treated with BG45S5 **(Figure 5)**.

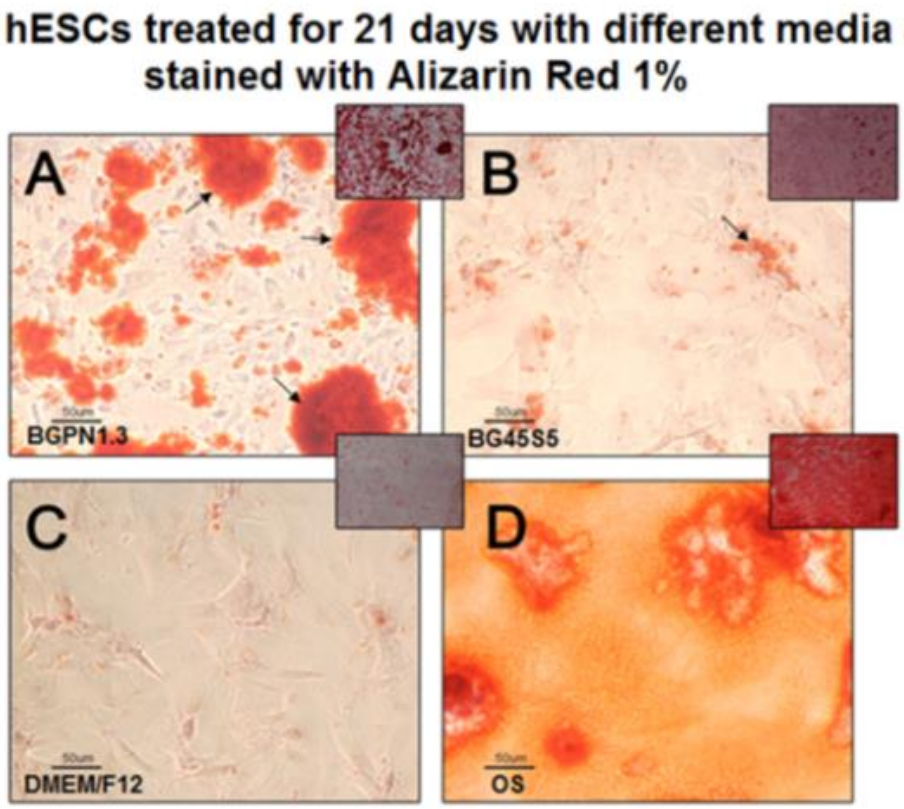

Figure 5. Micro and macrographs of calcium deposits within and around hESCs stained with alizarin red (1%) after 21 days of treatment with different media. The four large squares show micrographs (100× magnification) in which the red aggregates (indicated by the arrows) are calcium deposits. The small squares show the photographs taken of each well. Cells treated with osteogenic medium (OS) showed a fully mineralized matrix which means that most hESCs were in a late stage of differentiation to osteoblasts. Those cells treated with BGPN1.3 showed a greater degree of matrix mineralization than those treated either with BG45S5 or DMEM/F12. This study was carried out only for the BG45S5 and BGPN1.3 samples.

The products leached from bioactive glass seem to stimulate stem cells to proliferate and differentiate to osteoblasts by activating different intracellular pathways[6,8,46]. Lopes et al. observed that the incorporation of up to 1.3% of Nb_2O_5 by replacing the P_2O_5 in a SiO_2-Na_2O-CaO-P_2O_5-Nb_2O_5 system imposed significant structural changes on the glass, altering its solubility and the rate and magnitude of the Na, Ca, Si and P species leaching from the glass network, compared to niobium-free bioglass[31].

Although a receptor for Si has not been identified yet, this ion has been shown to be one of the main components of bioglass that is responsible for osteogenic stimulation[6,47,48]. As a component of silicic acid [$Si(OH)_4$], silicon has been shown to stimulate osteoblasts to produce collagen I, which is the main component of the extracellular bone matrix[46]. On the other hand, the receptors and intracellular pathways activated by Ca^{+2} in osteoblasts as well as its indirect roles in the bone formation process are very well described[46,49].

It is well known that calcium possesses both structural and signalling roles in regulating bone homeostasis[46,50-52]. Structurally, hypercalcemia is required to produce mineralized bone as it is combined with PO_4^{-3}, precipitating as calcium phosphate, which constitutes the inorganic phase of the bone matrix. Furthermore, Ca has an important role in regulating bone homeostasis by signalling pathways in bone-forming osteoblasts[46,50,52,53]. It has been reported that this ionic signalling enhances proliferation of stem and mature bone cells through binding to a G-protein, coupled to an extracellular calcium sensing receptor, in a process dependent on nitric oxide (NO) production. Downstream in this signalling, the P13K/Akt pathway is activated, ensuring the surveillance of the osteoblasts[46].

Niobium species seem to have a direct effect on cells. This fact was demonstrated by Obata et al. by treating mouse osteoblast-like cells (MC3T3-E1 cell) with media containing different concentrations of niobium ions (between 1×10^{-8} to 1×10^{-5} M)[27]. Their results showed that, independent of the concentration, niobium did not compromise cell proliferation. Besides this observation, they noted that the ions stimulated a significantly higher alkaline phosphatase activity (APA) in a dose-dependent manner, indicating cell differentiation after 14 days, even in a medium devoid of an osteogenic supplement. When osteogenic media was conditioned with the

same ion concentrations, a significant dose-dependent increase was observed in calcium deposition compared to that in the osteogenic medium without niobium ions, suggesting that the niobium ions stimulated greater calcium deposition, which is an indicator of cell maturation. Although we have not studied specific intracellular pathways, we suggest that the greater osteogenic differentiation stimulated by Nb-substituted bioglass observed in our study may have been caused by the presence of niobium species, since the amount of the other bioactive ionic species (based on Si, Ca, Na, P) were similar between the groups. This suggestion corroborates with the results of the aforementioned study[27].

It is worth mentioning that ICP-OES analysis allowed quantification of the ionized Na, Ca, Si, P, and Nb species released from the glass, but the results do not provide any information on their bioavailability or molecular structure. The dissolution products generated are likely to be in the form of compounds of the elemental constituents of the glass rather than individual ions. Thus, drawing conclusions based only on ion concentration may seem an oversimplification. Obviously, in more complex media, such as culture media or corporeal fluid, the presence of chelating molecules and the ionic strength of the medium may alter the release profile and bioavailability of these species. In order to determine the levels of each element and its bioavailability, the quantification of the leached species from the vitreous matrix, concomitant with molecular speciation studies in a complex, more realistic, media, would be an ideal study, but is a technically challenging experiment. Further studies should focus on determining specifically which compounds are released, which intracellular pathways take part in the osteogenic process, and which genes are regulated by the presence of the bioglass-derived compounds.

Bone formation stimulated by Nb-containing bioactive glass. *In vivo* experiments were performed in order to analyse the bioactive properties of osteostimulation and osteoconductivity of different Nb-containing glass compositions. Glass rods were implanted into the tibia in rats to test their biological properties by quantifying the newly formed subperiosteal bone and the thickness of the bone layer formed over and near the surface of the rod.

Comparison of subperiosteal bone area in the rod group tibia and those in a control group showed no significant difference after 14 days of implantation [F (3, 16) = 1.881, p= 0.174)] (**Figures 6 and 7**).

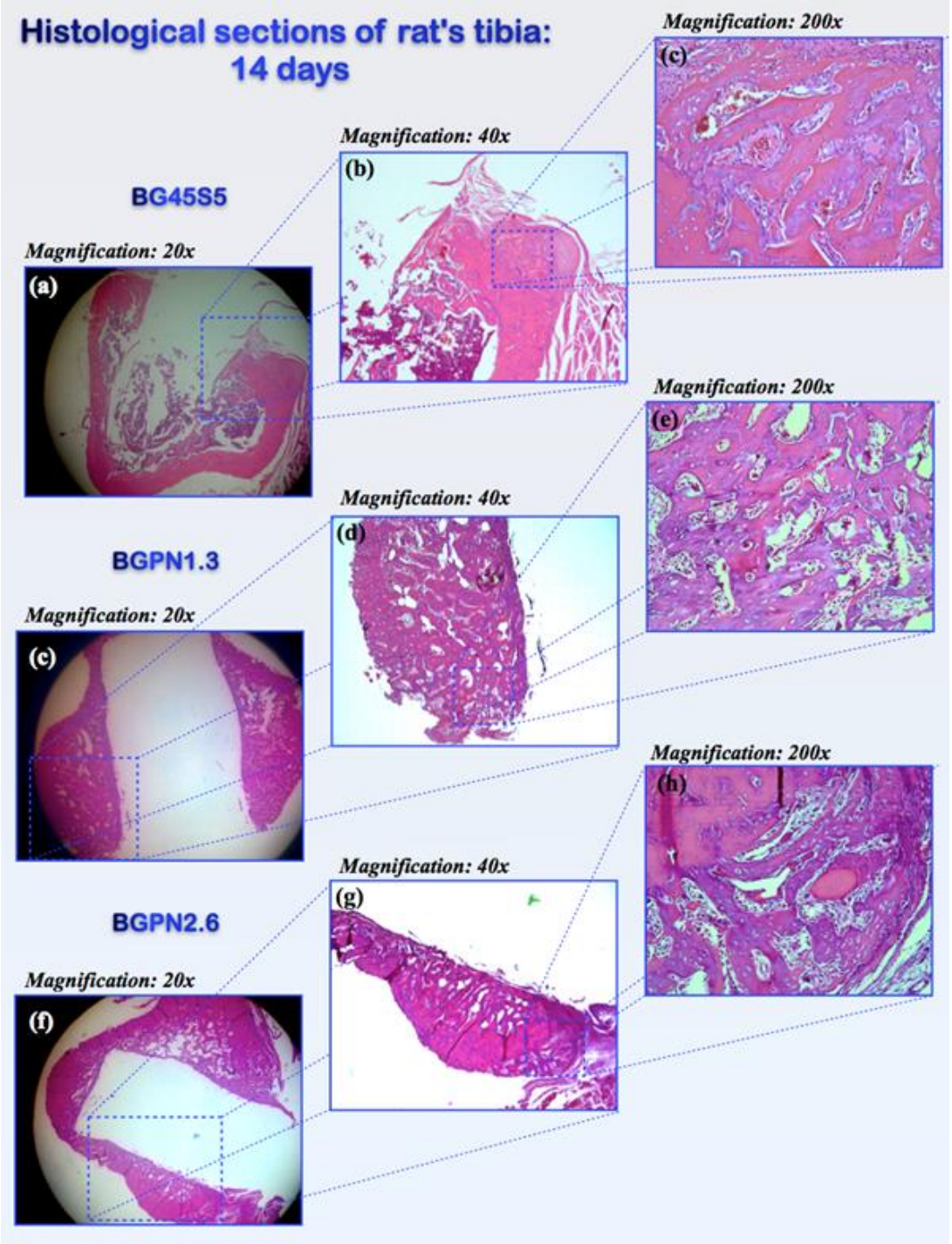

Figure 6. Micrographs of transversal histological sections of rat tibia tissues stained with Haematoxylin & Eosin after 14 days of implantation with different glass compositions. All groups showed similar amount of subperiosteal bone formation [F(3.16) =1.881, p= 0.174, ω= 0.34].

However, after 28 days, BGPN1.3 induced a significant effect on bone formation [F (3, 16) = 6.375, p= 0.005]. The tibia bones in which BGPN1.3 was implanted showed greater subperiostal bone area (51513.88 ± 2050.08 μ^2) than the control (BG45S5) (46537.19 ± 2050.08 μ^2) (**Figures 7 and 8**).

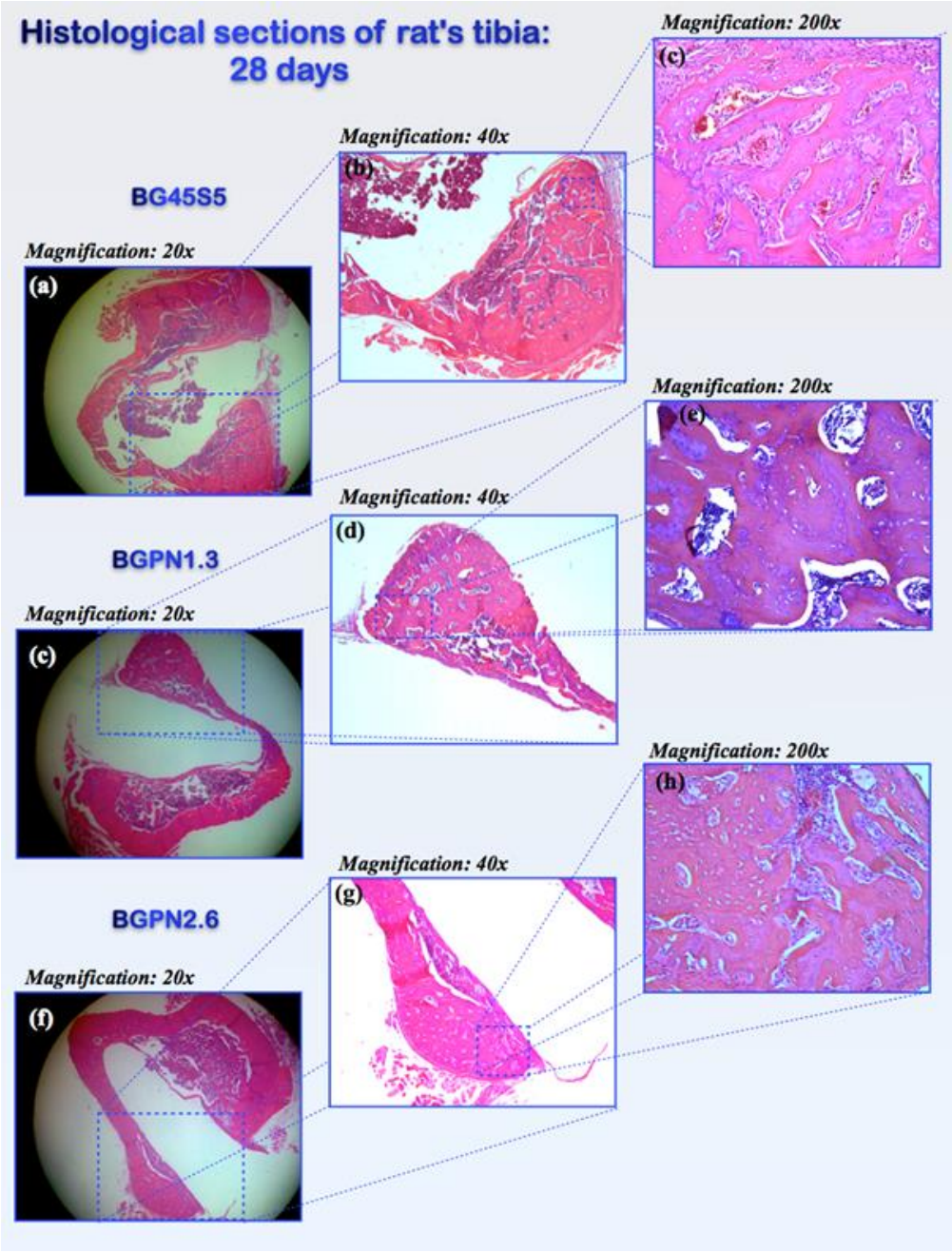

Figure 7. Micrographs of transversal histological sections of rat tibia tissues stained with Haematoxylin & Eosin after 28 days of implantation of different glass compositions. The groups differed regarding newly-formed bone area [F(3.16) = 6.375, p=0.005, ω= 0.67]. The group BGPN1.3 showed greater bone area (51513,88 ± 1265,13 μm2) than BG45S5 (46537.19 ± 2050.08 μm2) (p = 0.011) and BGSN1(40614.49 ±

3360.57 µm2) (p = 0.004) as can be seen on the micrographs in the right column (200× magnification).

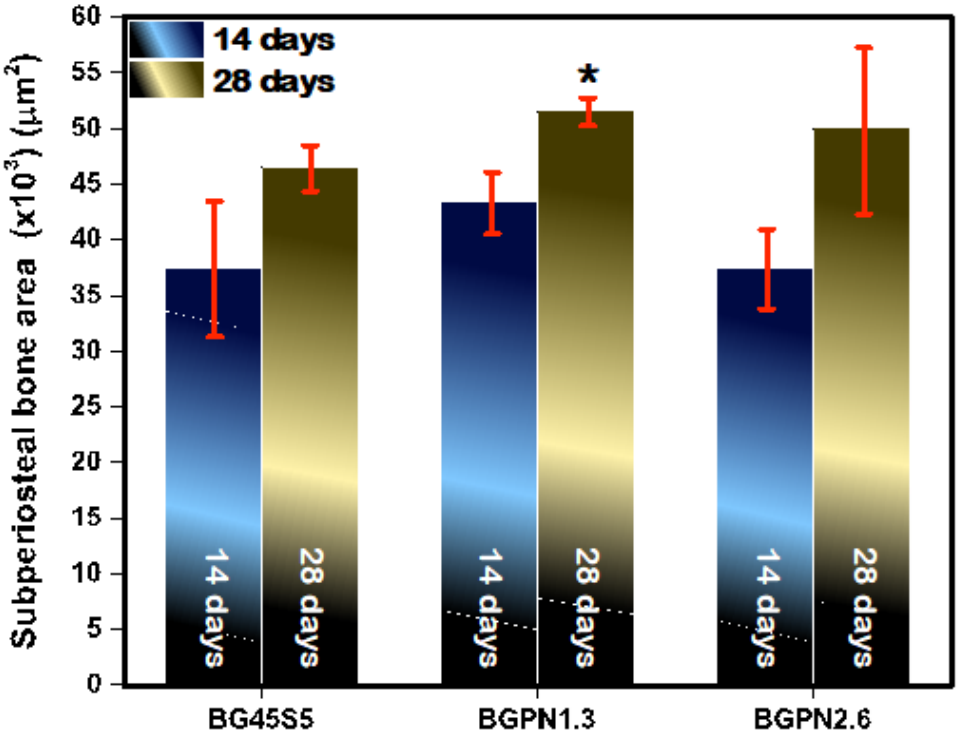

Figure 8. Quantitative analysis of the area of newly-formed subperiosteal bone in rats treated with the different bioactive glass. After 28 days the group treated with BGPN1.3 showed significantly greater bone formation than the control group (treated with BG45S5). All data are displayed as mean and SEM. For all comparisons $p < 0.005$ was considered.

Moreover, the presence of niobium did not alter the osteoconductivity of the glass, stimulating the formation of a bone layer over its surface, displaying thicknesses similar to the control group [$F(3,16) = 0.423$, $p = 0.739$] (**Figure 9**).

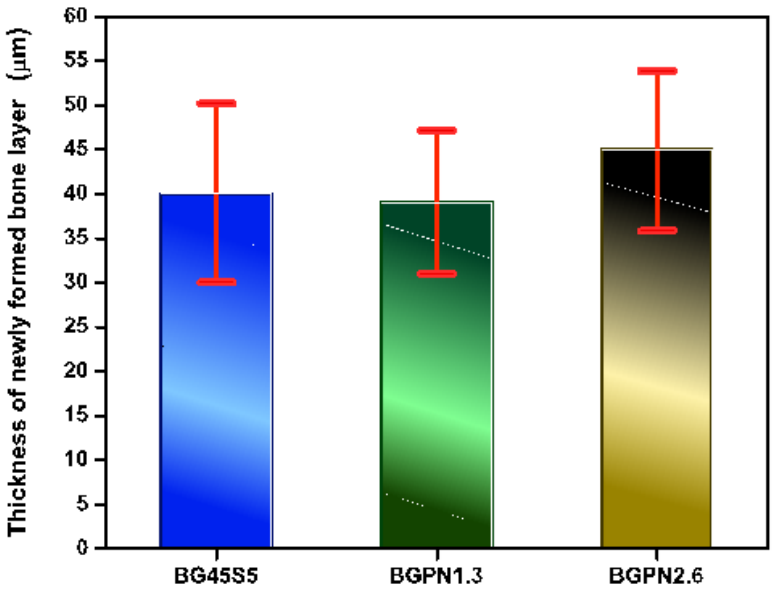

Figure 9. Quantitative analysis of the area of newly-formed subperiosteal bone in rats treated with the different bioactive glass. After 28 days the group treated with BGPN1.3 showed significantly greater bone formation than the control group (treated with BG45S5). All data are displayed as mean and SEM. For all comparisons $p < 0.005$ was considered.

We believe the greater bone formation stimulated by Nb-containing glass was caused by the release of Nb species that could have acted in two ways: (a) directly acting over cells by the mechanism explained by the mechanism explained previously in the in vitro section of this work and (b) by acting as nucleation agent, forming microscopic needle-shaped crystals on the surface of the glass[54]. This confers a microscopic complexity to the glass surface, which is thought to be critical for *in vivo* contact osteogenesis to occur[26]. It is stated that a micro or nanoscopic complexity allows greater protein, mainly fibrin, adsorption, and that platelets aggregate on this fibrin net and secrete cytokines that recruit osteogenic cells to the implant site[55]. These cells differentiate in osteoblasts and produce a collagen-rich matrix which is further calcified, and newly formed bone is strongly anchored to the surface of the material with an interfacial bond strength equal to or greater than the natural bone[9]. This mechanism explains the osteoconductivity displayed by all glass evaluated in the present study.

We believe that the greater subperiosteal bone formation of the different Nb glass formulations was caused by a direct effect of the leached ionic products (Si, Ca, Na, and P) on the periosteal osteogenic cells, possibly throughout the mechanisms previously discussed in the section "Osteogenic potential of Nb-containing bioglass" of this paper. In short, the leached ionic products may ultimately have caused the upregulation of the expression of important genes for cellular differentiation and maturation. For example, extracellular calcium ions are known to increase the upregulation of IGF-II, one of the main growth factors for bone formation[52,53].

CONCLUSION

To summarise, our results showed that the addition of Nb_2O_5, replacing P_2O_5, within glass networks increased bioactivity of the glass. All glass compositions derived from Bioglass® tested in the present study exhibited similar release profile for Si, Na and Ca species compared to BG45S5, in addition to the release of niobium species by the compositions of Nb-containing glass. The release of niobium species may have been responsible for the observed enhanced osteogenic and osteostimulative properties.

Solid state ^{31}P MAS NMR proved to be a very sensitive technique to elucidate the *in vitro* chemical reactivity and bioactivity of niobium bioactive glass. ^{31}P MAS NMR showed that glass containing lower quantities of Nb_2O_5 (BGPN1.3) exhibited enhanced early glass apatite formation, whereas for glass compositions containing higher amount of Nb_2O_5 (BGPN2.6) the opposite effect was observed.

Nb-substituted silicate glass is not toxic to hESCs and does not cause any problems for liver and kidneys of rats, proving their biocompatibility. The results suggested that hESCs differentiated toward osteoblast lineage after treatment with the dissolution products of Nb-containing glass, revealing the osteogenic capacity of niobium. *In vivo* experiments showed that after 28 days, Nb-containing bioglass induced a significant effect on bone formation. Based upon these results, we suggest Nb-substituted silicate glass may be an interesting alternative for biomedical applications.

MATERIALS AND METHODS

Preparation of Bioglass Samples. Details on the preparation of bioglass samples can be found in our previous publications[11,31,33,34]. High purity SiO_2, Na_2CO_3, $CaCO_3$, P_2O_5 powders (>99.9%), were weighed to obtain the glass compositions depicted in **Table 1**. All precursor reagents were purchased from Sigma-Aldrich (St. Louis, MO, USA), except for niobium oxide (Nb_2O_5, optical grade, >99.5%), which was donated by the CBMM (*Companhia Brasileira de Metaluria e Mineração, Araxá, Minas Gerais, Brazil*). Thirty-gram batches were melted in a platinum crucible at 1400 °C in air for 3 hours using a furnace (Lindberg/Blue M 1700 °C, Thermo Electron Corporation, Asheville, NC, USA). At the end of the refining process, the melts were quenched directly into cold water (frit cast), collected in a sieve, and dried to constant weight at 120 °C overnight. The different types of glass were then ground using an agate mortar and pestle, and sieved to separate fine (< 38 μm) and coarse (> 53 μm) particles. All experiments described in this work were carried out using glass particles size between 38-53 μm, excepting the *in vivo* studies for which cylindrical rods with 4 mm length x 2 mm diameter were used. These samples were prepared by casting method in a graphite mould (**Figure SI2**). Glass rods were annealed at 50 °C below the glass transition temperature (T_g) for 12 h and slowly cooled to room temperature to release the thermal stress associated with the quenching process.

Ion Leaching Experiments by ICP-OES. The ionic leaching patterns of the bioactive glass were determined by inductively coupled plasma optical emission spectrometry (ICP-OES). In this experiment, 300 mg of bioglass particles were dispersed in a beaker with 200 mL of buffer solution and maintained under continuous stirring (stirring rate of 75 rpm), at room temperature. The solution was buffered at pH 7.40 by using 50.69 mM HEPES (2-(4-(2-hydroxyethyl)piperazin-1-yl)ethanesulfonic acid) and 1 mM NaOH, both purchased from Sigma-Aldrich (St. Louis, MO, USA). Prior to the addition of the glass particles, 50.69 mM HEPES solution was passed through a 0.22 μm Millipore® filter to remove eventual aggregates or contaminants. During the leaching experiment, the beaker was kept sealed with parafilm in order to avoid any loss of liquid by evaporation, preventing changes in the ratio of glass/HEPES in the solution. After 3, 6, 12, 24 and 48 hours, 10 mL of solution was removed with a

syringe. Since the powder suspension was well dispersed and homogenous, the sample removal did not alter the solution concentration. For this reason, the solution was not refilled after collecting samples, resulting in a final volume of the solution of 150 mL. After each removal, the solution was immediately filtered with 0,22 μm Millipore® filters and analysed with an ICP-OES spectrometer (Optima 8300 ICP-OES, PerkinElmer, Inc., Shelton, CT, USA). The calibration curves were obtained from standard solutions containing Ca, Na, P, Si, and Nb. In order to ensure the accuracy of the calibration curve, the standard sample concentrations were measured periodically. Three replicates were measured for each element. The results obtained for the same element from different emission lines were averaged. Each point of the graphs shown is the result of the average of three dissolution experiments. Elemental concentration was reported in ppm.

Formation Rate of Calcium Phosphate Layer determined by ^{31}P MAS NMR Spectroscopy. The rate of formation of the calcium phosphate layer on bioglass surfaces was monitored by ^{31}P MAS NMR. Samples were prepared by adding 50 mg of bioactive glass particles to 5 mL of simulated body fluid (SBF)[*56*] (**see supplementary information – Table SI1**), and stirring in a thermostatic bath at 37 °C. After 3, 12, 24 and 48 hours the solution was filtered and the remaining powder was immediately dried between two filter papers. Soon after the drying procedure the material was packaged in the rotor and analysed by ^{31}P MAS NMR.

^{31}P MAS NMR study was carried out using an FT-NMR (AVANCE II+ 400, 9.04T, Bruker, Rheinstetten/Karlsruhe, Germany) at the resonance frequency 161.98 MHz, using standard Bruker double-resonance magic-angle sample spinning (MAS) probes. The glass particles were packed into a 4-mm cylindrical zirconia rotor and spun at the MAS frequency at the magic angle to remove any anisotropy effects. The samples were spun at 10 kHz at the ambient probe temperature. The ^{31}P MAS spectra were obtained using a high-power decoupling (HPDEC) pulse sequence with 2.50 μs pulses, 82 ms acquisitions, 5 s recycle delays, a 100 kHz spectral width, and 1024 scans. The ^{31}P chemical shifts were referenced to 85% H_3PO_4. The spectra were processed with TopSpin 2.1.6 software using Fourier transforms and an exponential filter of 50 Hz. The phase was manually adjusted, and the baseline was obtained using a five-order polynomial function.

Culture of Human Embryonic Stem Cells (hESCs). Human Embryonic Stem Cells (hES cells) CCTL12 were cultured in complete human embryonic stem cell medium (cHES) composed of Dulbecco's Modified Eagle Medium Nutrient Mixture F-12 (DMEM/F-12) supplemented with 2 mM of L-glutamine (Gibco®, Thermo Fisher Scientific Inc.) and 10 ng/mL of fibroblast growth factor 2 (FGF2, PepTech Corporation, Bedford, MA, USA). Before being used with hES cells, cHES was conditioned by incubation for 24 h with confluent cultures of mouse embryonic fibroblasts.

For all cell experiments the hES cells were cultured in flasks previously coated with BD Matrigel™ and using one of the following four culture media: (a) cHES; (b) Osteogenic Medium (OS), composed by cHES supplemented with 3mM β-glycerolphosphate, 0.1 mM ascorbic acid and 10^{-8} M dexamethasone (Sigma-Aldrich, St. Louis, MO, USA); (c) BG45S5 medium, in which BG45S5 powder was mixed with cHES medium at 10 mg/mL; and (d) BGPN1.3 medium, in which Nb-substituted bioglass was mixed with cHES at a concentration of 10 mg/mL. All glass-conditioned media were sterilized using a 0.22 μm pore filter (which also removed the powder particles) prior treating the cells. Cells were incubated at 37 ºC in a humid 5% CO_2 atmosphere.

Cell Viability – Resazurin Assay. Cell viability was determined by means of resazurin assay (Sigma-Aldrich, St. Louis, MO, USA). The culture medium was supplemented with 5 μM of resazurin and the cells were incubated at 37 °C and 5% CO_2 for 4-6 hours. The total metabolic activity was measured by scanning the cell plate at a plate reader (Synergy HT, BioTek® Instruments, Inc, Winooski, VT, USA) on the fluorometry mode with excitation filters centred at wavelengths of 540 nm and 590 nm.

Matrix Mineralization. The Alizarin red stains intracellular calcium deposits and calcium bound to proteins and proteoglycans[57]. This dye was used to analyse the deposition of mineralized matrix by osteoblasts, which is a marker of cell maturation. The test was conducted after 21 days of cell culture (the time required for observing matrix mineralization) within the four different experimental media. For the test, the cell monolayers were fixed with 70% ethanol for 1 hour at 4 °C and incubated in 1% Alizarin Red (Sigma-Aldrich, St. Louis, MO, USA) for 10 minutes. After this period five washes in distilled water were carried out and microphotographs at 100×

magnification were taken from each well. Each treatment was applied to five wells per plate and the whole assay was performed in duplicate.

In Vivo Assessment. In order to test the biological response incited by the bioactive glass, glass rods were implanted into rat tibia. For this, Brazilian College of Animal Experimentation (BCAE) guidelines were followed, and experiments were approved by Ethics Committee in Animal Use – ECAU/Unicamp (Protocol nº 2777-1). Rods composed of different types of glass (BGPN1.3, BGPN2.6, and BG45S5) were implanted into a round defect created in the tibia of rats that had been anesthetized with a mixture of ketamine (ANASEDAN®) at 80 mg/kg and xylazine (DOPALEN®) at 10mg/kg. Five rats were used per group. After pulling aside the periosteum a round transcortical defect was created using a spherical threfine bur (JET®) with a diameter of 2 mm. The glass rod (4 mm length × 2 mm diameter) was carefully introduced into the defect until total coupling, then the periosteum and the skin were sutured. After 14 or 28 days, the animals were euthanized, and the tibia was obtained from the animals and fixed for 24 h at 4 ºC in 10% zinc-buffered formalin (Sigma-Aldrich®). After fixation, they were decalcified in 5% EDTA (Synth Labsynth, Diadema, SP, Brazil), the glass rod was then carefully removed and the bones were paraffin-embedded and sectioned.

Systemic Toxicity. To assess the systemic toxicity of the glass implants we calculated the relative weights of rats' liver and kidneys. For this, immediately after euthanasia (14 or 28 days after implantation), liver and kidneys were dissected from the five rats of each group and weighed with a high precision scale (Unibloc®). The organ relative weights were calculated as the ratio between organ weight and body weight.

Morphometry. All histological sections were stained with haematoxylin and eosin dyes. A light microscope (80i) with a camera (DS-Ri1) and software (NIS-Elements software Advanced Research 3.0), all made by Nikon Corporation, Tokyo, Japan, were used to quantify the following parameters:

Area of newly-formed subperiostal bone. The area of the newly-formed subperiostal bone was measured at one field of each side of the cortical defect, directly underneath the periosteum and adjacent to where the glass rod was previously located, at 400× magnification. Five non-consecutive histological sections were analysed per animal. Five rats were used per group (n=5 per group). Thus, the mean and standard error of the mean were registered and further compared (**Figure SI3)**.

Thickness of newly-formed bone layer. Along the bone layer that formed around the implant we performed 20 measurements of thickness. All measurements were performed at 400× magnification. Five rats were used per group (n=5 per group). The mean and standard error of the mean were registered and further compared (**Figure SI4**).

Statistical Analysis. We used One-way ANOVA followed by Student Newman-Keuls test to compare the organ relative weights. Comparisons between means of subperiostal newly-formed bone and thickness of the bone layer formed around the implant were made using ANOVA one-way test with Tukey (homogeneous variances) or Games-Howell (non-homogeneous variances) post-hoc. For comparisons between the amounts of trabecular bone formed at 14 post-operative days, a Kruskal-Wallis test was used due to the non-normality of the data, matching the control group with each of the other groups through Mann-Whitney tests post hoc. For all tests $\alpha = 0.05$ was assumed. All data are presented as means and standard errors.

Acknowledgments

The authors acknowledge the use of the analytical instrumentation facility at Institute of Chemistry - University of Campinas, which is supported by the State of Paulo. This work was carried out with the financial support of the São Paulo Research Foundation – FAPESP (Grant: 2010/12376-5, 2010/00863-0, 2011/09240-9 and 2011/17877-7) and The National Council for Scientific and Technological Development (CNPq/PIBITI).

Author Contributions

J. H. L and L. P. L. S. contributed to the design and implementation of the research, to the analysis of the results and to the writing of the manuscript. J. H. L. manufactured the samples, performed the spectroscopic observations and analysed the results. L. P. L. S designed and performed the *in vitro* and *in vivo* experiments. D.E. assisted with ion leaching experiments. C. A. B., I. O. M., J. A. C. and R. M. contributed to the final version of the manuscript. C. A. B. and J. A. C supervised the project.

Additional Information

Competing financial interests: The authors declare no competing interests as defined by Nature Research, or other interests that might be perceived to influence the results and/or discussion reported in this paper.

Supplementary Information – SI

SI1. Glass rods preparation

Figure SI1. Devices used for the preparation of glass rods for in vivo tests: Graphite mould and suction system to force filling of the glass in the graphite mould. The vacuum pump was used to suction the molten glass, overcoming the high surface tension of the melt and allowing it to fill the 2 mm diameter graphite mould.

SI2. Preparation of SBF solution

The acellular simulated body fluid (SBF) solution was prepared with concentrations of ions equal to those of blood plasma, including Cl^- and HCO_3^- .The pH value of 7.40 was obtained using the Hepes buffer at concentration 50.69 mmol/L. Details about the concentrations of the ions present in the SBF solution is presented in **Table SI.**

Table SI1. Nominal ion concentrations of the SBF in comparison with those of human blood plasma.

Ions	**Concentration/mM**	
	Blood Plasma	**SBF**
Na^+	142.0	142.0
K^+	5.0	5.0
Mg^{2+}	1.5	1.5
Ca^{2+}	2.5	2.5
Cl^-	103.0	103.0
HCO_3^{2-}	27.0	27.0
HPO_4^{2-}	1.0	1.0
SO_4^{2-}	0.5	0.5

SI3. Ion release in 50.69 mM HEPES solution at pH 7.40 for BG45S5 and Nb-substituted bioactive glass

Figure SI3 shows a linear function with the square root of time up to about 120 min for all compositions.

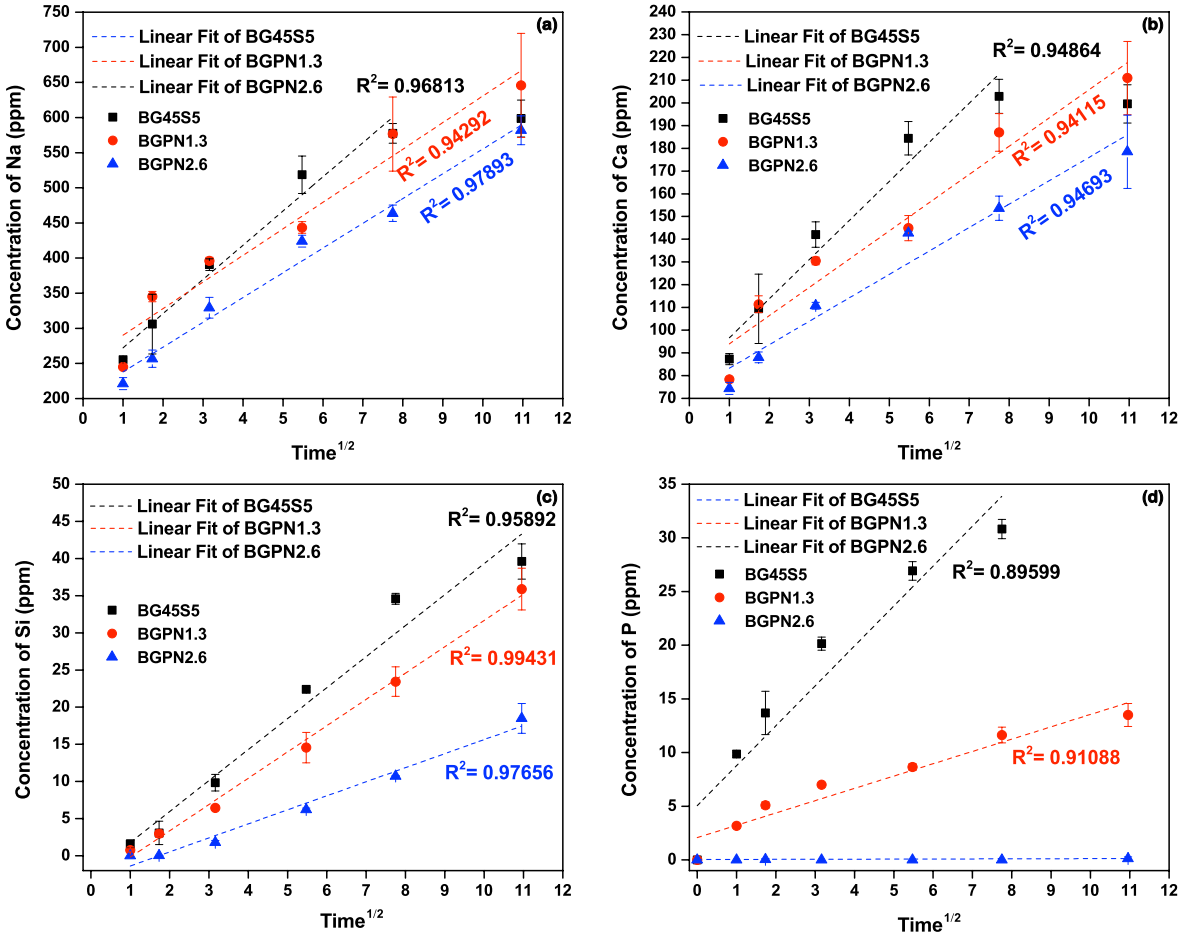

Figure SI3. ICP data: ion release as a function of square root of time in 50.69 mM HEPES solution at pH 7.40 for BG45S5 and Nb-substituted bioactive glass. The data displayed in (a), (b), (c), and (d) are related to leached of Na, Ca, Si, and P species, respectively, from glass derived from substitution of P2O5 by Nb2O5. Lines are linear regression of dissolution data up to 120 min.

The elemental concentrations of sodium, calcium, silicon, and phosphorus exhibited a linear function of the square root of time up to about 120 min for all compositions, which indicates a two-step degradation mechanism with initial dissolution controlled by diffusion (exhibits a $t^{1/2}$ dependence).

SI4. **Morphometry**

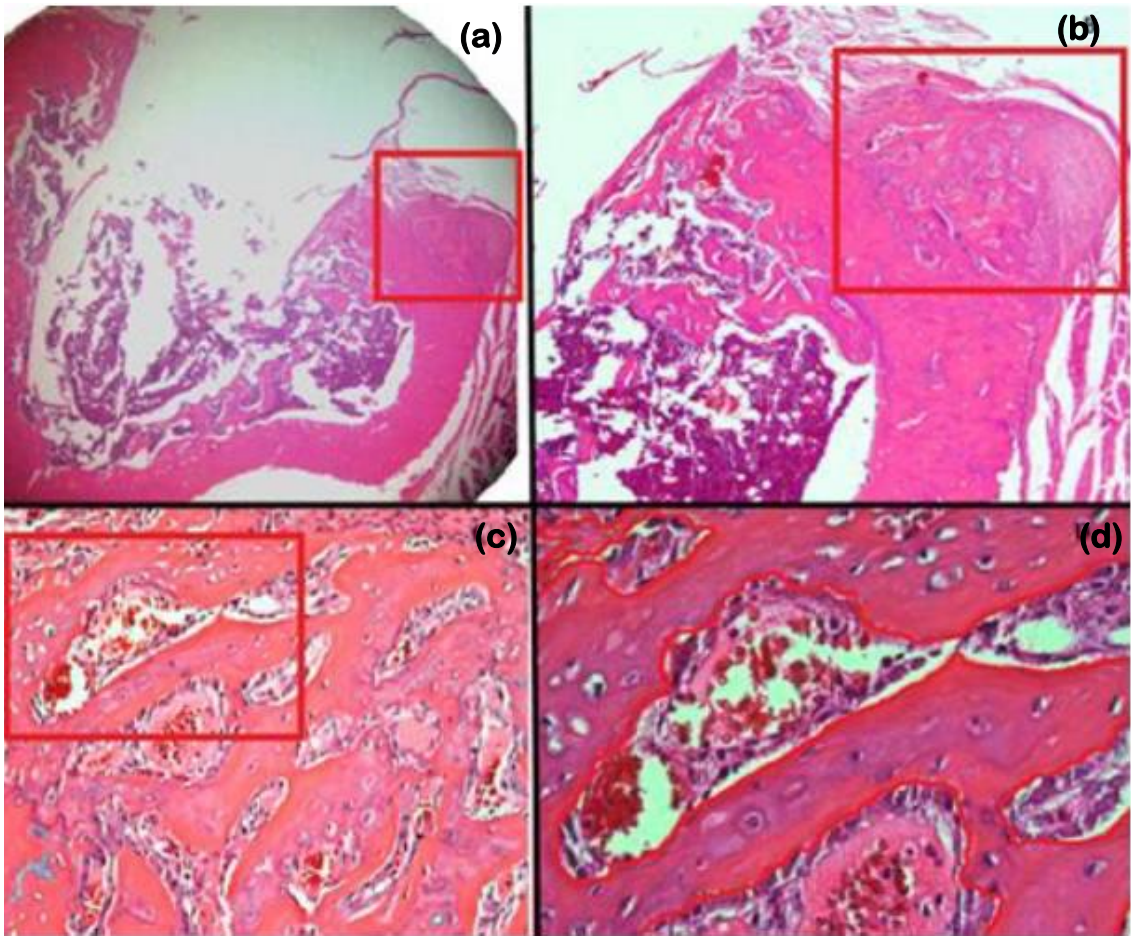

Figure SI4.1. Micrographs showing H&E stained histological sections of rat tibia tissues at 40×, 100×, 200×, and 400× magnifications and quantification of the area of newly-formed subperiostal bone. The area of the newly-formed subperiostal bone was measured in one field of each side of the cortical defect, directly underneath the periosteum and adjacent to where the glass rod was previously located at 400× magnification. Five non-consecutive histological sections were analysed per animal. Five rats were used per group (n = 5 per group). Thus, the mean and the standard error of the mean were recorded and further compared

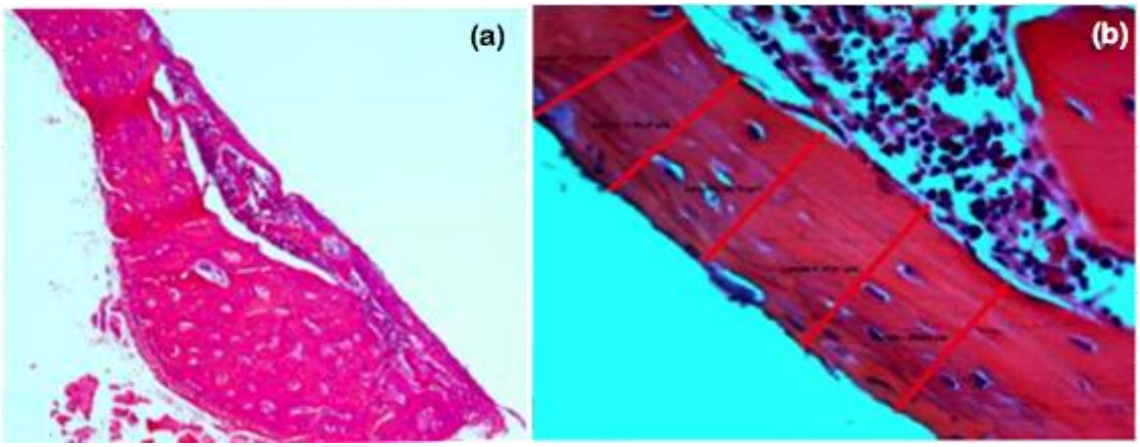

Figure SI4.2. Micrographs showing H&E stained histological sections of rat tibia at 40×, 100×, 200×, and 400× magnifications. Measurement of the thickness of newly-formed bone layer that formed around the implant was repeated 20 times, and all measurements were performed at 400× magnification. Five rats were used per group (n = 5 per group). The mean and the standard error of the mean were recorded and further compared.

ARTICLE 2: Osteogenic capacity of novel melt-derived Nb-substituted 45S5 bioglass: in vitro and in vivo studies

**The following manuscript layout follows the guidelines of the journal "Advanced Functional Materials".*

DOI: 10.1002/ ((please add manuscript number))

Article type: Full Paper

Osteogenic capacity of novel melt-derived Nb-substituted 45S5 bioglass: in vitro and in vivo studies

‡*João H. Lopes*, ‡*Lucas P. L. De Souza**, *Juliana A. Domingues, Filipe V. Ferreira, Moema de Alencar Hausen, Davi Encarnação, José A. Camilli, Richard A. Martin, Eliana Aparecida de Rezende Duek, Italo O. Mazali, Celso A. Bertran.*

Dr. J. H. Lopes, Dr. C. A. Bertran, D. Encarnação

Department of Physical Chemistry, Institute of Chemistry, University of Campinas – UNICAMP, P.O. Box 6154, 13083-970, Campinas, SP, Brazil.

Dr L. P. L. De Souza, Prof. J. A. Domingues, Prof. J. A. Camilli

Department of Structural and Functional Biology, Institute of Biology, University of Campinas – UNICAMP, 13083-862, Campinas, SP, Brazil.

E-mail: (lpls2002@hotmail.com)

Dr. F. V. Ferreira

School of Chemical Engineering, University of Campinas - UNICAMP, 13083-970, Campinas, SP, Brazil.

Dr. M. A. Hausen, Dr. E. A. R Duek

Department of Physiological Sciences, Biomaterials Laboratory, Pontifical Catholic University of São Paulo - PUC- SP, 18030-070, Sorocaba, SP, Brazil

Dr R. A. Martin

School of Engineering & Applied Sciences, Aston Institute for Materials Research, Aston University, B47ET Birmingham, United Kingdom.

Dr. I. O. Mazali

Department of Inorganic Chemistry, Institute of Chemistry, University of Campinas – UNICAMP, P.O. Box 6154, 13083-970, Campinas, SP, Brazil.

[‡] *These authors contributed equally.*

Keywords: bioactive glass, bioglass, niobium, osteogenic, bone

Abstract

This paper reports and discusses the results of a systematic evaluation of the bioactive properties of Nb-substituted silicate glass derived from Bioglass® 45S5. Substituting low concentration of Nb_2O_5 caused minimal variation in the dissolution compared to 45S5 apart from the presence of Nb ions. An amorphous calcium phosphate / apatite layer was seen to form on 45S5 BG and the 1% doped Nb glass within 3 hours, whilst 2.5 % Nb glass took 12 hours. Cytocompatibility of Nb-doped glass and bone marrow-derived mesenchymal stem cells (BMMSCs) revealed that Nb-substituted glass is not toxic to BMMSCs. In addition, replacing 1 mol% of SiO_2 with 1 mol% of Nb_2O_5 significantly enhanced cell proliferation after four days of treatment. The compositions BGSN1 and BGSN2.5 stimulated osteogenic differentiation of BM-derived MSCs after 21 days of treatment. For the *in vivo* experiments, trial glass rods were implanted into circular defects in rat tibia in order to evaluate their osteoconductivity and osteostimulation. Two morphometric parameters were analyzed: (i) thickness of new-formed bone layer and (ii) area of new-formed subperiostal bone. Results showed that Nb-doped glass is osteoconductive and osteostimulative. Therefore, these results indicate that Nb-substituted glass is suitable for biomedical applications.

1. Introduction

Musculoskeletal disorders are the most widespread human health issue with bone fractures standing among the most debilitating ones.[1] Recent investigations showed that men and women aged 50-64 account for nearly 30% of most types of fractures. Furthermore, most tibia fractures occur in working-age individuals. Therefore, fractures not only compromise the quality of life of people but also represent an economic burden due to the medical costs associated with fracture repair, the related lost work productivity and disability to the working age population.[1, 2]

The progressive increase in the number of fractures has prompted the development of synthetic materials for bone replacement. Currently, the most widespread treatments for bone replacement include autologous bone, allografts, xenografts, and various types of biomaterials.[3] Autologous bone is considered a gold standard for the treatment of large fractures but presents some drawbacks, such as donor site morbidity, limited availability, and some degree of resorption. Both allografts and xenografts possess potential risk of disease transmission, unpredictable resorption rate, and graft rejection. To overcome these challenges, synthetic materials have been developed, and bioactive glass-ceramics are therefore of great importance.[3-6]

The history of biomaterials designed to treat bone disorders can be easily distinguished in three different generations. The first generation of biomaterials was designed with the only requirement of achieving similar physical properties of those from the replaced tissue whilst being biocompatible (e.g. metallic implants).[7-10] The second generation of biomaterials was defined by their ability to interact with biological environment to enhance tissue bonding as well as progressively degrade while the new tissue regenerates and heals (e.g. hydroxyapatite).[8] Today, we are in the era of third generation of biomaterials, which have the additional ability to stimulate specific cellular responses at the molecular level (e.g. Bioglass® 45S5).[8-10]

The first biomaterial of the third generation was the Bioglass® 45S5.[7] This biomaterial is a glass that is biocompatible and also forms bonds with hard and soft tissues, which ultimately optimizes the stability and lifespan of implants. Many investigations describe several biological properties of Bioglass® 45S5, such as angiogenesis, osteostimulation, osteoconduction, and osteoinduction, which are essential for a biomaterial for bone replacement.[8] These effects on living tissues are

determined by the chemical composition of the glass. Hence, several researchers have been designing variations of the original Bioglass® 45S5 in order to improve its mechanical and biological performance.[4, 6, 8, 9, 11-14]

Recent investigations reported the ability of niobium to optimize mechanical and biological performance of synthetic implants.[1, 3, 9, 11, 12, 14, 15] Niobium first appeared in biomaterials as a component of metallic alloys.[16] The introduction of Nb in alloys substituting vanadium, for instance, was shown to enhance biocompatibility.[17] In one study Nb-2Zr was reported to exhibit excellent corrosion resistance, fatigue strength, and crack propagation in simulated body fluids.[17, 18] It is noteworthy that Nb_2O_5 is an effective nucleating agent and generally leads to the development of glass-ceramic in silica-poor compositions, such as Bioglass® 45S5.[7]

In one of our previous studies, we replaced the network former P_2O_5 with Nb_2O_5 and undertook a detailed structural characterization using ^{29}Si, ^{31}P, and ^{23}Na solid-state MAS NMR and Raman spectroscopy, we concluded that Nb_2O_5 participates in the silicate network by breaking the Si-O-Si bonds to form structures, such as -Si-O-Nb-O-Si- chains.[14, 19, 20] These alterations modified the glass dissolution rate and magnitude, which we believe increases the lixiviation of ions with biological importance such as Si, Ca, Na, and Nb.[20] Some recent investigations incorporated niobium into the structure of fluorapatites and phosphate-inverted glass and tested their cytocompatibility, osteostimulation and osteoinduction.[11, 12] They observed that the presence of niobium resulted in greater biocompatibility and enhanced bioactive properties.[3, 11, 12] Furthermore, osteogenic differentiation of human Mesenchymal Stem Cells (hMSCs) was achieved after 21 days of culture on Nb-doped fluorapatite glass-ceramics.[3] Nb doped glasses are also reported into increase vascularization [21]. Even though Nb-substituted silicate glass appears to possess interesting bioactive properties, its effect over pluripotent cells and bone regeneration has not been investigated so far.

The present study aimed to evaluate the cytocompatibility, osteostimulation, and osteoinduction of Nb-containing bioactive glass. For this purpose *in vitro* and *in vivo* experiments were carried out. In the *in vivo* assay, glass rods were implanted into circular defects in rat tibia and bone formation was quantified. The *in vitro* experiments consisted of treating bone-marrow-derived mesenchymal stem cells (BMMSCs) isolated from rats with the dissolution products from the glass and verifying their viability and

osteogenic differentiation. We also investigated the leaching profile of Si, Ca, Na, P, and Nb species from the bioglass using ICP as well as the kinetics of apatite formation using P NMR.

2. Results and Discussion

2.1 Glass preparation

A series of Nb doped bioactive glasses were successfully prepared using the melt quench technique. The glass compositions were based on Bioglass® 45S5 with 1, 2.5 and 5 mol % of the SiO_2 concentration replaced by Nb_2O_5 as shown in Table 1. (Bioglass® 45S5 was used as the control and all glasses had a fixed Na_2O:CaO:P_2O_5 ratios. Despite Nb being a known nucleating element the glasses there were no visible signs of crystallization.[14]

2.2 Dissolution studies.

Figure 1 illustrates the release of Na, Ca, Si and P from the glass and **Figure 2** shows the concentration of Nb ions as determined by inductively coupled plasma optical emission spectrometry (ICP-OES). The release of soluble ions from bioactive glasses is known to be the key first step in the bio-mineralization process as described by Clark and Hench.[7, 10, 22] The release of Ca and P creates a supersaturated solution which then precipitates into amorphous calcium phosphate which then crystallizes in apatite. Furthermore, the controlled release of Si, Ca, Na, P, and Nb species from the bioglass has been associated with the promotion of bioactivity, angiogenesis, osteostimulation, osteoconduction, and other important properties for bone regeneration.[2, 8-10] The 45S5 bioglass composition is also presented for the purpose of comparison

As shown there is a rapid release of ions following immersion in HERPES solution. From the release of Na and Ca ions (Figure 1 a, b) it appears at first glance as though the 45S5 bioglass is the most soluble and that the solubility decreases upon increasing concentrations of Nb. However it is important to note that the molar mass of Nb_2O_5 is ~ 4.4 times heavier than SiO_2. Therefore a 300 mg sample of BGSN5 will contain 15% less CaO, Na_2O and P_2O_5 compared to BG45S5. Taking this into consideration and given the errors the release of Ca and Na is similar for the glasses

with the exception of the BGSN5 which is clearly much less soluble. The Si concentrations shows a slight increase in solubility for the 1 and 2.5% Nb glasses despite it having a lower SiO_2 concentration.

The increase in Si solubility is attributed to the degree of matrix fragmentation caused by both the reduction of Si and more importantly the additional oxygen atoms provided by Nb_2O_5 compared to SiO_2. The higher the niobium content the more non-bridging oxygen atoms and the greater the number of Si-O-Nb bonds.[14, 19, 20]

The release profile of phosphorus suggests a maximum concentration (approximately the solubility limit), from which there is a dramatic reduction, presumably associated with the removal of some of the soluble phosphate species to form the calcium phosphate layer on the bioglass surface (**Figure 1d**). The results indicate that an amorphous calcium phosphate is rapidly deposited for BG45S5 and BGSN1, with delay and a reduction for BGSN2.5 whilst BGSN5 appears to insoluble to release sufficient P (or Ca) to begin to form ACP.

A characteristic common to all leaching curves for sodium, calcium, silicon, and phosphorus species in the earliest dipping times is the mechanism of the species lixiviation. The initial elemental concentrations up to about 120 min for all compositions are a linear function of the square root of time, which indicates a diffusion-controlled process (**Supplementary Information - Figure SI1 a-d**).

The profile shape of niobium species at early soaking times are similar to those observed for P, i.e., a sudden increase in the Nb concentration in the medium, reaching a maximum value, followed by a characteristic reduction of concentration value for each glass. This initial increasing is related to the leaching of niobium species near surface and/or release of isolated NbO_6 units, which are more labile since their release does not require extra energy to break bonds in comparison with the Nb-O-Nb groups.. The rate at which the niobium species are removed from the solution is gradual and can be mostly attributed to polymerization of the niobate species (Nb-O-Nb), which are continuously subtracted from the medium to form the niobium gel layer on the bioglass surface.[20] The Nb-OH groups are chemically stable (Brønsted and Lewis acid sites), as well as effective nucleation centers for the removal of the leached niobium species from the glass.[14] Consequently, the concentration of free niobium decreases as the niobium

gel layer is established on the surface of the bioglass, i.e., the limit solubility of niobium is reduced.

2.3 Apatite layer formation ability by ^{31}P MAS NMR spectroscopy

Amorphous calcium phoasphate / apatite formation on the bioglass surface in simulated body fluid (SBF) has been verified by ^{31}P MAS NMR (**Figure 3 (a-d)**). As shown the local structural arrangement of phosphorus changes rapidly even for early soaking times.[6, 20]

The ^{31}P MAS NMR spectra of unreacted BG45S5, BGSN1, BGSN2.5 and BGSN5 exhibit a single broad resonance around 11 ppm with peak maximum at 11.9, 11.8, 11.6 and 8.5 ppm, respectively. The ^{31}P resonances are attributed to the $_{P}Q^{0}$ isolated orthophosphate units (charge balanced byNa^{+} and Ca^{2+}.[20, 23] In addition, as the niobium content increases there is a tiny shift to lower frequencies followed by a more significant shift for the BGSN5 suggesting that Nb interacts with phosphorus, presumably forming P-O-Nb bonds. The data extracted from the ^{31}P MAS NMR spectra such as peak positions and full width half maximums (FWHM) for BG45S5 and Nb-substituted glass, unreacted and after 3, 12, and 24 hours of immersion in in simulated body fluid (SBF) are listed **Table 2**.

^{31}P MAS NMR data show a trend that describes the evolution in the chemical environment of the phosphorus during the chemical transformations at the bioglass/solution interface as a function of the soaking time in SBF. All ^{31}P resonances are characterized by notable shift to lower frequencies during the soaking time in SBF, reaching the frequency of approximately 4 ppm, which is similar to the signal observed in the spectrum of hydroxyapatite. Such spectral changes and the decrease in FWHM values describe the partial degradation of glass and precipitation of amorphous calcium phosphate and its progressive crystallization.[20] ^{31}P MAS NMR spectra for BG45S5 **(Figure 3a)** and BGSN1 **(Figure 3b)** suggest that 3 hours of incubation in SBF are enough to establish an ACP/ apatite layer. While for BGSN2.5 glass the time required is considerably longer, approximately 12 hours **(Figure 3c)**. Although subtle, the changes observed in the BGSN2.5 spectrum in the range of 13-24 hours are related mainly to the gradual increase in the crystallinity of calcium phosphate (increase of long-range order). In contrast, ^{31}P MAS NMR spectrum for the BGSN5 exhibit a progressive increase in the FWHM values of the resonance peak as a function of the soaking time in SBF

(Figure 3d). This is a result of some P remaining in the glass network at ~11ppm whilst some P starts to form an ACP/ apatite precipitated on the glass surface ~4ppm resulting in a much wider distribution of frequencies. For the BG45S5, BGSN1 and BGSN2.5 samples, almost all of the phosphorus present in the glass network is continuously leached into the solution, where it is precipitated in the form of calcium phosphate in the gel layer (silica- and/or niobosilica-gel) formed on the bioglass surface.

In summary, all vitreous compositions have been able to form the phosphate layer, but as the niobium content increases the chemical stability of the bioglass increases, and the dependence of an external source of phosphorus for apatite composition increases. In accordance with this assumption, ^{31}P MAS NMR spectra display resonance peaks with slight asymmetry on the left-hand side of the peak owing to the residual glass fraction.

2.4 Cytocompatibility assessment. The cytocompatibility is an essential feature that must be ensured in any type of biomaterial. Any sign of toxicity may represent a risk for the recipient organism and therefore must be avoided. In this work we evaluated the cytocompatibility of the dissolution products of different compositions of Nb-doped glass (BGSN1, BGSN2.5 and BGSN5) with Bioglass® 45S5 as the control with rat bone marrow mesenchymal stem cells (BM-MSCs) by MTT and Live/Dead assay. We treated cells with culture media conditioned with the dissolution products of the different glasses for up to four days. Cells treated with complete DMEM were used as positive controls meanwhile cells killed with dimethyl sulfoxide (DMSO) or 70% Methanol served as negative controls. None of the glass-conditioned media was cytotoxic to this cell type (**Figures 4a and 4b**). This result demonstrates that the incorporation of niobium dioxide into the structure of Bioglass® 45S5 does not compromise its cytocompatibility. As it can be seen on figure 4b the viability of cells treated with medium conditioned with the composition BGSN1 were considerably higher than the Bioglass® 45S5 glass and the positive control group (complete DMEM) which indicates that this glass enhances cell proliferation.

Several other studies have also shown that the addition of niobium into biomaterials do not result in cytotoxicity. These investigations include tests with different materials such as fluorapatite glass-ceramics,[3] phosphate glasses,[24] bioglass-niobium granules,[15] hydroxyapatite bioceramics,[25] and calcium silicate cements with

different cell lines.[26] In one of these assays human osteogenic cells (SAOS) were incubated with Nb-doped hydroxyapatite for 72 hours and cell viability was tested by means of a MTT assay. They observed no difference or even a statistically significant increase in cell proliferation when compared to the control group (reference material) which allowed them to conclude that Nb-doped hydroxyapatite has the ability to support cell proliferation.[25] Furthermore, a very recent investigation evaluated the cytocompatibility of calcium silicate-based cements combined with niobium oxide (Nb_2O_5) micro and nanoparticles, comparing the response in four different cell lines: (a) human dental pulp cells – hDPCs; (b) human dental follicle cells – hDFCs; (c) human osteoblast-like cells (SAOS-2); and (d) mouse periodontal ligament cells – mPDL. After 24 hours of incubation within media conditioned with the materials they measured cellular viability by means of MTT assay. The authors concluded that calcium silicate cements combined with Nb_2O_5 micro and nanoparticles presented cytocompatibility and can be used as an alternative radiopacifier agent for calcium silicate cements. Therefore, our results complement the existing literature demonstrating that Nb-doped bioactive glass is cytocompatible and also constitutes a safe biomaterial for biomedical applications.

2.5 Osteoinductive potential of Nb-containing bioglass. Over the past few years the role of engineered scaffolds complexed with mesenchymal stem cells (MSCs) for bone regeneration has been a main research topic in regenerative medicine.[27-29] The bone- marrow- derived mesenchymal stem cells (BM-MSCs) are multipotent cells that are able to self-renewal and to differentiate into several cell types depending on which chemical or mechanical stimulus they are subjected.[30] The bone formation that is required for integration of biomaterials relies on the presence of multipotent cells that are capable of differentiating into osteoblasts.[30] As BM-MSCs constitute one of the most abundant multipotent cell types present at the fracture site they play major roles in supporting faster bone formation along implants.

In some studies MSCs were complexed with different types of biomaterials such as calcium phosphate[24, 28] and biodegradable poly(lactide) (PLA) scaffolds.[27] The incorporation of human BM-MSCs in macroporous calcium phosphate cement (CPC) promoted great cell attachment, osteogenic differentiation and mineralization. When these BM-MSCs – containing scaffolds were used to treat cavarials defects in rats new bone and blood vessels were generated between 4 and 24 postoperative weeks. In

summary, the authors concluded that seeding stem cells with CPC increased new bone and new blood vessel density, compared to CPC without cells, suggesting this material can be used for craniofacial and orthopedic applications.[28] In other very recent investigation[27] human gingival mesenchymal stem cells (hGMSCs) were cultured with three-dimensional printed PLA scaffolds pre-treated with hGMSCs – derived - extra cellular vesicles (EVs) in order to test the *in vitro* osteogenic performance of this material by means of alizarin red staining, gene expression of RUNX2 and BMP-2 (RT-PCR), and the concentration of the proteins RUNX2, BMP-2, and β-Actin (Western Blot). The combination of hGMSCs + 3D-PLA + EVs promoted excellent osteogenic differentiation indicating that the combination of pluripotent cells and inorganic scaffolds enhances bone regeneration of calvarial defects.[27]

The formation of bone requires not only the recruitment and/or migration of potentially osteogenic cells but also their differentiation towards the osteoblastic lineage. We believe that scaffolds composed of Nb-doped glass may favor MSCs to differentiate into osteoblasts because some investigations have reported that the incorporation of niobium into other types of biomaterials such as fluorapatites and phosphate-inverted glass has incited osteogenic differentiation of hMSCs[2] and maturation of mouse osteoblast-like cells (MC3T3- E1 cell).[11] The study of Obata and his collaborators[11] is of particular importance for the scope of the present work because they tested the osteostimulative capacity of niobium ions over MC3T3-E1 cells. They reported that both ALP activity and calcium deposition of MC3T3-E1 cells was significantly higher in the medium containing niobium at a concentration of 10^{-7} M when compared with control or other Nb- containing media, even though none of the tested media contained osteogenic supplements. The authors proposed that this may indicate that the niobium ions not only enhance but also induce osteogenic differentiation.[11]

The osteoinduction capacity of Nb- doped bioactive glass may result in a higher number of osteoblasts within the implant and consequently at the fracture site. In order to test the capacity of different compositions of Nb-doped bioactive glass to stimulate the osteogenic differentiation of BM-MSCs we stained mineralized nodules at the extracellular matrix with Alizarin Red after 21 days of treatment with culture media conditioned with the dissolution products of different Nb-containing glasses. We also marked matrix-mineralization-related protein osteocalcin with and fluorescent antibody

and obtained micrographs using a Laser Scanning Confocal Microscope to demonstrate the presence of this protein which is also a marker of osteogenic differentiation.

The formation of mineralized nodules marks the final step of the process of osteogenic differentiation. In short, this process follows the subsequent stages: (i) proliferation of multipotent cells (as differentiation only progresses after this step we chose to wait BM-MSCs to form a monolayer before starting to treat them with the different cell media); (ii) formation of non-mineralized matrix mostly composed of type I collagen; and (iii) mineralization of the matrix forming calcium-rich nodules. Our results showed that the compositions BGSN1 and BGSN2.5 stimulated the formation of nodules comparable to the positive control group (MSCs treated with an osteogenic culture medium) (**Figure 5, six upper squares**) which is an ultimate sign of osteogenic differentiation. In addition, osteocalcin was present in the bone matrix corroborating with the previous result (**Figure 5, four lower squares**). These results support the claim that Nb-doped bioactive glass may be used to produce high-bioactive scaffolds for bone tissue engineering because it not only serves to support migration of BM-MSCs but also stimulates osteogenic differentiation of these cells, increasing the population of mature secretory osteoblasts in the fracture site which may hasten bone regeneration.

2.6 Bone formation stimulated by Nb-containing bioactive glasses. *In vivo* experiments were performed in order to analyze the properties of osteoconductivity and osteostimulation of Nb-containing glass. Osteoconductivity is often referred in the biomaterial literature as the capacity of a material to allow bone to grow onto its surface.[31] Despite this definition correctly describes the event it does not explain exactly how it happens. In fact, what makes a new bone form onto a material's surface in a particular direction is the migration of multipotent cells coming from the bone-marrow (bone marrow-derived MSCs), blood (blood- derived MSCs) or, in a minor extent, from surrounding tissues (e.g. myocytes from the muscles and pericytes from the blood vessels). Just the migratory activity of these cells over the surface responds for the expansion of a bone spicule.[32] As soon as a material is placed into a surgically made defect (as in our experiment) it rapidly undertakes a series of ion exchange with the body fluid that culminates with a drastic increase in the surface's roughness (**Figure 6**).

Rough surfaces are more easily coated with many proteins, lipids, ions, and sugars which will dictate which cell types will subsequently attach.[32] It is known that some characteristics of the material's surface, such as its topography, chemical composition, charge, and energy, directly influence protein adsorption and consequently cell adhesion and migration.[32] Hence, biomaterials designed for bone replacement must provide suitable surface for the adhesion and migration of osteogenic cells that will populate the surface, differentiate into osteoblasts and produce a mineralized matrix. As the composition BGSN1 showed better performance in the *in vitro* experiments and a significant increase in topographical complexity of its surface it was chosen for the *in vivo* investigation. We implanted glass rods made of BGSN1 into the tibia of rats and looked for the formation of a bone layer around the implant. The composition BG45S5 was used as a control. We observed the presence of a bone layer around both glass compositions and calculated their thickness in order to compare the groups (**Figure 7**).

In the present work we demonstrate *in vivo* osteoconductivity of Nb_2O_5-containing bioactive glass. Nevertheless, the ability of other type of niobium- containing materials to support bone growth onto their surfaces was demonstrated *in vivo* by Matsuno and his collaborators.[33] They introduced a wire of 99.9% niobium, 1.0 Ø x 7.0mm in size in rat femur bone marrow and evaluated bone formation around the implant after 14 and 28 days. They observed new bone formation onto niobium implant's surface after 28 days, confirming its osteocondutivity.[33] In another investigation cylindrical implant made of Ti-Nb alloy was implanted into medial tibia of beagles for 2, 4 and 12 weeks.[34] New bone formation was observed to grow in contact with the material's surface after 4 weeks. In the same study the authors reported that the incorporation of Nb to the metallic alloy increased its surface roughness (Ti-Nb: 1.79 ± 0.23 µm compared to pure Ti: 1.63 ± 0.17 µm) and reduced its contact angle (Ti-Nb: 81.75 ± 2.94º compared to pure Ti: 96.46 ± 3.56º) (more hydrophilic). It is generally accepted that osteogenic cells respond to microroughness (<25µm) and tend to adhere to more hydrophilic surfaces.[35]

As a matter of fact the surface characteristics determine which types of proteins will adsorb and as a consequence which cell types will be attracted to it.[32] Thus, it is believed that the incorporation of Nb into these materials provided them with a more suitable surface for adhesion and maturation of osteogenic cells. We believe that a similar mechanism was involved in the formation of the bone layer onto BG45S5 and

BGNS1 (**Figure 7**). We suggest that osteogenic cells coming from the bone marrow and the periosteum contributed to the observed bone formation. As the surface of the material was in direct contact with the periosteum at the outer surface of tibia cortical we believe that osteogenic cells started to migrate from the periosteum onto material's surface by haptotaxic migratory movement. This pattern of migration is described as a directional motility of cells towards cellular adhesion sites or surface-bound chemoattractans.[36] In addition, bone- marrow- derived MSCs also may have substantially contributed to bone formation attaching to the material's surface probably attracted by its favorable physical, chemical, and/or biological characteristics. The bone formation on the surface reveals that it presented ideal features that favored protein adsorption and consequently cell migration and adhesion followed by subsequent osteogenic differentiation. To confirm this scenario and fully understand the mechanisms underlying the formation of the observed bone layer more comprehensive studies should focus on the characteristics of Nb- containing bioactive glass such as surface topography and hydrophobicity.

It is worth mentioning that direct contact is not the only way by which materials can influence living cells. In fact, inorganic ions were shown to influence formation, regulation and maintenance of bone.[37] In our dissolution studies we showed that BGSN1 presents a pattern of ion release very similar to BG45S5 except for the Nb, obviously only found in the Nb- containing glass. The biological roles of BG45S5-derived ions are well described in the literature,[37, 38] whereas the role of Nb soluble ions over osteogenic cells started to be investigated only recently.[11] Ca ions were shown to affect osteoblasts *in vitro*. In low concentrations (2-4 mmol) Ca stimulates osteoblasts to proliferate whereas in medium concentrations it boosted cell differentiation and matrix mineralization. In high concentration (> 10 mmol) Ca ions were shown to be toxic to cells.[39] Soluble P was reported to promote expression of matrix 1a protein (MGP) which is an essential protein for bone formation.[39] It is well accepted that Si participates in the process of bone formation probably by inducing precipitation of hydroxyapatite in the early stages of matrix mineralization.[36, 37] The only study that investigated the effect of Nb ions on osteoblast- like cells (MC3T3-E1 cells) concluded that in a dose- dependent manner (3×10^{-7} M) these ions induce differentiation and mineralization of osteogenic cells rather than adhesion and proliferation.[11]

While the investigations of the effect of soluble ions over cells provide good insights regarding the probable mechanism by which bioactive materials perform its non- contact biological effects it is not without problems. It is important to take into account the fact that these ions will mostly be complexed in large molecules, thus, the observed effects of the glass- derived ions might actually be caused by the compounds of the elemental constituents of the glass rather than individual ions. Despite the specific ionic compounds formed after dissolving from the bioactive glasses not being well described they were shown to possess an overall effect over gene expression of osteoblasts.[40] Xinus *et al*.[40] prepared a bioactive glass conditioned medium containing 1% w/v of Bioglass® 45S5 in DMEM and filtered the medium to remove glass particulates (0.2 μm filter). Thus, they treated human osteoblasts with this medium for 24 hours and performed cDNA microarrays to analyze gene expression. Their results showed that bioglass dissolution products were able to up- regulate many genes related to osteoblast metabolism, cell proliferation, cell-cell and matrix-cell adhesion up to 5 fold.[40]

We believe that immediately after implantation glass rod started to exchange ions with the body fluid, releasing ionic products that acted over osteogenic cells located in the adjacent periosteum and bone marrow. The glass dissolution products may have stimulated periosteal osteogenic cells to differentiate into polarized secretory osteoblasts that began to produce new bone onto the preexistent bone promoting appositional bone growing forming a very clear cement line (arrows in **figure 8**).

This chain of events is believed to have happened for both glass compositions, as the two of them showed histological signs of subperiosteal bone formation. The comparison of subperiosteal bone area in the BGSN1 group and in the control group (BG45S5) showed significant larger bone area in the control group after 28 days of implantation [$F(3, 16) = 1.881$, $p = 0.174$)] (**Figure 8**) despite both glasses clearly stimulated periosteal cells to differentiate and produce new bone.

The present study have gathered sufficient information to claim that Nb-containing glasses are cytocompatible with BM- derived MSCs in addition to stimulate these cells to differentiate into osteoblast. Furthermore, we showed this material possess the bioactive properties of osteoconductivity and osteostimulation *in vivo*.

3. Conclusion

To summarize, our results showed that when incubated in buffered solution the glass composition BGSN1 released similar amounts of Ca, Na, P, and Si compared to BG45S5. However, BGSN1 also released Nb into the solution. The Nb-containing glasses BGSN1 and BGSN2.5 exhibited the ability to form an apatite layer onto their surfaces, which is a sign of bioactivity. In addition, the immersion of BGSN1 and BG45S5 into complete culture media for 24 h promotes significant increase in surface's roughness. Furthermore, Nb-doped glasses are non toxic to BM-derived MSCs, instead, BGSN1 stimulated greater cell proliferation after up to 4 days of treatment than the control group. The dissolution products of the glass compositions BGSN1 and BGNS2.5 are osteogenic as they differentiated BM-derived cells towards osteoblast lineage after 21 days of treatment. *In vivo* experiments showed that BGSN1 was osteoconductive enabling the formation of a bone layer onto its surface. In addition, BGSN1 stimulated the osteogenic cells of the periosteum to form bone (from a very clear cement line) which indicates good osteostimulative capacity for this glass composition even though it was lower than that stimulated by BG45S5. These results let us conclude that the addition of 1% of Nb_2O_5 substituting SiO_2 in Bioglass® 45S5 generates a cytocompatible material with great bioactive properties with significant potential for biomedical applications.

4. Experimental Section

Preparation of bioglass samples. The detailed process of preparation of bioglass samples is fully described in our previous publications.[14] High purity SiO_2, Na_2CO_3, $CaCO_3$, P_2O_5 powders (>99.9%) (Sigma-aldrich®) were weighed to obtain the glass compositions depicted in **Table 1.** The niobium oxide was donated by the CBMM (*Companhia Brasileira de Metaluria e Mineração, Araxá, Minas Gerais, Brazil*). The different types of glass were ground and sieved to isolate the desired particle size (between 38μm and 53μm). For the *in vivo* studies cylindrical rods with 4 mm length x 2 mm diameter were prepared by casting method in a graphite mould. (**Supplementary**

Information - Figure SI1). These rods were annealed at 50 °C below the glass transition temperature (T_g) for 12 h and slowly cooled to room temperature to release the thermal stress associated with the quenching process.

Ionic leaching patterns of bioactive glass by ICP-OES. We used inductively coupled plasma optical emission spectrometry (ICP-OES) to verify the ionic leaching patterns of bioactive glass. In brief: 300 mg of bioglass particles were dispersed in a beaker with 200 mL of buffer solution and maintained under continuous stirring (stirring rate of 75 rpm), at room temperature. Using a 50.69 mM HEPES (2-(4-(2-hydroxyethyl)piperazin-1-yl)ethanesulfonic acid) (Sigma-Aldrich®) and 1 mM NaOH (Sigma-Aldrich®) the solution pH was adjusted to 7.40. The solution was filtered using a 0.22 µm pore filter (Millipore®) in order to remove contaminants and aggregates. The glass was then added to the solution and allowed to mix for 3, 6, 12, 24 and 48 hours. At each time point 10 mL of solution was collected with a syringe and passed through a 0.22 µm pore filter (Millipore®) and analyzed with an ICP-OES spectrometer (Optima 8300 ICP-OES, PerkinElmer, Inc., Shelton, CT, USA). Three replicates were measured for each element.

Analysis of the calcium phosphate layer by ^{31}P MAS NMR spectroscopy. ^{31}P MAS NMR was performed to analyze the rate of formation of the calcium phosphate layer on bioglass surfaces. Samples of 50 mg of bioactive glass particles were added to 5 mL of simulated body fluid (SBF) (**see supplementary information - Figure SI2**) and the mixture was stirred in a thermostatic bath at 37 °C. After 3, 12, 24 and 48 hours the solution was filtered and the remaining powder was immediately dried between two filter papers. Soon after the drying procedure the material was packaged into a 4-mm cylindrical zirconia rotor and spun at the MAS frequency at the magic angle to remove any anisotropy effect. The samples were spun at 10 kHz. The ^{31}P MAS spectra were obtained using a high-power decoupling (HPDEC) pulse sequence with 2.50 µs pulses, 82 ms acquisitions, 5 s recycle delays, a 100 kHz spectral width, and 1024 scans. The ^{31}P chemical shifts were referenced to 85% H_3PO_4. The spectra were processed with TopSpin 2.1.6 software using Fourier transforms and an exponential filter of 50 Hz. The phase was manually adjusted, and the baseline was obtained using a five-order polynomial function.

Culture of BM- derived Mesenchymal Stem Cells (MSCs). Bone- marrow-derived Mesenchymal Stem Cells (BMMSCs) were isolated from the tibia and femoral of five adult Wistar rats weighing 250 - 300g. For this, the bone epiphyses were removed and discarded. The bone shafts were centrifuged at 1500 rpm for 15 minutes in order to precipitate their bone marrows. The pellet (composed by the precipitated bone marrow) was resuspended in Dulbecco's modified Eagle's medium (DMEM) supplemented with 1% penicillin/streptomycin solution and 10% fetal bovine serum (FBS) (Complete DMEM) in a 37 °C–5% CO_2 incubator Cells, up to their fourth passage, were maintained in supplemented DMEM . All media were changed every other day.

Cell viability – MTT assay. Cytotoxicity was analyzed using 3-(4,5-dimethylthiazol-2-yl)-2,5-diphenyltetrazolium bromide (MTT) assay (Sigma-Aldrich, St. Louis, MO, USA). For this, 5000 BMMSCs were cultured in conditioned media containing 10 mg/mL of each of the glass compositions (BG45S5, BGSN1, BGSN2.5 and BGSN5), for a period of four days. Cells grown in complete DMEM served as a positive control while cells previously incubated in Dimethyl sulfoxide (DMSO) for 30 minutes served as a negative control. The MTT assay was performed following the manufacturer's instructions. In short, 12 mM stock solution of MTT was prepared and diluted 10 x in phenol red free medium before being added to the cells, which were incubated for 4 h at 37 °C. After the incubation 75 μL of medium was replaced by 50 μL of Dimethyl sulfoxide (DMSO) and left to incubate at 37 °C for 10 min. MTT was reduced to formazan by metabolically active cells and the optical density was measured using a spectrophotometer (at 570 nm). This assay was performed in quintuplicate.

Cell viability – Live/Dead assay. 10,000 BM- derived MSCs were seeded per well and treated for 72 h with conditioned media containing the dissolution products of Bioglass®45S5, BGSN1, BGSN2.5, and BGSN5 at a concentration of 10 mg/mL. Following the incubation period, a negative control of dead cells was established by incubating cells with 70% methanol for 30 min. Cells treated with regular growth media served as a positive control. The polyanionic dye calcein-green is retained within live cells, producing an intense uniform green fluorescence. Ethidium homodimer-1 (EthD-1) enters cells with damaged membranes and undergoes a 40-fold enhancement of fluorescence upon binding to nucleic acids, thereby producing a bright red fluorescence in dead cells. To stain BM- derived MSCs working concentrations of calcein-green at 2

μM and EthD-1 at 4 μM were combined into one solution and used to treat cells. Cells were overlaid with 200 μL of staining solution.

Staining mineralized nodules with Alizarin Red 1%. BM-derived MSCs were cultured in complete medium until reach monolayer (~10 days). Following the formation of the monolayer cells were treated for three weeks with one of the experimental media: (a) complete DMEM; (b) osteogenic medium, composed by complete DMEM supplemented with 0.1 mM ascorbic acid, 3mM β-Glycerolphosphate and 10^{-8} M dexamethasone (Sigma-Aldrich, St. Louis, MO, USA); (c) BGSN1 (Complete DMEM + 10mg/mL of BGSN1); (d) BGNS2.5 (Complete DMEM + 10mg/mL of BGSN2.5; or (e) BGSN5 (Complete DMEM + 10mg/mL BGSN5). After 21 days of incubation the monolayerswere stained with Alizarin Red 1% (Sigma-Aldrich, St. Louis, MO, USA) in order to analyze the presence of mineralized nodules, which is a marker of osteogenic differentiation. In short, cell monolayers were fixed with 70% ethanol for 1 hour at 4 °C and incubated in 1% Alizarin Red for 10 minutes. Thus, plates were washed five times with distilled water and microphotographs at 100× magnification were taken from each well. Five well were used per group.

Immunofluorescence for Osteocalcin. 20,000 BM- derived MSCs were cultured per well. Cells were treated for 21 days with culture media conditioned with the dissolution products of BG45S5 and BGSN1. Cells treated with osteogenic medium (StemPro™ Osteogenesis Differentiation Kit, ThermoFisher) were used as a positive control. After 21 days of treatment cells were fixed with 4% paraformaldehyde for 30 minutes and treated with a 0.25% solution of Triton X-100 for 30 minutes. Cells were then incubated in Osteocalcin primary antibody (Abcam) at 1:100 for 1 hour at room temperature. After washing with saline solution, cells were incubated in the secondary antibody (Alexa-Fluor 647 goat to rat, Abcam) for 1 hour at room temperature. The cellular nucleuses were stained with DAPI. Images were obtained with a Laser Scanning Confocal Microscope (LSCM, Leica TCS SP5) in PMT mode. Reflection images of laser in TRANS mode were obtained in order to identify mineralized matrix.

Atomic force microscopy (AFM). Surface roughness of bioglass before and after immersion in culture medium was measured by atomic force microscopy (AFM) using a NX-10 atomic force microscope (Park System) operating on intermittent contact. The nominal spring constant and resonant frequency of the silicon tip (Nanosensors) were

42 N/m and 320 kHz, respectively. Firstly, the bioactive glass discs were polished in a similar way and immersed in culture medium and maintained at 37 °C for 24 hours. Then, the samples were allowed to completely dry for 48 h at room temperature. The images were recorded at room temperature and Gwyddion software was used to process the AFM images. The root mean square (RMS) surface microroughness was obtained on 30 x 30 μm scans.

Scanning electron microscopy (SEM). The surface roughness was qualitatively characterized by scanning electron microscopy (SEM) using FEI Inspect F50 available at LNNano, Campinas. The operating voltage and working distance were 20 kV and 10.5 mm, respectively. The samples before and after immersion in culture medium were fixed on a metal stub using carbon tape and coated with gold before observations.

In Vivo analysis. Glass rods were implanted into rat tibia. For this, Brazilian College of Animal Experimentation (BCAE) guidelines were followed, and experiments were approved by Ethics Committee in Animal Use – ECAU/Unicamp (Protocol nº 2777-1). Rods composed of BG45S5 or BGNS1 were implanted into a round defect created in the tibia of rats that had been anesthetized with a mixture of ketamine (ANASEDAN®) at 80 mg/kg and xylazine (DOPALEN®) at 10mg/kg. Five rats were used per group. A round transcortical defect was created using a spherical threfine bur (JET®) with a diameter of 2 mm after pulling aside the periosteum. The glass rod (4 mm length × 2 mm diameter) was carefully introduced into the defect until total coupling, then the periosteum and the skin were sutured. After 28 days, the animals were euthanized, and the tibia was obtained from the animals and fixed for 24 h at 4 ºC in 10% zinc-buffered formalin (Sigma-Aldrich®). After fixation, they were decalcified in 5% EDTA (Synth Labsynth, Diadema, SP, Brazil), the glass rod was then carefully removed and the bones were paraffin-embedded and sectioned.

Morphometry. All histological slides were stained with hematoxylin and eosin dyes and a light microscope (Nikon 80i model, Nikon Corporation, Tokyo, Japan) with a camera Nikon Model DS-Ri1 and NIS-Elements software: Advanced Research 3.0 were used to quantify: (i) area of new-formed subperiostal bone and (ii) thickness of new-formed bone layer (for a fully detailed description of these analysis see **Supplementary Information SI4**)

*Statistical Analysis***.** The comparison between means of subperiostal new formed bone and of the thickness of the bone layer formed around the implant were done through ANOVA one-way test with tukey (homogeneous variances) or Games-Howell (non-homogeneous variances) post-hoc. For all tests $\alpha = 0.05$ was assumed. All data are described in mean and standard error.

Supporting Information

Supporting Information is available from the Wiley Online Library or from the author.

Acknowledgements

The authors acknowledge the use of the analytical instrumentation facility at Institute of Chemistry - University of Campinas, which is supported by the State of Paulo. This work was carried out with the support of the São Paulo Research Foundation – FAPESP (Grant: 2010/12376-5, 2010/00863-0, 2011/09240-9, 2011/17877-7, and 2016/09588-9) and The National Council for Scientific and Technological Development (CNPq/PIBITI) that provided financial support. The authors would like to thank Brazilian Nanotechnology National Laboratory (LNNano) for technical support during SEM and AFM analyzes especially Dr. Carlos Alberto Rodrigues Costa for his technical assistance with AFM analysis. João H. Lopes and Lucas P. L. De Souza contributed equally to this work

Received: ((will be filled in by the editorial staff))

Revised: ((will be filled in by the editorial staff))

Published online: ((will be filled in by the editorial staff))

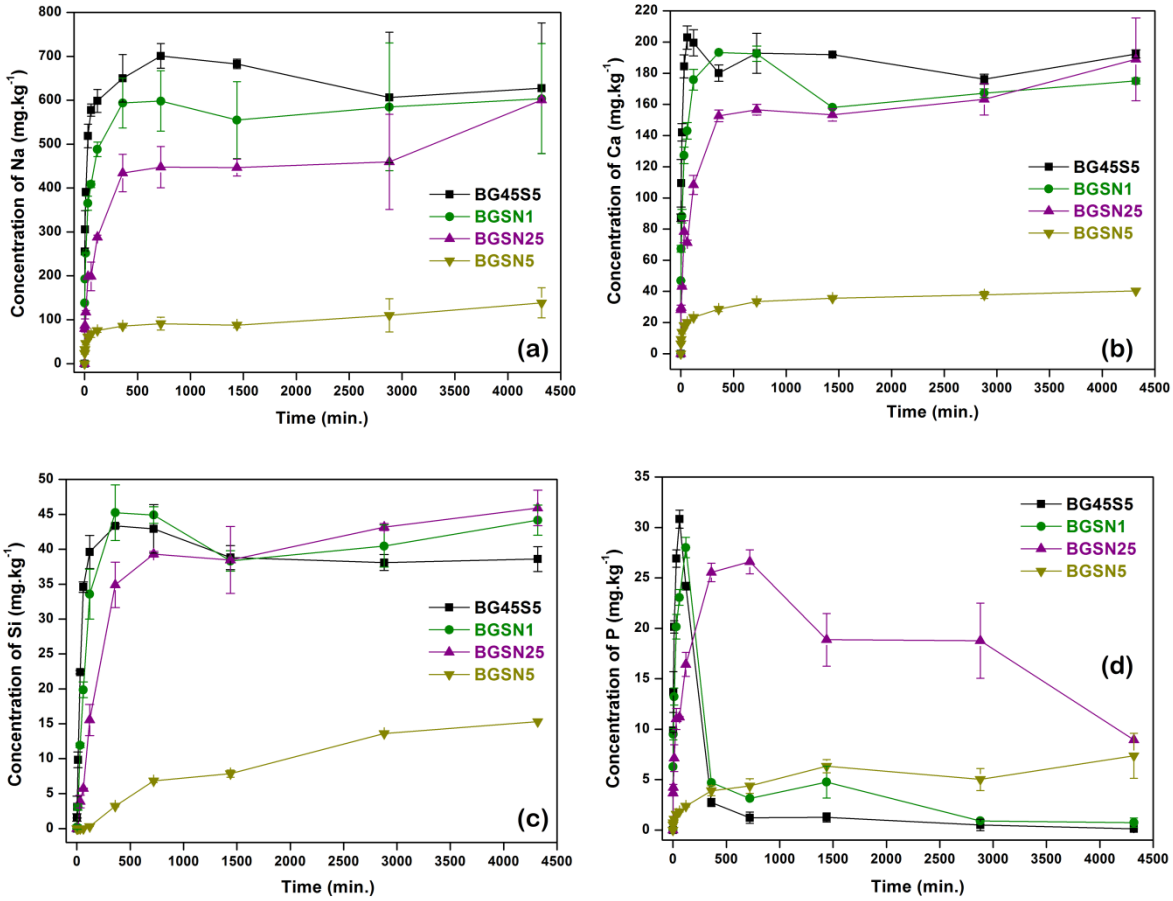

Figure 10. ICP data: ion release vs. time in 50.69 mM HEPES solution at pH 7.40 for BG45S5 and Nb-substituted bioactive glass. The data displayed in (a), (b), (c) and (d) are related to leached Na, Ca, Si, and P species from glass derived from substitution of P_2O_5 for Nb_2O_5.

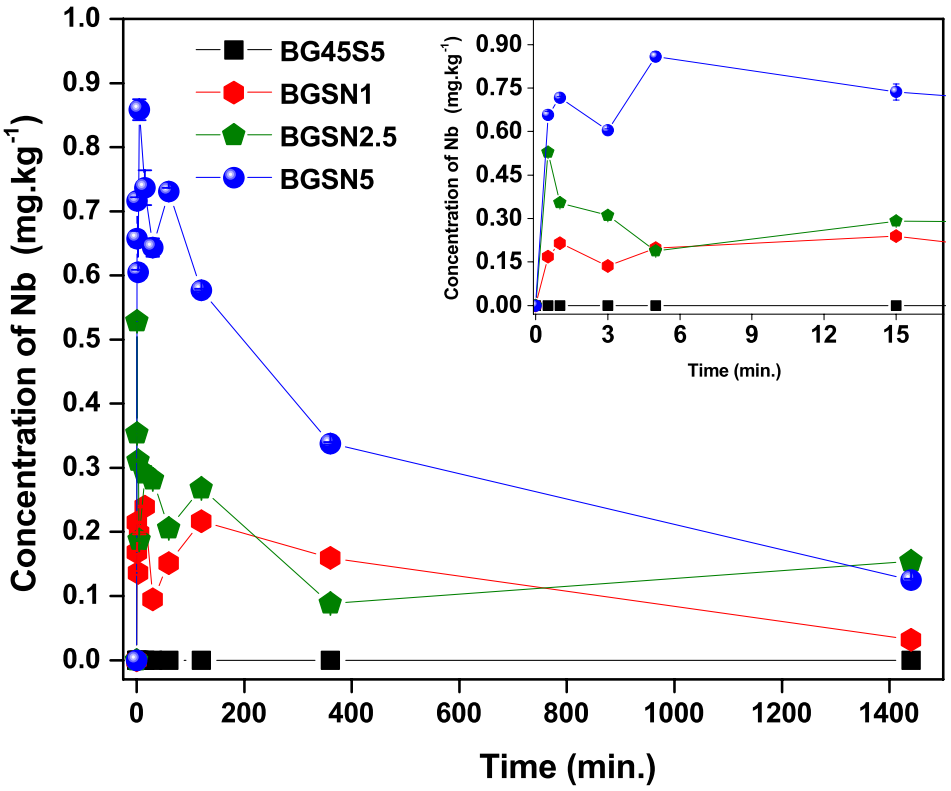

Figure 11. ICP data: Nb ion release vs. time in 50.69 mM HEPES solution at pH 7.40 for BG45S5 and Nb-substituted bioactive glass. The amounts of niobium determined by ICP-OES is consistent with the niobium content in each sample, i.e. BGSN5 exhibits a higher peak of niobium concentration compared to the BGSN1 bioglass. As expected, no niobium was detected for BG45S5.

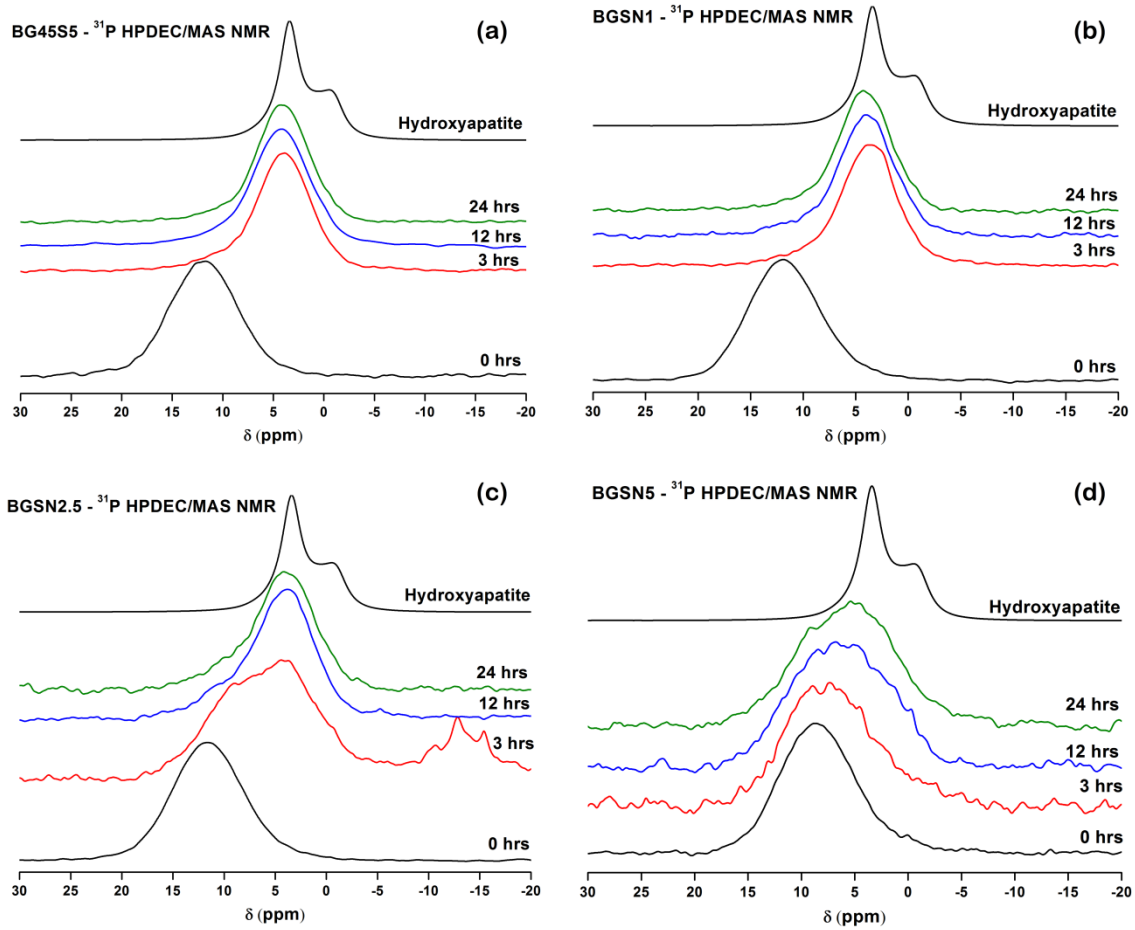

Figure 12. 31P MAS-NMR spectra for the different glass compositions, recorded at a magnetic field strength of 9.4 T and a spinning speed of 10 kHz: (a) BG45S5, (b) BGSN1, (c) BGSN2.5, and (d) BGSN5. The chemical environmental for 31P shifts progressively evolves to lower values of δ, reaching a peak position similar to the 31P spectrum observed in the hydroxyapatite control.

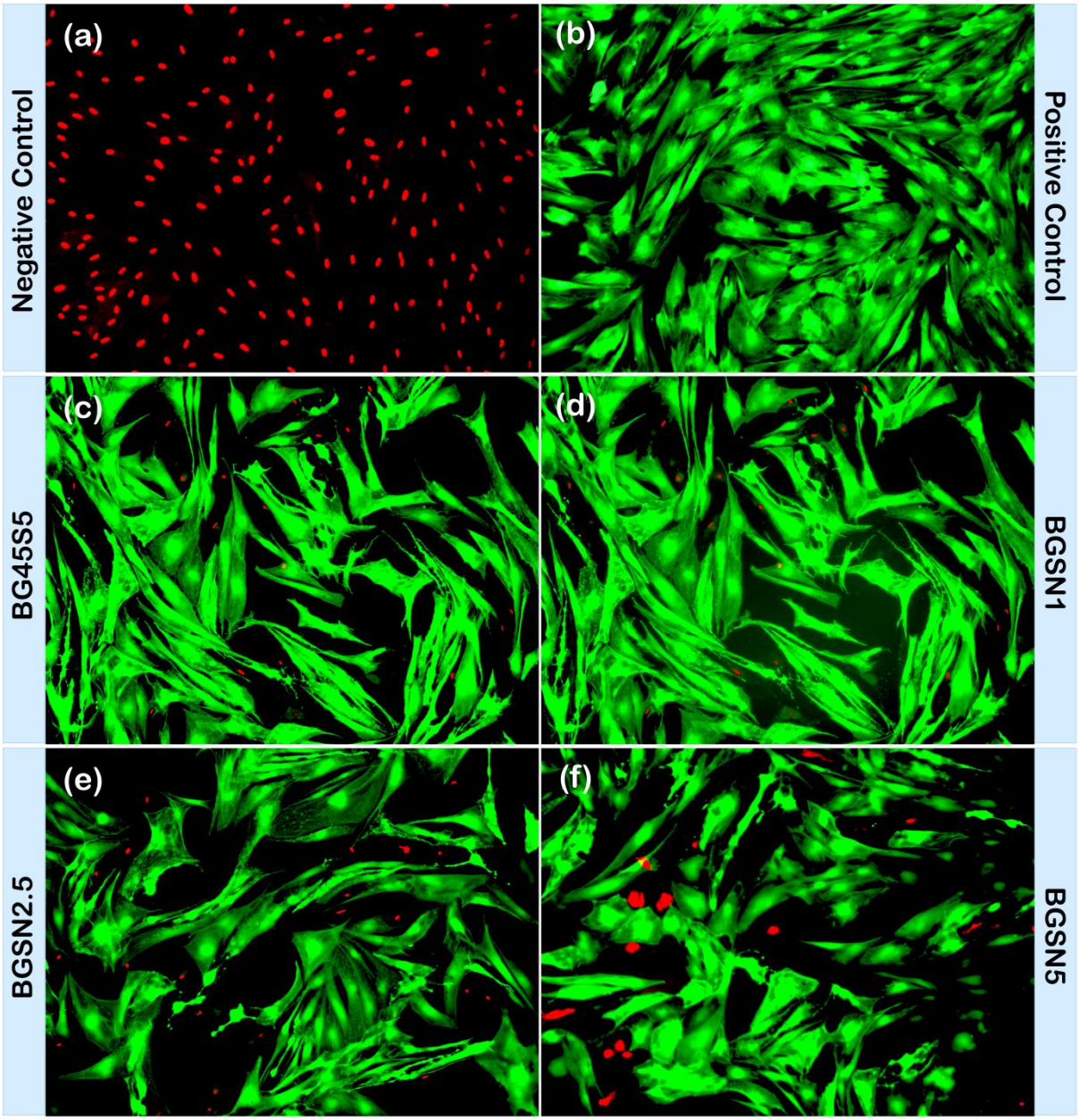

Figure 13a. Micrographs of BM- derived MSCs treated for 72 h with culture media conditioned with the dissolution products of: BG45S5 (c), BGSN1 (d), BGSN2.5 (e), and BGSN5 (f) at a concentration of 10 mg/mL. Following the incubation period, a negative control of dead cells was established by incubating cells with 70% methanol for 30 min (a). Cells treated with regular growth media served as a positive control (b). Dissolution products of none of the glass compositions were toxic to the tested cell line.

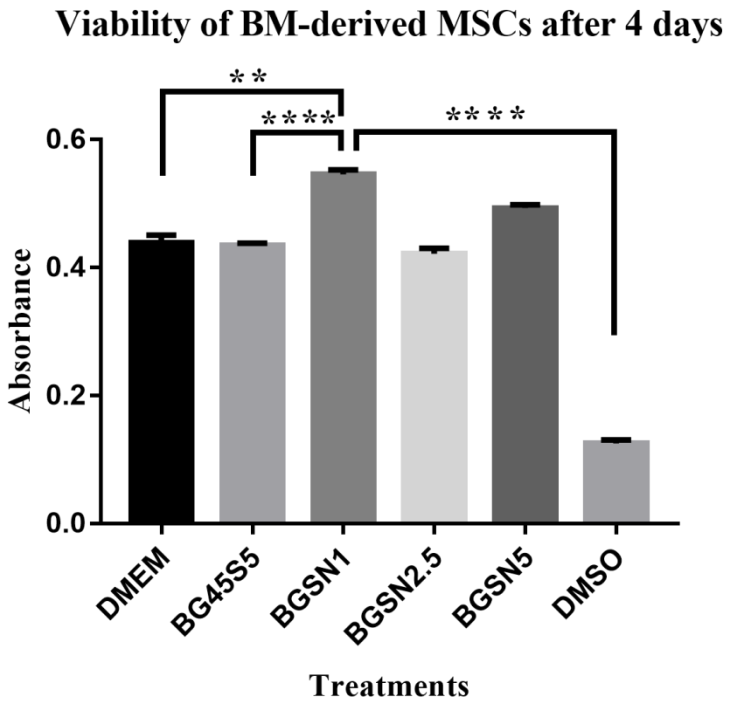

Figure 4b. Viability of bone-marrow-derived mesenchymal stem cells (BM-MSCs) after 4 days of treatment with different glass-conditioned media measured by MTT assay. DMEM was used as a positive control and cells killed with DMSO as negative control. Results are expressed in mean and SEM. One-way ANOVA followed by Tukey's test was used to compare the groups. None of the glass-conditioned media (BG45S5, BGSN1, BGSN2.5 and BGSN5) reduced cell viability in comparison with the control group (DMEM). The group BGSN1 showed significantly higher absorbance than DMEM ($p=0.0014$) and BG45S5 ($p<0.0001$) after 4 days, suggesting superior cell proliferation.

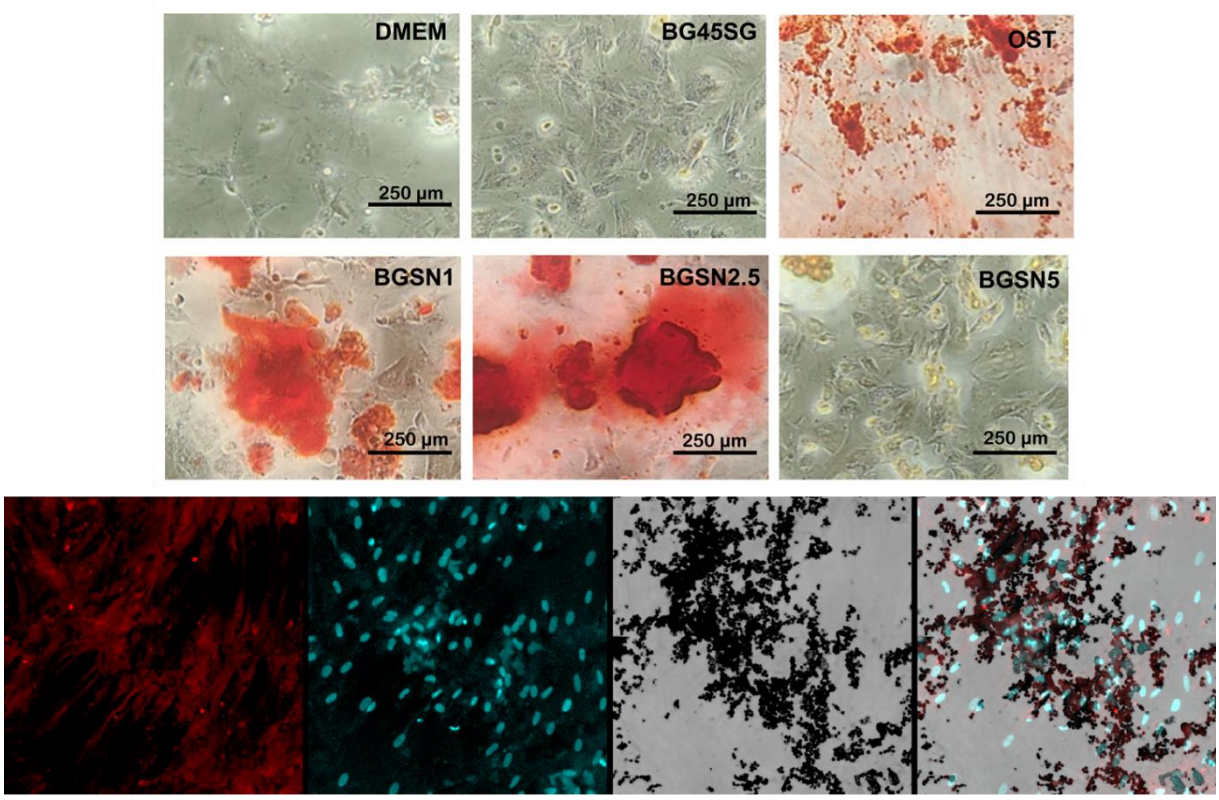

Figure 5. Micrographs of calcium deposits within and around BM- derived MSCs stained with alizarin red (1%) and osteocalcin immunofluorescence after 21 days of treatment with different media. The six superior squares show micrographs (100× magnification) of BM-MSCs in which the red aggregates are calcium deposits. Cells treated with osteogenic medium (OST) showed a fully mineralized matrix which meaning that most cells were in a late stage of differentiation to osteoblasts. Those cells treated with BGSN1 and BGSN2.5 showed matrix mineralization.The four inferior squares display laser scanning confocal micrographs of BMMSCs treaded with BGSN1 showing osteocalcin immunofluorescence (in red), cell nucleuses stained with DAPI (in bright blue), mineralized matrix by reflection of laser in TRANS mode (black) and an overlapping of matrix and nucleuses.

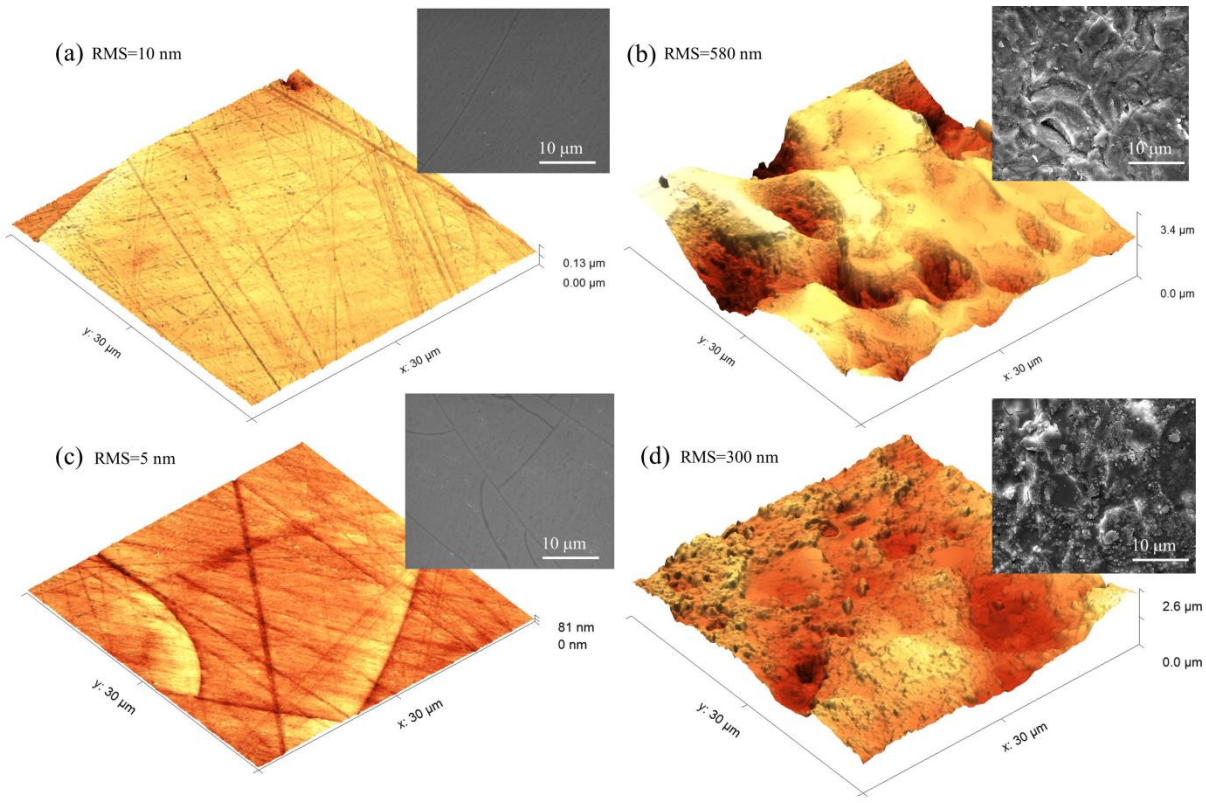

Figure 6. Three-dimensional surface AFM images for an area of 30 x 30 µm and SEM micrographs at magnifications of 3000× of bioglass 45S5 (a) before and (b) after 24 hours of immersion in complete culture medium; BGSN1 (c) before and (d) after 24 hours of immersion in complete culture medium showing the increase of surface roughness.

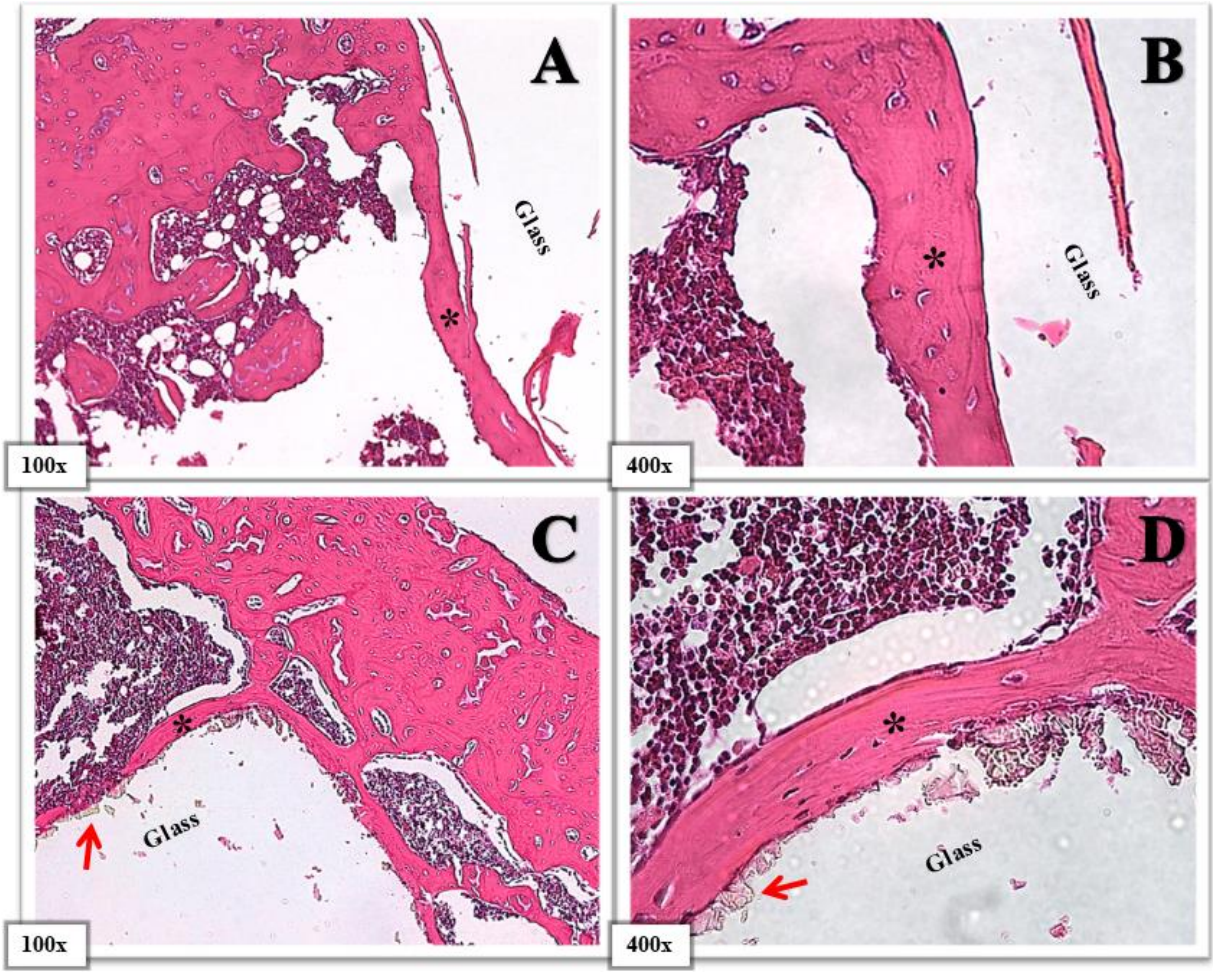

Figure 7. Micrographs of transversal histological sections of rats' tibias treated with glass rods for 28 days and stained Haematoxilin and Eosin at 100 and 400 x magnification. The glass implants were removed after decalcification to allow the preparation of the histological sections (empty areas marked with "Glass" are where the glass rods were located for 28 days), but, some fragments of the glass can still be seen (red arrows). The micrographs show the bone layer (marked with "*") that formed around the glass implant. Images A and B illustrate the group treated with BG45S5 whilst images C and D represent rats treated with BGSN1. A t-student test showed no significant different between thickness of the bone layer formed in the rats treated with BGSN1 and the control group (BG45S5) ($p=0.9568$). For this analysis $p<0.05$ was considered.

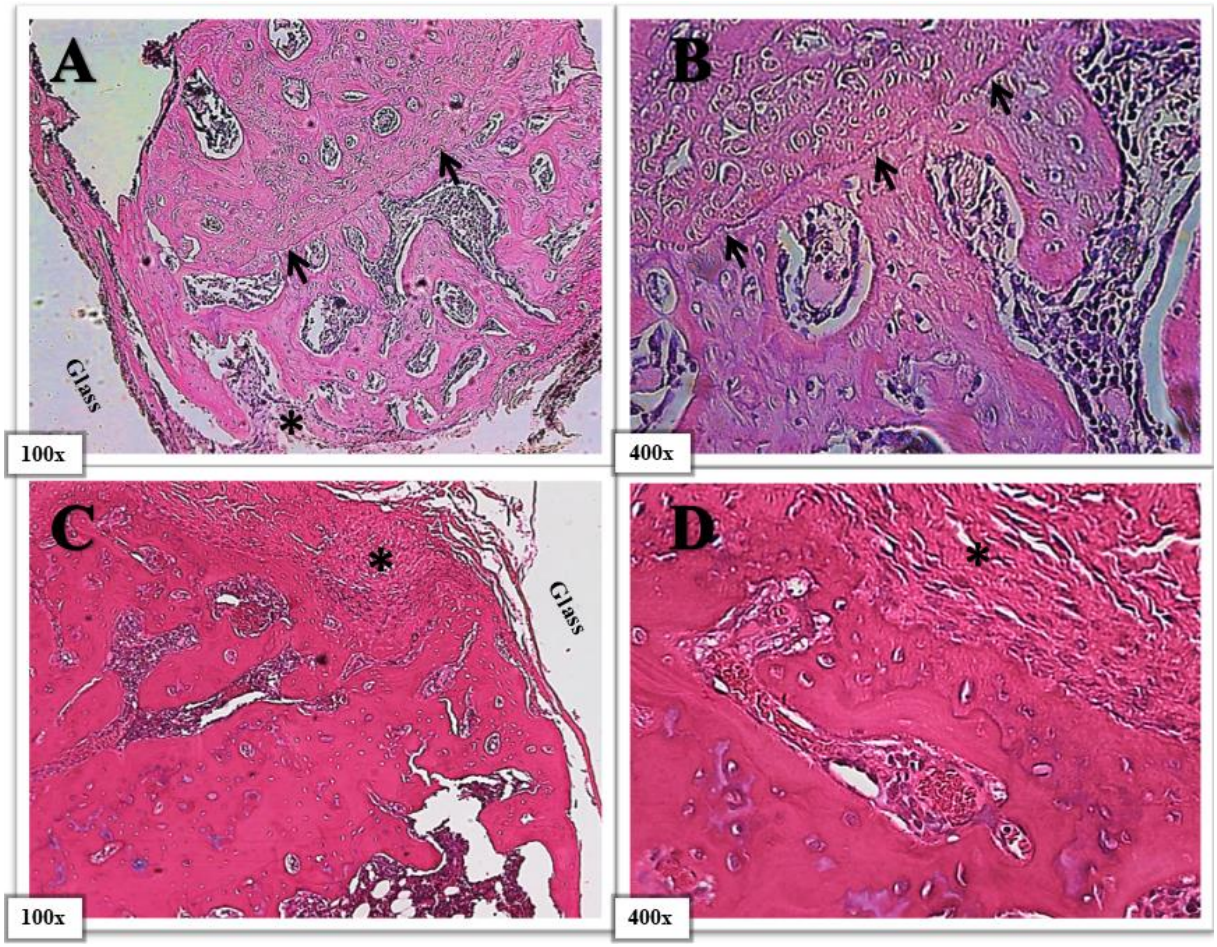

Figure 8. Micrographs of transversal histological sections of rats' tibias treated with glass rods for 28 days and stained Haematoxilin and Eosin at 100 and 400 x magnifications. The glass implants were removed after decalcification to allow the preparation of the histological sections (empty areas marked with "Glass" are where the glass rods were located for 28 days). The micrographs show the formation of bone by the osteogenic cells present at the inner layer of the periosteum (marked with an "*"). The cement line (black arrows in images A and B) mark where the new bone started to form after the implantation of the material. Images A and B illustrate the group treated with BG45S5 whilst images C and D represent rats treated with BGSN1. A t-student test revealed that the group treated with BG45S5 (46469±804.5µm) presented a significantly larger sub periosteal bone area than the group treated with BGSN1 (40615±1503µm) (P=0.0085). For this analysis p=0.05 was considered.

Table 1. Glass compositions of BG45S5 and Nb-substituted 45S5 bioglass.

Glass	SiO_2	CaO	Na_2O	P_2O_5	Nb_2O_5
BG45S5	*46,1*	*26,9*	*24,4*	*2,6*	-
BGSN1	*45,1*	*26,9*	*24,4*	*2,6*	*1,0*
BGSN2.5	*43,6*	*26,9*	*24,4*	*2,6*	*2,5*
BGSN5	*41,1*	*26,9*	*24,4*	*2,6*	*5,0*

Table 2. 31P MAS NMR peak positions and full width half maxima (FWHM) for BG45S5, Nb-substituted 45S5 bioglass and commercial hydroxyapatite.

The table of contents entry should be 50–60 words long, and the first phrase should be bold.

Nb-substituted silicate glass possesses enhanced osteoinductive properties. The replacement of 1 or 2.5 mol% of SiO2 with Nb2O5 in Bioglass® 45S5 significantly enhances cell proliferation after four days of treatment. BM-derived MSCs differentiate into osteoblasts in 21 days. Glass rods composed by Nb-containing glass enable bone growth onto its surface and release ionic products that promote subperioestal bone formation.

Keywords: bioactive glass, bioglass, niobium, osteogenic, bone

João H. Lopes, Lucas P. L. De Souza, Juliana A. Domingues, Filipe V. Ferreira, Moema de Alencar Hausen, Davi Encarnação, José A. Camilli, Richard A. Martin, Eliana Aparecida de Rezende Duek, Italo O. Mazali, Celso A. Bertran.*

Osteogenic capacity of novel melt-derived Nb-substituted 45S5 bioglass: in vitro and in vivo studies

Supporting Information

Osteogenic capacity of novel melt-derived Nb-substituted 45S5 bioglass: in vitro and in vivo studies

João H. Lopes, Lucas P. L. De Souza, Juliana A. Domingues, Filipe V. Ferreira, Moema de Alencar Hausen, Davi Encarnação, José A. Camilli, Richard A. Martin, Eliana Aparecida de Rezende Duek, Italo O. Mazali, Celso A. Bertran.*

Supplementary Information 1. *Ion release in 50.69 mM HEPES solution at pH 7.40 for BG45S5 and Nb-substituted bioactive glass*

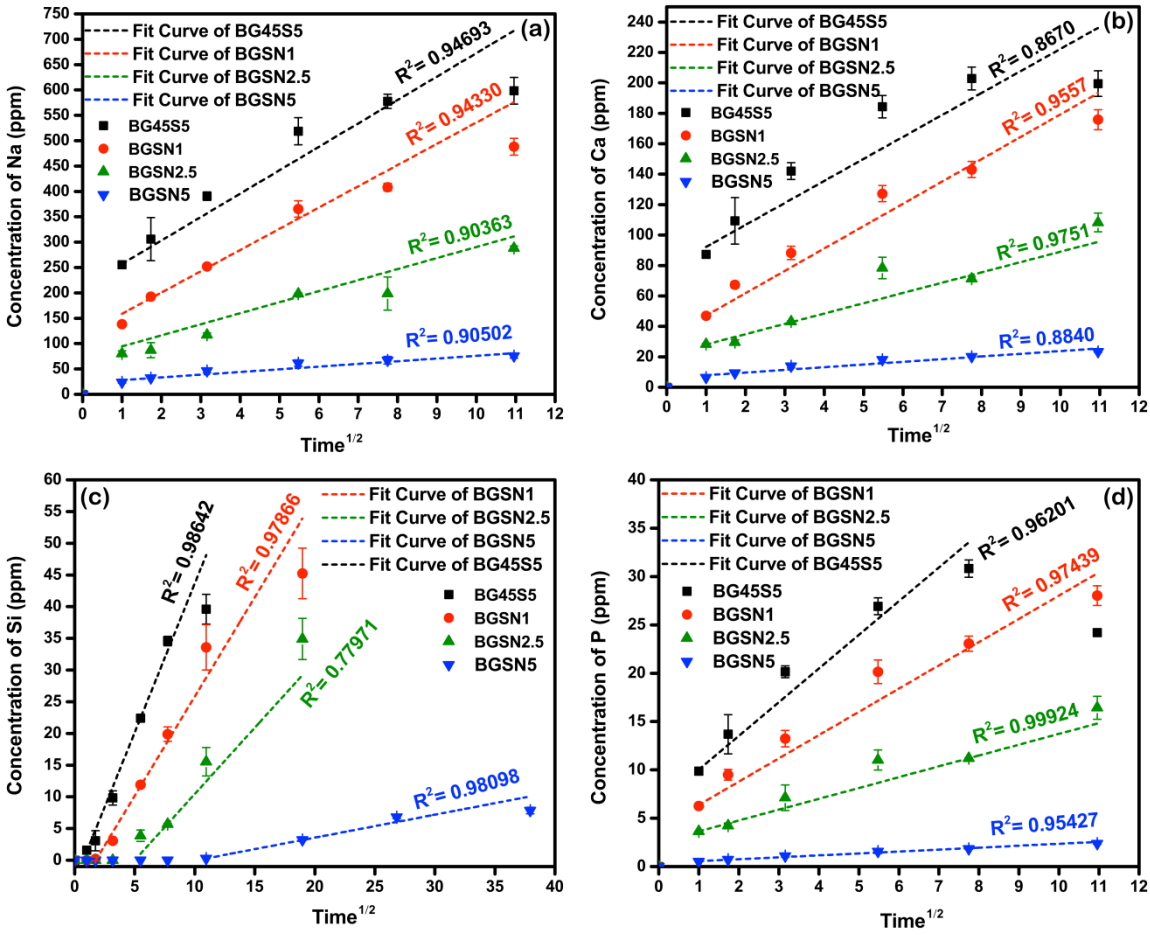

Figure SI1. ICP data: ion release as a function of square root of time in 50.69 mM HEPES solution at pH 7.40 for BG45S5 and Nb-substituted bioactive glass. The data displayed in (a), (b), (c), and (d) are related to leached of Na, Ca, Si, and P species, respectively, from glass derived from substitution of P2O5 by Nb2O5. Lines are linear regression of dissolution data up to 120 min.

Supplementary Information 2. *Preparation of SBF solution*

The acellular simulated body fluid (SBF) solution was prepared with concentrations of ions equal to those of blood plasma, including 〖Cl〗^- and 〖HCO〗_3^-. The pH value of 7.40 was obtained using the Hepes buffer at concentration 50.69 mmol/L. Details about the concentrations of the ions present in the SBF solution is presented in **Table SI2.**

Table SI2. Nominal ion concentrations of the SBF in comparison with those of human blood plasma.

Ions	**Concentration/mM**	
	Blood Plasma	**SBF**
Na^+	142.0	142.0
K^+	5.0	5.0
Mg^{2+}	1.5	1.5
Ca^{2+}	2.5	2.5
Cl^-	103.0	103.0
HCO_3^{2-}	27.0	27.0
HPO_4^{2-}	1.0	1.0
SO_4^{2-}	0.5	0.5

Supplementary Information 3. *Glass rods preparation*

Figure SI3. Devices used for the preparation of glass rods for in vivo tests: Graphite mould and suction system to force filling of the glass in the graphite mould. The vacuum pump was used to suction the molten glass, overcoming the high surface tension of the melt and allowing it to fill the 2 mm diameter graphite mould.

Supplementary Information 4. *Histom*orphometry

Area of newly-formed subperiosteal bone

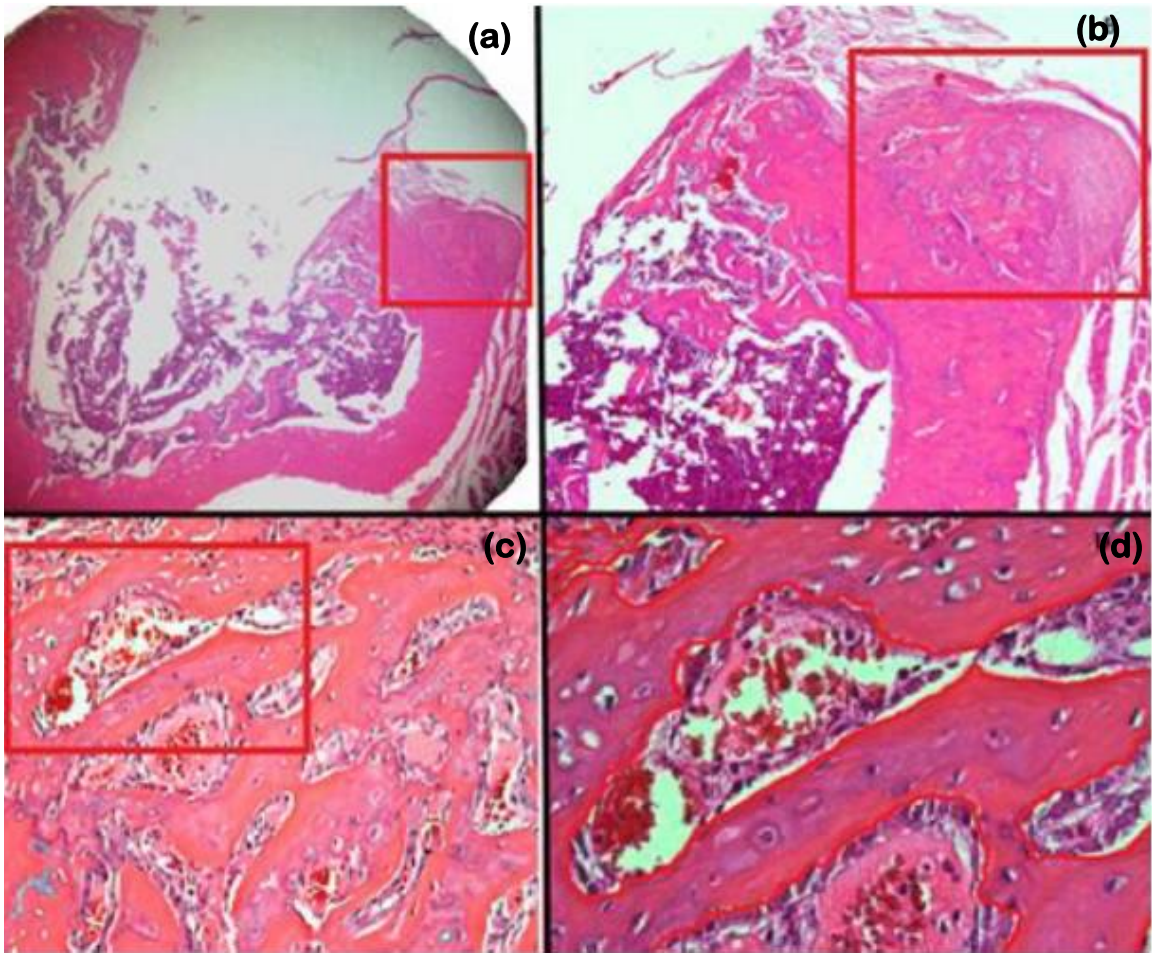

Figure SI4.1. Micrographs showing H&E stained histological sections of rat tibia tissues at 40×, 100×, 200×, and 400× magnifications and quantification of the area of newly-formed subperiostal bone. The area of the newly-formed subperiostal bone was measured in one field of each side of the cortical defect, directly underneath the periosteum and adjacent to where the glass rod was previously located at 400× magnification. Five non-consecutive histological sections were analyzed per animal. Five rats were used per group (n = 5 per group). Thus, the mean and the standard error of the mean were recorded and further compared.

Thickness of newly-formed bone layer

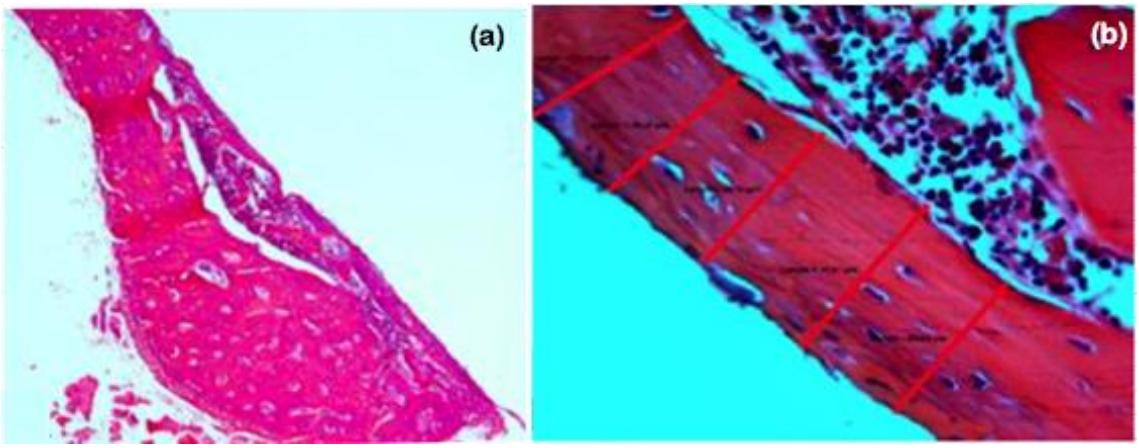

Figure SI4.2. Micrographs showing H&E stained histological sections of rat tibia at 40×, 100×, 200×, and 400× magnifications. Measurement of the thickness of newly-formed bone layer that formed around the implant was repeated 20 times, and all measurements were performed at 400× magnification. Five rats were used per group (n = 5 per group). The mean and the standard error of the mean were recorded and further compared.

ARTICLE 3:

BIOCOMPATIBILITY AND OSTEOSTIMULATIVE PROPERTIES OF NIOBIUM- CONTAINING BIOACTIVE GLASS: AN EXPERIMENTAL *IN VITRO* AND *IN VIVO* STUDY

[1]Lucas Pereira Lopes De Souza‡, [2,3]João Henrique Lopes‡, [4]Filipe Vargas Ferreira, [5]Richard Alan Martin, [3]Celso Aparecido Bertran, [1]José Angelo Camilli

AUTHOR INFORMATION

L. P. L. De Souza

[1]Department of Structural and Functional Biology, Institute of Biology, University of Campinas – UNICAMP, 13083-862, Campinas, SP, Brazil.

E-mail: (lpls2002@hotmail.com)

J. H. Lopes

[2]Department of Chemistry, Division of Fundamental Sciences (IEF), Technological Institute of Aeronautics (ITA), 12228-900, Sao Jose dos Campos-SP – Brazil.

[3]Department of Physical Chemistry, Institute of Chemistry, University of Campinas – UNICAMP, P.O. Box 6154, 13083-970, Campinas, SP, Brazil.

E-mail: (lopes@ita.br)

F. V. Ferreira

[4]School of Chemical Engineering, University of Campinas - UNICAMP, 13083-970, Campinas, SP, Brazil.

E-mail: (filipevargasf@gmail.com)

R. A. Martin

[5]School of Engineering & Aston Research Centre for Healthy Ageing, Aston University, B47ET Birmingham, United Kingdom.

E-mail: (r.a.martin@aston.ac.uk)

C. A. Bertran

[5]Department of Physical Chemistry, Institute of Chemistry, University of Campinas – UNICAMP, P.O. Box 6154, 13083-970, Campinas, SP, Brazil.

E-mail: (bertran@iqm.unicamp.br)

J. A. Camilli

Department of Structural and Functional Biology, Institute of Biology, University of Campinas – UNICAMP, 13083-862, Campinas, SP, Brazil.

E-mail: (jcamilli@unicamp.br)

[‡] *These authors contributed equally*

Abstract

Introduction: The development of safe biomaterials for the treatment of large bone defects and non-unions is still challenging. Objective: We aimed to test the biocompatibility and bioactive properties of a bioactive glass containing niobium dioxide (Nb2O5) for bone replacement application. Materials and Methods: Glass biocompatibility was tested by in vitro and in vivo experiments. In vitro study consisted of assessing the cytocompatibility of Nb-doped glass with bone-marrow-derived mesenchymal stem cells (BM-MSCs). Systemic biocompatibility was verified by means of the quantification of biochemical markers and histopathology of liver (TGO/AST, TGP/ALT), kidneys (creatinine), and muscles (total CK). The glass genotoxicity was tested by the micronucleus test. The regeneration of a calvarial defect using was assessed using both qualitative and quantitative analysis of 3D microcomputed tomography images. Results: The Nb-doped glass was not cytotoxic to BM- derived MSCs. It is systemically biocompatible causing no signs of damage to high metabolic and excretory organs such as liver and kidneys. No mutagenic potential was observed in the micronucleus test. MicroCT images showed Nb-containing glass was able to nearly fully regenerate a critical-sized calvarial defect and was far superior to standard 45S5 Bioglass®. Defects filled with Nb doped bioglass showed over 90% coverage compare to just 66% for 45S5 Bioglass®. For one animal the defect was completely filled in 8 weeks. Conclusion: Taken together these results make clear that Nb-containing bioactive glass is a safe and effective biomaterial for bone replacement.

1.0 Introduction

Bone fractures are the most widespread large- organ traumatic injury that affects humans[1]. The regeneration process after fractures normally achieves a successful healing outcome yet up to 10–15% of the patients show an impaired healing, delaying the process or even leading to a non-union[2]. Fractures represent not only a burden for the patient's life, but the costs with surgery and hospitalization also constitutes a considerable cost for socio- economic and health care systems[2]. In fact, it has been reported that the treatment of an established non- union of a bone costs over $10,000 on average[2]. The estimated number of fractures for the year 2000 was 9.0 million worldwide, but, as some fractures cause disability for a period longer than 1 year this number was estimated at approximately 50 million[3]. This high number of fractures stimulates the development of synthetic materials for bone replacement.

In 1971 the researcher Larry Hench developed the first bioactive material, the Bioglass® 45S5 [4]. This material is a glass composed of 46.1 mol. % SiO_2, 24.4 mol.% Na_2O, 26.9 mol.% CaO and 2.6 mol.% P_2O_5[5]. By means of ion exchange with the body fluids, Bioglass®45S5 spontaneously forms a layer of hydroxyl carbonate apatite ($Ca_5(PO_4)_3OH$) (HCA) on its surface, which is the main inorganic component of bone[6]. Due to its micro-/nano-scale complexity the HCA layer gives support to osteogenic cells to attach, spread and produce mineralized bone matrix whilst the biomaterial slowly dissolves until it be completely substituted by the new-formed bone[5–7]. Seeking to improve the mechanical and biological properties of Bioglass®45S5 many variations of the original composition have been designed and investigated[6].

The incorporation of niobium into biomaterials appears to be an interesting approach to improve their mechanical and biological properties[8–18]. Niobium is of interest for biomedical applications and has been incorporated into metallic alloys for dental implants where it imparts superior corrosion resistance, low cytotoxicity, and enhanced wear resistance [13]. Furthermore, some investigations reported that sol–gel-derived niobium oxide gels promote apatite formation within a week of immersion in simulated body fluid which indicates that this element is a good candidate for bioactive glass for bone replacement[19,20]. Niobium has already been incorporated into calcium phosphate invert glasses Containing [9] and in fluorapatite glass-ceramics[20] showing great

biocompatibility and also stimulating osteogenic differentiation of human mesenchymal stem cells (MSCs) and maturation of Mouse osteoblast-like cells (MC3T3- E1 cell) by means of direct contact[20] or through its ionic dissolution products[9]. Nb doped glasses are also reported into increase vascularization[21]. However, despite its great potential for biomedical applications niobium has rarely been incorporated in silicon-rich bioactive glass such as Bioglass®45S5. In view of that, we altered that composition of the original Bioglass®45S5 replacing all content of P_2O_5 (2.6 mol %) with Nb_2O_5 and investigated the biocompatibility, genotoxicity and the potential for osteointegration of this new Nb-containing glass. The biocompatibility of Nb-containing glass was tested by *in vitro* and *in vivo* experiments. The *in vitro* approach consisted of assessing the cytocompatibility of Nb-doped glass with Normal Human Osteoblasts (NhOsts) by quantitative MTT analysis and qualitative Live/Dead assay. Systemic biocompatibility was verified by means of quantification of biochemical markers of hepatic (TGO, TGP, and GamaGT), renal (creatinine and urea), and cardiac damage (total CK). In addition, histological sections of liver and kidneys were examined for any sign cellular or tissular damage. The glass genotoxic potential was tested by the micronucleus test. The regeneration of a 5mm sized calvarial defect was examined by means of both qualitative and quantative analysis of 3D microcomputed tomography images.

2.0 Materials and Methods

2.1 Preparation of bioactive glasses and conditioned cell culture media

We tested a variation of melt-quench derived Bioglass® 45S5, $(SiO_2)_{46.1}(CaO)_{26.9}(Na2O)_{24.4}(P_2O_5)_{2.6}$. In this variation 2.6 mol% of P_2O_5 were replaced by 2.6 mol% of niobium dioxide (Nb_2O_5), resulting the composition named BGPN2.6. The glass was prepared by thoroughly mixing the precursors oxides SiO_2 (Alfa Aesar, 99.5%), $CaCO_3$ (Alfa Aesar, 99.95-100.5%), Na_2CO_3 (Sigma-Aldrich, ≥99.5%), $NH_4H_2PO_4$ (Sigma-Aldrich, ≥99.5%), and Nb_2O_5 (Sigma-Aldrich,≥99.99%). The batches were melted at 1400ºC for 90 minutes in platinum crucibles. The melt was then poured into graphite mould which had been preheated to 370 °C and annealed at this temperature overnight before being allowed to cool slowly to room temperature. After cooling down the glasses were ground to powder. The particle size was standardized

between 40 and 60 µm using a series of micro sieves. For the experiments with the cells glass- conditioned media were prepared. For this, powders of BGPN2.6 and BG45S5 were added to cell culture medium (DMEM/F12) at a concentration of 10µg/ml, mixed for 24 hours and filtered using an ultrafine filter (0.22µm pore size) and the media were left within the cell incubator for 4 hours (time necessary for pH buffering, as observed in the results of the experiment described in the item 2.3).

2.3 Determining pH behaviour of culture media containing bioactive glasses prior cell treatment

Cell culture medium has bicarbonate ions in its composition. These ions react with CO_2 in the cell incubator buffering the medium, maintaining pH in an ideal level for cells. Glass dissolution affects the pH of the medium, usually increasing it, and pH directly influences cell behaviour. However it is known that the body naturally buffers the pH[22]. In view of this, we studied the kinetics of media buffering in the cell incubator over time in order to determine how much time would be necessary for neutralizing their pH before adding the cells. For this, 500µl of each medium were added to each well of a 24-well plate, in duplicate. The pH was measured prior incubation and after increasing time intervals up to 72 hours.

2.4 Cell Culture

Normal Human Osteoblasts (NhOsts, Lonza, Walkersville, MD) were cultured in growth medium (Osteoblast Growth Medium Bullet Kit, Lonza, Walkersville, MD). Cell flasks were kept in incubator at 37ºC in an atmosphere of 5% of CO_2. The culture medium was changed every other day. All procedures using osteoblasts were carried out following the manufacturer's protocol.

2.5 MTT

Cell culture media conditioned with BG45S5 and BGPN2.6 were used to treat 3000 NhOsts for 72 hours. A positive control group of NhOsts was treated with growth medium. A negative control group of cells were killed by incubation in ETOPOSIDE.

MTT (3-(4,5-dimethylthiazol-2yl)-2,5-diphenyltetrazolium bromide) is a soluble tetrazole salt in water that produces an yellowish solution when prepared in culture medium or in saline without phenol red. When dissolved, MTT is converted into insoluble purple formazan through the cleavage of the tetrazole ring by dehydrogenases. This insoluble formazan was solubilized using Dimethyl Sulfoxide (DMSO). The dissolved material was spectroscopically quantified as it produces an absorbance that is proportional to the concentration of the converted dye.

To quantify cell viability we followed manufacturer's protocol. Briefly, 10µl of MTT (stock solution at the concentration of 5mg/ml) were added to each well (containing 100µl of phenol red-free culture medium) incubating for 4 hours in the cell incubator at 37°C and 5% CO_2. After the incubation time the formed formazan was solubilized with DMSO incubating it for 10 minutes. The absorbance of the converted formazan was measured at the wavelength of 570nm.

2.6 Live/dead assay

For this assay cells were treated with the same media described for the MTT assay (Control, BG45S5, BGPN2.6, and ETOPOSIDE), following the same conditions and timeframe (72 hours). In this assay live cells are distinguished by ubiquitous intracellular esterase activity, which is determined by enzymatic convertion of the virtually nonfluorescent cell-permeant calcein AM to the intensely fluorescent calcein. Calcein is retained within live cell's cytoplasm, producing an intense green fluorescence (~495nm)[23].

EthD-1 enters cells with damaged membranes and undergoes a 40-fold enhancement of fluorescence upon binding to nucleic acids, thereby producing a bright red fluorescence in dead cells (ex/em ~495 nm/~635 nm). EthD-1 is excluded by the intact plasma membrane of live cells[23]. For this assay all procedures were carried out on human osteoblasts following the instructions of the manufacturer (ThermoFisher-Scientific®).

2.7 Animals

We used 90 adult rats weighing between 350 and 460 g provided by the Central Bioterium of UNICAMP (CEMIB). The rats were maintained in the Bioterium of the Department of Anatomy, in the Institute of Biology (IB), UNICAMP. They stayed in standard boxes in controlled environmental conditions (12 hours' bright/dark cycles) with standard food and water.

Table 1 shows the sample size of the experimental groups and subgroups. All experimental protocols are in accordance with the ethical principles for animal experimentation adopted by the Brazilian College of Animal Experimentation (COBEA) and were approved by the Committee for Ethics in Animal Use of the University of Campinas – CEUA/UNICAMP (Protocol Number: 3467-1).

Table 1. Sample division into the different experimental groups

	Number of rats		
Material	14 days	28 days	56 days
Control	6	6	6
Sham	6	6	6
BG45S5	6	6	6
BGPN2.6	6	6	6
Total: 72 rats			

2.8 Surgical Procedure:

Before the surgery animals were weighed and transferred into individual boxes. A pre-anaesthetic dose of Tramadol (TRAMAL® - RETARD) (5mg/kg) was applied 15 minutes before the injection of anaesthetics. Animals were anaesthetized by means of an intraperitoneal injection of a mixture of Xilazin (Xilazin – Syntec) (0,3mg/kg/weight) and ketamine hydrochloride (0,8mg/kg/weight). A prophylactic dose of 1mg/kg/weight of Enrofloxacin (Biofloxacin – Biovet) was applied to prevent bacterial contamination. The full description and photos of the surgical technique can be found in figure 7.

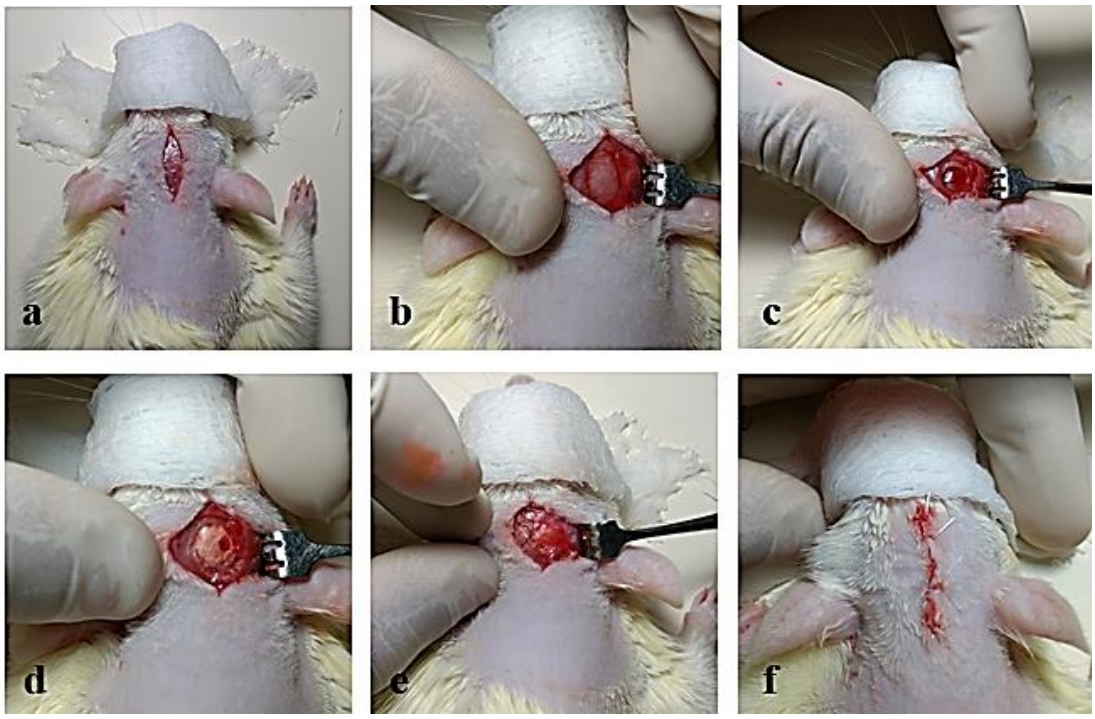

Figure 2. Development of a critical size calvarial defect in rat: a. an incision was made starting at the nose bridge, and ending at the base of the skull, using a scalpel. b. Skin, subcutaneous tissue, temporal muscle, and the periosteum were pulled aside for complete exposure of the parietal bones. c. 5 mm round full-thickness calvarial defect was created in the parietal bone with a 5 mm-diameter tissue punch (Richter®). d. In the control group, the defect was left empty, in the other groups it was filled with different glass compositions (in powder form). e. The periosteum was sutured using a 6-0 Nylon non-absorbent monofilament (ETHILON®). f. The skin was sutured using a 4-0 Nylon non-absorbent monofilament (ETHILON®). In the SHAM group the periosteum and skin were sutured immediately after step "b", without making the bone defect.

2.9 Systemic Toxicity

After the experimental time (14, 28 or 56 postoperative days) rats were euthanized and their blood, liver, and kidneys were collected. The specimens of liver and kidneys were fixed with Bouin solution for 24 hours and embedded in paraplast (Sigma-Aldrich®). All paraffin-embedded histological sections were stained using Hematoxilyn and Eosin and histopathologically examined under a light microscope. Systemic toxicity was also analysed by the quantification of biochemical toxicological markers from kidneys (Creatinine), liver (TGO, TGP) and muscles (Total Creatine

Kinase – Total CK). The markers were quantified by means of enzymatic kits (Interkit®).

2.10 Micronucleus test

Micronucleus induction is a key characteristic of genotoxic compounds and the analysis of micronuclei formation resulting from DNA strand breakage (clastogens) or interference with chromosome segregation (aneugens) is an important component of toxicology screening of new biomaterials. For this assay, we collected bone marrow from rat's femur using a disposable syringe containing 1 mL of 0.9% saline at room temperature. The harvested bone marrow was transferred to a sterile tube, homogenized and centrifuged for 10 minutes at 900 rpm and part of its supernatant was discarded.

The sediment was re-suspended in the remaining supernatant. One drop of this bone marrow suspension was placed on one extremity of a microscope slide. Using another glass slide a smear was made and left to dry at room temperature. The dry slides were fixed in 100% methanol for 10 minutes and dried at room temperature. Once fixed, the slides were stained with Giemsa diluted in Sorensen buffer (Na_2HPO_4 0,06M e KH_2PO_4 0,06M – pH 6,8), at the proportion of 1 mL of Giemsa for 20 mL of buffer solution for 10 minutes, washed with distilled water, and dried at room temperature. Entellan® was used to mount the histological slides that were further analysed.

For the calculation of the relative number of micronucleus 3000 erythrocytes were counted per animal in five animals per group (BG45S5, BGPN2.6 and SHAM). The means of micronucleus were compared to the SHAM group.

2.11 Computed Microtomography of rats' calvaria.

Immediately after the euthanasia, the calvarias were dissected and fixed with 10% buffered formaldehyde for 24 hours and kept in 70% ethanol up to the analysis. Prior to the microcomputed tomography scanning specimens were left to dry at room temperature for at least 60 minutes. We scanned 5 calvarias per group. Scanning was performed using SkyScan 1278 with 84.6 µm of pixel size, 53kV, 0.5 mm of Al filter and 0.18° of rotation. For the image reconstruction a correction of 10% of Beam

Hardening was applied together with a ring artefact correction of 5 and Gaussian smoothing of zero. The amount of bone formed within the defect was calculated as a percentage of the total volume of a pre-determined volume of interest and normalized by the mean values of the SHAM group (which represented 100%). The amount of bone found in the control group served as a blank that was subtracted from the other values.

3.0 Results

3.1 pH behaviour in culture media containing bioactive glasses

It is known that pH is a variable that significantly affects cell behaviour. For the cell culture experiments we decided to remove this variable in order to investigate the precise role of the ionic products derived from glass dissolution. For this, we studied the kinetics of media buffering in the cell incubator over time to determine how long it would take to neutralize media's pH.

We observed that all glass compositions caused an increase in pHand this is attributedto the release of positively charged ions such as Ca^{2+} and $Na^{+}$from the glass into the cell medium. After 24 hours mixing the different glass compositions in media at a concentration of 10 mg/ml we measured their pH. The pH reached 10.27 in the medium conditioned with BG45S5 and 9.46 in the group BGPN2.6 (Figure 2). No glass was added to the control group (growth medium) and osteogenic group (osteogenic medium) and their pHs were 7.77 and 8.22 respectively.

Cell culture medium containing living cells tends to become acidic over time due to normal cell metabolism reactions. The chemical reaction between HCO_3^- present in the cell medium and the CO_2 present in the cell incubator is responsible for buffering the system maintaining medium's pH around 7.4-8.0 which is suitable for living mammals cells. We observed that it takes 4 hours inside the incubator for the media's pH to reach physiological levels (Figure 1). Thus, to exclude pH as a variable all media were left to buffer in cell incubator for 4 hours prior being used to treat cells as it is wekll known that the body will naturally buffer the pH.

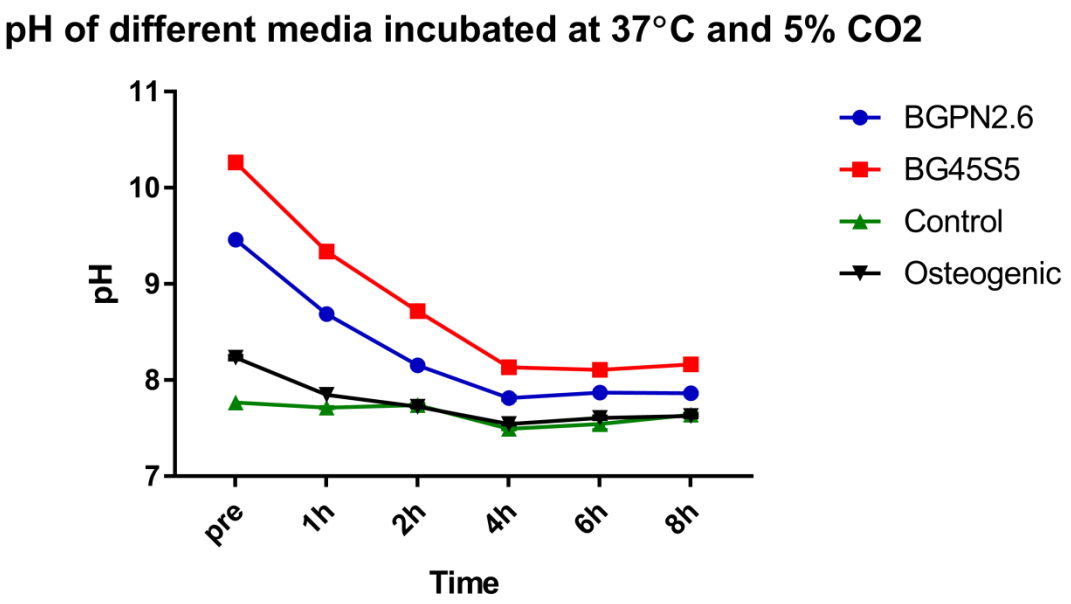

Figure 3. pH variation of different culture media along 8 h of incubation at 37ºC and 5% CO_2. It takes 4 hours inside the cell incubator for the media's pH to reach physiological levels (7.4 – 8.0).

3.3 Viability of bone-marrow-derived MSCs

The survival of Normal Human Osteoblasts (NhOsts) within the different media over 72 hours was assessed using MTT and Live/Dead assay. It can be seen in figure 4 that none of the glass-conditioned media were cytotoxic to the cells. It proves that the addition of niobium dioxide (Nb_2O_5) did not compromise the cytocompatibility of BG45S5 and can replace phosphorous pentoxide (P2O5) without damaging living cells (Figure 3).

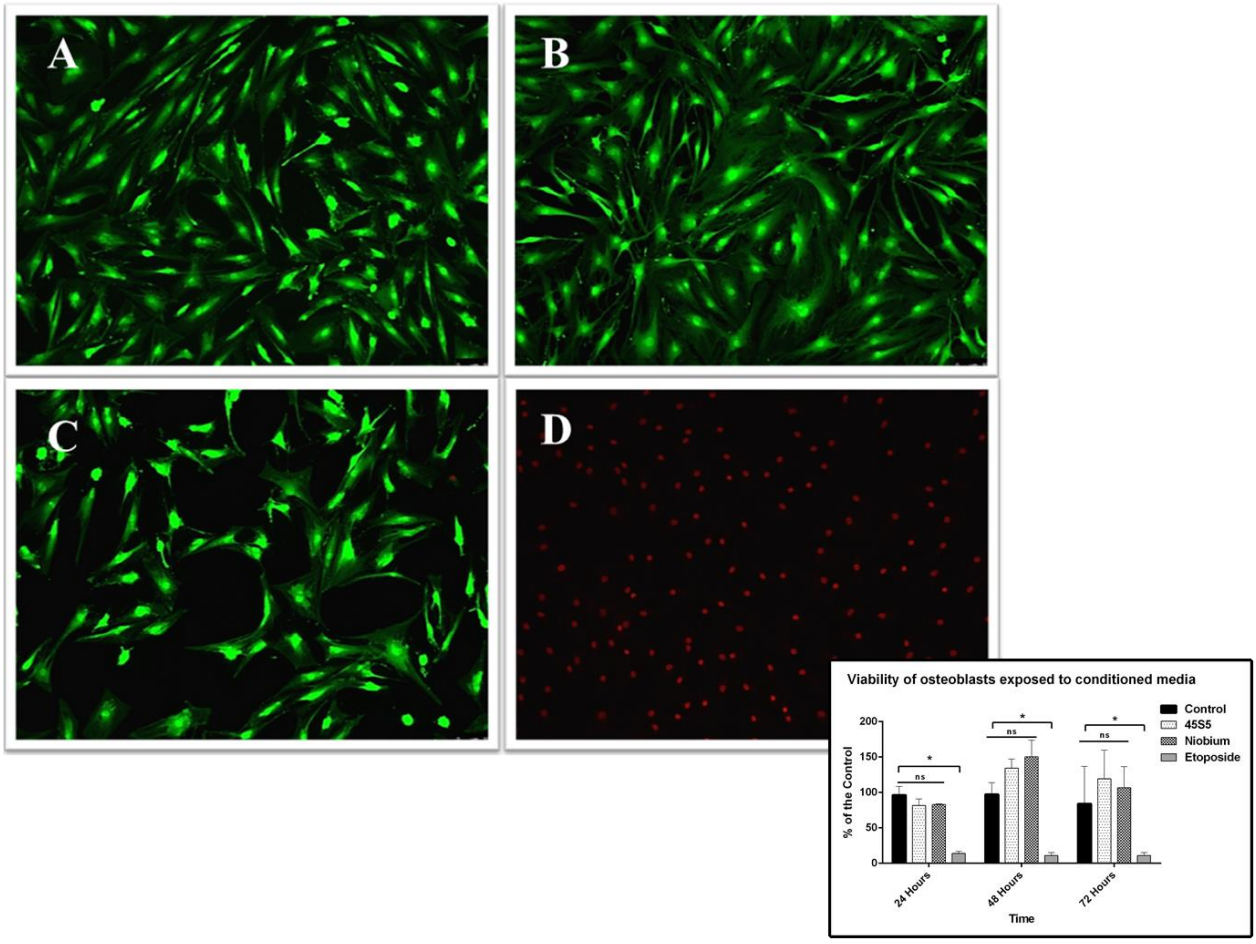

Figure 4. Viability of Normal human Osteoblasts (NhOsts) after 72 hours of treatment with Control Medium (A), BG45S5 (B), BGPN2.6 (C), and ETOPOSIDE (D). None of the glass conditioned media was cytotoxic to the human osteoblasts. Quantification of MTT assay displaying the absorbance as % of the control group. No significant difference was observed between groups treated with glass- conditioned media and the control group (ns bars). All groups showed significantly higher viability than the negative control group (*). Live/Dead assay photomicroscopies of NhOsts treated with the different media for 72 hours (100 x magnification). Living cells appear in bright green whereas the dead cells appear in red.

3.4 Systemic Biocompatibility

3.4.1 Biochemical Markers

In all groups the levels of TGO/AST, TGP/ALT and were similar to those of the control and SHAM groups (Figure 3, upper row). This result shows that the presence of implants did not cause any kind of damage to the hepatic cells. Results of the levels of renal (Creatinine) and cardiac (Total CK) biochemical markers support the claim that

these materials are biocompatible as none of them showed significant difference between the glass-treated rats and those from the control and SHAM groups (Figure 3, bottom row).

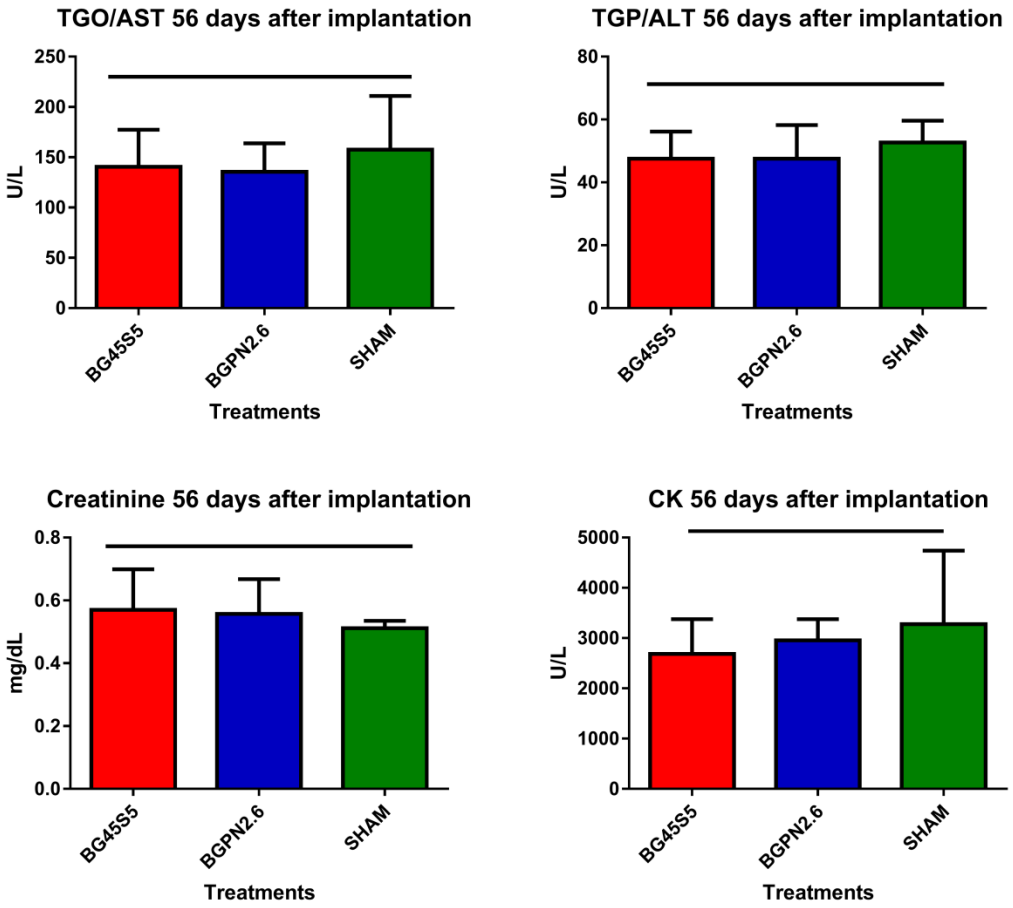

Figure 5. Concentration of biochemical markers of hepatic, renal and muscular damage after 56 postoperative days. Data are displayed as mean and SEM. One- way ANOVA and Tukey's post-test were performed to compare the experimental groups (BG45S5 and BGPN2.6) to SHAM group. No significant difference was found between treatment groups and SHAM group. This result reveals that none of the glass compositions were toxic to these three organs.

3.4.2 Histopathology

Histological sections of liver and kidneys were stained with Haematoxylin and Eosin and were qualitatively analysed. We looked for any sign of tissue damage or cellular disturbance. A thorough examination of the organs confirmed the results for the biochemical markers. After 56 postoperative days no organ showed any noticeable sign

of damage (Figure 5). In the livers all hepatocytes presented normal morphology as did the hepatic parenchyma, showing no aggregates of connective tissue or any inflammatory cell which could be sign of toxicity (Figure 5, upper row). In the kidneys, their functional units, the glomerulus appeared normal as well as the proximal and distal convoluted tubules (Figure 5, bottom row). Just as in the liver, no sign of inflammation or tissue damage was observed in any group attesting the integrity of the kidneys.

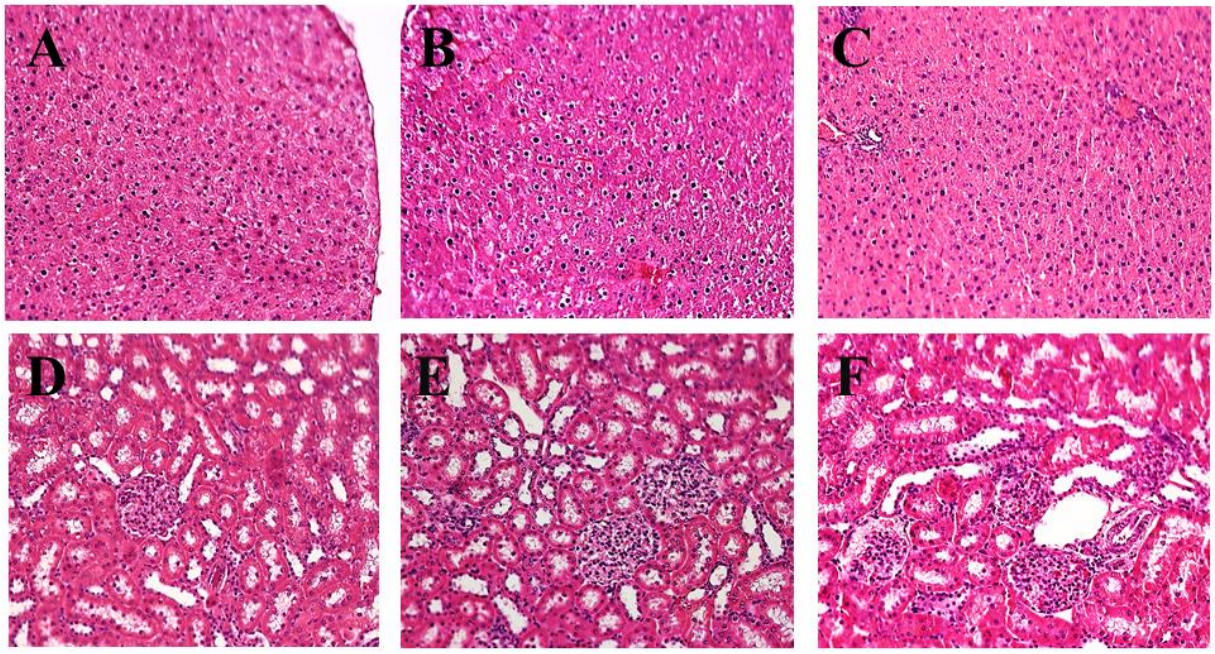

Figure 6. Photomicrographies of histological sections of liver (upper row) and kidneys (lower row) after 56 postoperative days. Magnification 200 x. Haematoxylin and Eosin staining. No signs of damage were observed in any of the analyzed organs. None of the glass compositions were toxic to these organs.

3.4.3 Mutagenic Potential

The carcinogenic risk of Nb-containing glass was tested by means of the micronucleus test (MN) which is a method for to assess chromosomal damage in cells exposed to genotoxic agents. We counted 3000 erythrocytes per animal and compared the mean of each group with the SHAM group. The SHAM group exhibited, on average, 1.87 micronucleus in a thousand erythrocytes. No significant difference was observed between the experimental groups and the SHAM group (Figure 6). This result

reveals that none of the glass compositions are genetically toxic and display no mutagenic potential.

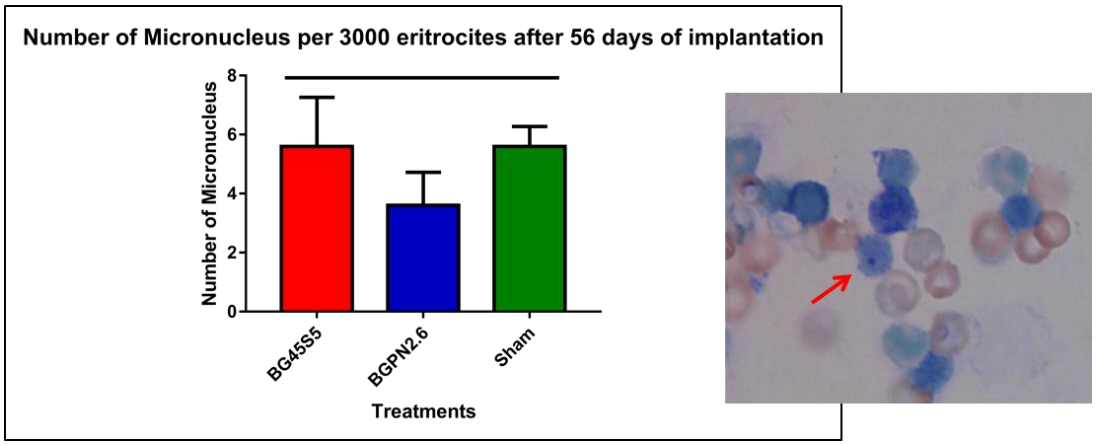

Figure 7. Number of micronuclei per 3000 erythrocytes. Data are displayed as mean and SEM. One- way ANOVA and Tukey's post-test were performed to compare the experimental groups (BG45S5 and BGPN2.6) with SHAM. No significant difference was found between the experimental groups and the SHAM group (p=0.0863). This result shows that none of the glass compositions possesses mutagenic potential.

3.5 MicroCTs of rat calvaria

The regeneration of a 5 mm calvarial defect was assessed by means of microcomputed tomography (microCT). This analysis is a powerful tool for the evaluation of bone tissue because it provides access to the 3D microarchitecture of the bone. In the present work the qualitative and quantitative microCT analysis of the rat`s calvarias were performed *ex vivo*. MicroCT images showed that the calvarial defect maintained its size even 56 days after surgery in the control group, proving to be a critical-sized defect. The treatment with BG45S5, on average, filled 65.63% of the bone defect whereas BGPN2.6 filled 91.66% of the defect, on average. In one rat BGPN2.6 completely filled the defect (figure 7).

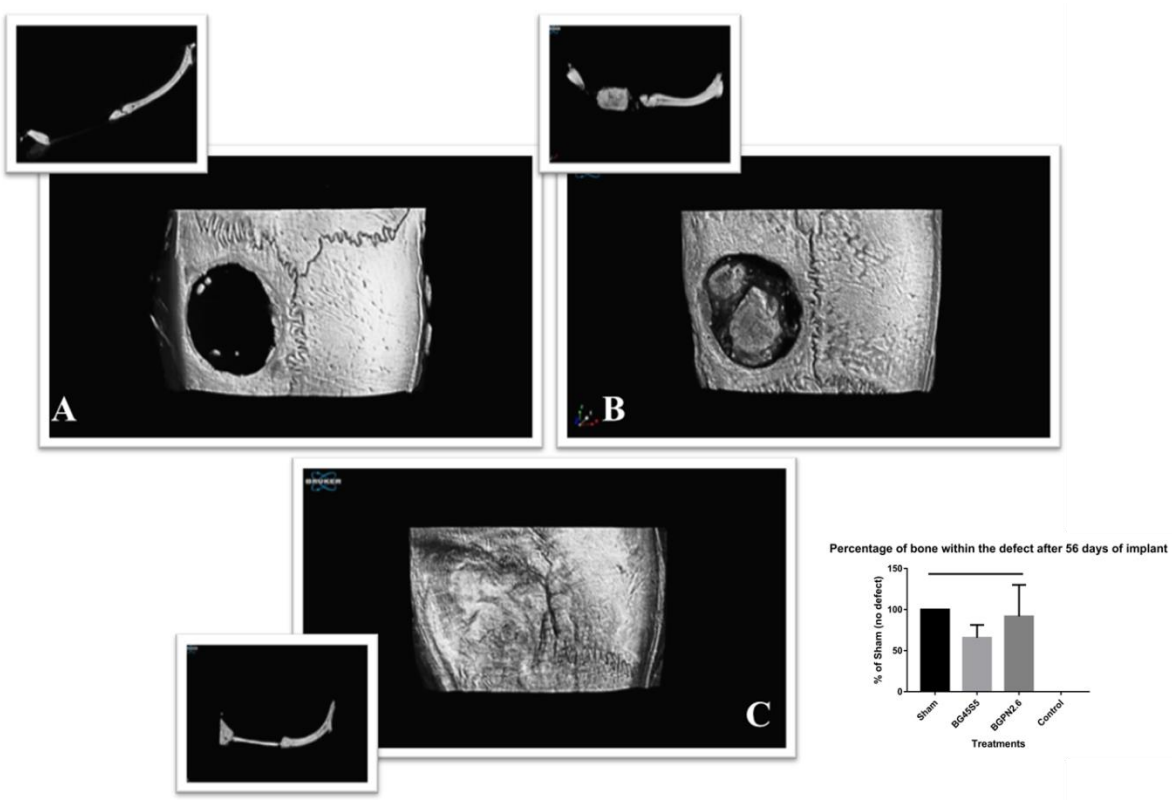

Figure 8. 3D reconstructions of microcomputed tomography images of rats' calvarias of the three experimental groups (Upper row). Tranversal sections of the calvarial defect of the three experimental groups. Imagens taken after 56 postoperative days using SkyScan 1278. Almost no bone formation can be observed in the control group after 56 days. The group treated with BG45S5 showed a good amount of bone within the defect yet not enough to completely fill it. The composition BGPN2.6 was the only one that was able to completely fill the 5 mm calvarial defect after 56 days in one of the subjects.

4.0 Discussion

We performed both *in vitro* and *in vivo* analysis in order to verify the biological properties of Nb-cointaining bioactive glass. The glass showed great biocompatibility as it was compatible with normal Human Osteoblasts (NhOsts) in the *in vitro* assay and in the *in vivo* experiments it did not compromise high metabolic and excretory organs such as liver and kidneys along 8 weeks. Through microcomputed tomography we observed that Nb-containing glass was capable of stimulating the regeneration of a 5-mm calvarial defect in 56 days.

When implanted into the body a biomaterial for bone replacement must be gentle to its surrounding cells in order to enable efficient osteointegration. Previous reports demonstrated the cytocompatibity of niobium in some other types of biomaterials with several types of cells. Pure niobium discs were shown to be cytocompatible with mesenchymal stem cells derived from human bone marrow (hBMSCs) seeded and grown onto its surface up to 10 days[8]. Cells adhered well to the surface of pure-niobium discs presenting a spread morphology which is an evidence that they were active[8]. Mesenchymal stem cells were also observed to attach and proliferate well onto niobium-doped fluorapatite glass-ceramics. The dissolution products of Nb-doped glass-ceramic were also shown to stimulate greater osteogenic differentiation of hMSCs when mixed with osteogenic medium[10]. Pure metalic Nb also proved to be bioinert when implanted into rats for 4 weeks[24].

Despite the cytocompatibility which is a good sign of non-toxicity we also need to take into account the fact that the implant will progressively dissolve and be replaced by living tissue. Part of its dissolution products and even microscopic particles get into the blood stream and may end up in high metabolic and excretory organs such as liver and kidneys. This is the first time organs have been studied to test the systemic behavior of these materials to ensure that no damage was caused by the dissolution products of Nb-containing glass after 8 weeks (Figures 3 and 4). These results are in accordance with an investigation in which Swiss male mice were treated with a single dose (1 mL) of 3 % niobium oxide (Nb_2O_5) diluted in phosphate-buffered saline (PBS), intraperitoneally (i.p.). In this cited study rats hepatocytes showed some signs of degeneration between the third and seventh day after the intraperitoneal application. However, after 12 days all livers appeared regenerate with cellular mitoses[25]. In our investigation we did not observe signs of degeneration nor regeneration at any of the studied time points. We believe that in the aforesaid investigation they might have provoked a mild hepatic degeneration due to the direct intraperitoneal injection of a higher dose of Nb_2O_5 (~30µg per rat) than ours (~3.4 µg per rat).

The assessment of the genotoxic potential of new biomaterials is imperative. In order to evaluate the genotixicity of Nb-containing glass we performed micronuclei analysis (MA). This is considered to be one of the gold-standard analyses for the recognition of the mutagenic potential of any treatment. In the present study 3000 eritrocytes were taken into account per animal and the number of microcunclei found

was compared to the SHAM group (group in which no fracture nor treatment was performed). Nb-doped glass showed no sign of genotoxicity demonstrating that, at least in this particular dose, niobium is a safe metal to be used in biomaterials. Other metallic ions have been shown to possess genotoxic effects. Vanadium, one of the components of the titanium alloy (Ti-6Al-4V), a well-recognized primary metallic biomaterial for orthopedic implants, can generate long-term health problems such as peripheral neuropathy, osteomalacia and Alzheimers disease[26]. Furthermore, lanthalum and nickel were shown to cause some degree of DNA damage[27,28]. Therefore, Nb-containing glass appears to be a safe biomaterial that causes no cellular or DNA damage being a very interesting candidate for use in biomedical devices for bone replacement.

The osteoestimulative capacity of Nb-containing glass was tested by treating critical-sized calvarial defect for up to 8 weeks. A critical size defect is defined as "the smallest size tissue defect that will not completely heal over the natural lifetime of an animal"[29]. For the rat calvarial defect, 8 mm is generally accepted to be of critical size[30]. Nevertheless, we chose to work with 5 mm size defect because it can be made in one rat's parietal bone without crossing the sagittal suture. The sutures are nearly immovable fibrous joints that connect two or more bones. In the case of the sagittal suture it connects the two parietal bones. It is important to take into account the fact that fibrous joints (such as the sagittal suture) show a very different pattern of regeneration from flat bones (such as parietal bones). In view of this, we believe the occurrence of these two different rates of regeneration at the fracture site might constitute an extra variable that could confuse the interpretation of the results as the bioactive glass may interact with these two tissues in different ways. Furthermore, even though our 5 mm size calvarial defect showed very low regeneration along 8 weeks, to avoid any influence of such regeneration over the results the mean value of the control group (empty defect) served as a blank that was subtracted from the means of all other groups.

The analysis of MicroCT images showed that treating circular calvarial defect with Nb-doped glass promoted great fulfillment after 8 postoperative weeks revealing the great osteostimulative capacity of this glass (Figure 6). Our study is the first one to report osteostimulative effects of Nb-containing bioactive glass using critical-sized calvarial defect. Two other studies investigated the osteintegrative properties of other types of Nb-containing biomaterials[8,13]. Wang at al. implanted Ti–Nb–Zr–Ta–Si alloy into rabbit's femur to assess its mineral apposition rate and bone-implant contact[13]. The

authors concluded that Ti–Nb–Zr–Ta–Si alloy showed significantly higher mineral apposition rate compared to CpTi implants after 4 postoperative weeks and showed no difference in bone-implant contact (BIC). They suggested that Ti–Nb–Zr–Ta–Si alloy had favorable biocompatibility and had an effect on the promotion of osteogenesis[13]. Furthermore, Bartolomé and colleagues verified the biological tolerance of new zirconia/Nb biocermets implants in rabbit's tibias. Their results showed effectiveness of osseointegration after 6 postoperative months as new bone was observed around the implants at retrieval date[8]. Together these results indicate that the presence of niobium in the bulk of biomaterials seems to improve material's biocompatibility and increases bioactive properties such as osteoconduction and osteostimulation.

It is important to considerate that the calvarial defect serves as a model for intramembranous bone formation and thus may be less applicable to biomaterials or strategies for endochondral bone formation[30]; thus, this result may be applicable mainly for large fractures in flat bones such as those of the skull, ribs, pelvis and some parts of the vertebras.

5.0 Conclusion

In summary we conclude that the Nb-containing glass BGPN2.6 is not cytotoxic to Human Osteoblasts. Its biocompatibility was confirmed by the results of the *in vivo* experiments that showed the material does not cause any harm to high metabolic and excretory organs such as liver and kidneys. Moreover, the Nb-containing glass does not show any genetic toxicity, therefore can be used without risk of mutagenicity. These results attest this glass composition is biocompatible and, up to the used concentration, can be implanted into the body without any harm. Microcomputed tomography demonstrated that Nb-doped glasses stimulated the regeneration of a large calvarial defect and the results showed a 40% increase in defect repair compared to 45S5 bioglass. Taken together these results support the claim that Nb-containing bioactive glass is a safe and efficient biomaterial that can be used for bone replacement.

Acknowledgments

The authors acknowledge the use of the analytical instrumentation facility at Institute of Chemistry - University of Campinas, which is supported by the State of

Paulo. This work was carried out with the support of the São Paulo Research Foundation – FAPESP (Grant: 2016/24372-2) and The National Council for Scientific and Technological Development (CNPq/PIBITI) and the Coordination for the Improvement of Higher Level -or Education- Personnel (CAPES) for the financial support. We also would like to acknowledge Prof. Dr. Antonio Carlos Boschero for providing us with the SkyScan 1278 (FAPESP EMU 2009/54121-8) for the μCT analysis.

Author Contributions

J. H. L. and L. P. L. S. produced the bioactive glasses. L. P. L. S conceived and performed the experiments and analyzed the results. J. H. L. and L. P. L. S. wrote the paper. All authors reviewed the paper.

Additional Information

Competing financial interests: The authors declare no competing financial interests.

PART TWO: THE DEVELOPMENT AND CHARACTERISATION OF GALLIUM DOPED BIOACTIVE GLASSES FOR POTENTIAL BONE CANCER APPLICATIONS

Objectives of this study

In this study, we have developed a series of novel gallium oxide doped bioactive glasses to specifically target osteosarcoma cells whilst aiding new bone formation. The methods and results of this study are described in the following scientific paper:

Article 4: ***The development and characterisation of gallium doped bioactive glasses for potential bone cancer applications.*** **(Published in the journal: ACS Biomaterials Science & Engineering. DOI: 10.1021/acsbiomaterials.7b00283)**

ARTICLE 4: The development and characterisation of gallium doped bioactive glasses for potential bone cancer applications.

Karan Rana, **Lucas Pereira de Souza**, Mark A. Isaacs, Farah Raja and Richard A. Martin*

Aston Institute of Materials Research, School of Engineering & Applied Science and Aston Research Centre for Healthy Ageing, University of Aston, Birmingham, B4 7ET, UK.

Corresponding Author

*Email: r.a.martin@Aston.ac.uk. Tel.: +44 (0)121 204 5111

ORCID

Richard A. Martin 0000-0002-6013-2334

Notes

The authors declare no competing financial interests regarding this work.

ABSTRACT

In this study we have developed a series of novel gallium oxide doped bioactive glasses to specifically target osteosarcoma cells whilst aiding new bone formation. The results show that osteosarcoma (Saos-2) cell death is induced through the addition of gallium oxide. Relative to the gallium-free control glass (0% Ga) glasses containing 1, 2 and 3% Ga decreased Saos-2 cell viability in a dose dependant manner. After 72 hours in media preconditioned with 3% Ga Saos-2 cell viability was reduced by over 50%. Corresponding studies undertaken on primary normal human osteoblast cells (NHOst) demonstrated no adverse effects to the gallium containing glasses. Hydroxyapatite formation was observed for all glasses when exposed to simulated body fluid.

INTRODUCTION

Survival for osteosarcoma patients is poor despite the aggressive use of surgery, chemotherapy, and/or radiotherapy[1]. Therefore, to improve the clinical outcome safe and effective therapeutic materials are required. The minimum key requirements for an effective biomaterial targeted towards osteosarcoma therapy are (1) to successfully eradicate any residual tumour not excised during the surgery without being cytotoxic to the surrounding tissue and (2) to provide a suitable platform for the regeneration of new bone. A potential solution to this problem is to engineer materials capable of replacing damaged tissue whilst simultaneously preventing reoccurrence and/ or metastases of tumours after surgery. The development of synthetic alternatives that help regenerate bone by acting as active temporary scaffolds is associated with considerable research activity. However there have been very few reports of synergistic scaffolds which can help manage cancer and simultaneously promote wound healing.

Bioactive glasses are one of the most promising bone replacement/ regeneration materials because they bond to existing bone, are degradable and can stimulate new bone growth by the action of their dissolution products on cells[2,3]. Bioglass®, $(SiO_2)_{46.1}(CaO)_{26.9}(Na_2O)_{24.4}(P_2O_5)_{2.6}$, exhibits class A bioactivity meaning it bonds to bone and stimulates new bone growth even away from the glass–bone interface[4-6]. Direct comparisons with hydroxyapatite *in vivo* have shown that 45S5 Bioglass® forms a more rapid and stronger bond with bone[7,8]. Bioglass® was originally developed to provide a controlled release of calcium and phosphorous ions under physiological conditions[5]. The calcium and phosphorous ions precipitate into amorphous calcium phosphate which then crystallises into hydroxyapatite to form new bone mineral[9-11]. Bioglass® has received FDA approval and has been in clinical use since 1985. Whilst there has been considerable interest in developing and optimising bioactive glasses for bone regeneration little or no research has been undertaken on bioactive glasses specifically for bone cancer applications.

Gallium (Ga) is the most widely used metal ion for cancer treatment with the exception of platinum[14]. Gallium has the ability to localise in tumour cells via surface transferrin receptors[15]. Based on its clinical efficacy, gallium nitrate (Ganite™) is used as a treatment for cancer-associated hypercalcaemia[16]. Furthermore, gallium nitrate has been shown to inhibit increased bone turnover and to decrease osteolysis in patients

with bone metastases from a variety of different cancers[16]. Bockman *et al* (1995)[17] demonstrated that administrating low, non-toxic doses of gallium nitrate to patients with Paget's disease of bone, a disease characterised by abnormal bone remodelling and increased bone resorption, rendered bone more resistant to resorption by blocking osteoclast function without affecting their viability. Several studies indicate that gallium nitrate may have an application in diseases associated with increased bone loss such as osteoporosis, multiple myeloma and bone metastases. Uptake of bioavailable gallium is however low when administered orally as a salt. The recommended mode of administration for gallium nitrate is therefore via a continuous intravenous infusion for 5–7 days. However, this treatment is very inconvenient since patients receive this drug either intravenously in hospital or as an outpatient via a pump device. A scaffold that can provide a site specific controlled delivery of gallium would therefore be highly advantageous. Gallium ions have previously been incorporated into phosphate based glasses to deliver a controlled antimicrobial effect[18,19]. Wren *et al.* and Towler *et al.* incorporated Ga into bioactive glasses for bone cement applications and for antimicrobial functionality[20-22]. More recently, Frachini *et al*. and Lusvardi *et al.* have incorporated gallium oxide into bioactive glasses for antimicrobial applications[23,24]. However no studies have been undertaken on osteosarcoma cells. The present study therefore investigates the potential of incorporating gallium into bio-degradable bioactive glasses specifically targeted towards bone cancer applications.

MATERIALS AND METHODS

Glass synthesis. Melt-quench derived 45S5 Bioglass, $(SiO_2)_{46.1}(CaO)_{26.9}(Na_2O)_{24.4}(P_2O_5)_{2.6}$, and the gallium doped analogues were prepared using SiO_2 (Alfa Aesar, 99.5%), $CaCO_3$ (Alfa Aesar, 99.95–100.5%) and Na_2CO_3 (Sigma-Aldrich, ≥99.5%), $NH_4H_2PO_4$ (Sigma-Aldrich, ≥99.5%), and Ga_2O_3 (Alfa Aesar, 99.99%)[25]. In brief, the precursors were weighed in the appropriate molar ratio to give $(Ga_2O_3)_X(SiO_2)_{46.1-3X}(CaO)_{26.9}(Na_2O)_{24.4}(P_2O_5)_{2.6}$ where X=1, 2 and 3%. The compositions were carefully selected to maintain a network connectivity of 2.11 which exhibits optimal bioactivity (see supplementary section). Precursors were thoroughly mixed and placed into a 90% platinum - 10% rhodium crucible. The crucible was placed into a furnace at room temperature and heated at a rate of 10°C min^{-1} to 1450 °C and held at this temperature for 90 min. The melt was then poured into a graphite mould

which had been preheated to 370 °C and annealed at this temperature overnight before being allowed to cool slowly to room temperature.

Glass discs were cut in discs using an IsoMet™ 1000 Precision Diamond Saw (Buehler). Discs, 10mm diameter and 2mm thick, were polished using a MetaServ® (Buehler) polishing machine to a finish of 0.06μm using colloidal silica. Glass particles were prepared using a planetary ball mill (PM100, Retsch) and the particles were sieved to give a size distribution between 40 to 60 microns.

Hydroxyapatite formation. A simulated body fluid (SBF) solution was prepared using the method outlined by Saravanapavan and Hench [26]. SBF emulates the salt ion concentrations found in human blood plasma and can be used to test for the formation of hydroxyapatite *in vitro*. The three gallium containing glasses 1%, 2% and 3% together with the control glass (45S5) were placed in separate containers and 40 ml of SBF salt ion solution was added. The samples were sealed and maintained at 37 °C for 7 days. After reacting in SBF the samples were removed and rinsed with distilled water and acetone to remove any residual salts and halt reactions. Samples were dried at 60 °C and then assessed for apatite formation using X-ray diffraction.

X-ray diffraction experiments were conducted using a Bruker D8 diffractometer operating at the copper k_α wavelength of 1.54 Å. Finely powdered glasses were measured over a two theta range of 10 to 80° in 0.02° steps. Measurements were taken at one second per point and no smoothing was undertaken.

Dissolution. Stock solutions of 10mg/ml of ground glass in ultra-pure water were prepared for quantitative ionic profile using inductively coupled plasma optical emission spectrometry ICP-OES (iCAP™ 7000 Plus Series). Solutions were maintained at 37 °C for up to 3 days. Reference standards were used to calibrate the concentrations and the amount of each ion was calculated from the linear portion of the generated standard curve.

Preparation of conditioned media. Stock solutions of conditioned media were prepared by dissolving glass particles in complete McCoy's 5A medium to treat Saos-2 cells and Clonetics OGM Osteoblast complete growth media to treat osteoblasts. Stock solutions were prepared at a concentration of 10mg/ml and left to incubate in a shaker incubator at 250rpm at 37 ºC for 24 hours. Following the 24 hour incubation period,

stock solutions were filtered using 0.2 micron syringe filter. 3ml of each media was taken to record stock solution pH values following glass dissolution. To allow for the natural buffering of the body pH neutralisation was completed by preparing conditioned media and storing it in humidified atmosphere of 5% CO_2/95% air and 37 ºC overnight to allow CO_2 mediated buffering.

Cell culture. Human osteosarcoma (Saos-2) cells were purchased from the American Tissue Culture Collection and maintained in McCoy's 5A medium containing 1.5mM L-glutamine and 2200mg/L sodium bicarbonate. Media was supplemented with 1% penicillin, streptomycin and 15% fetal bovine serum (FBS). Primary Normal Human Osteoblasts (NHOst) were purchased from Lonza and cultured in Clonetics OGM Osteoblast growth media supplemented with 10% FBS, 1% L-glutamine and 1% penicillin, streptomycin. Both cell lines were maintained at 37 ºC in a humidified atmosphere of 5% CO_2/95% air.

Live/Dead cell viability assay. 10,000 cells per well were seeded of both Saos-2 and NHOst cells and treated for 72 hours with conditioned media containing the dissolution products of 45S5, Ga 1, 2 and 3% at a concentration of 10mg/ml. Following the incubation period, a positive control of dead cells was established by incubating cells with 70% ethanol for 30 minutes. Cells treated with regular growth media served as a negative control. The polyanionic dye calcein-green is retained within live cells, producing an intense uniform green fluorescence. Ethidium homodimer-1 (EthD-1) enters cells with damaged membranes and undergoes a 40-fold enhancement of fluorescence upon binding to nucleic acids, thereby producing a bright red fluorescence in dead cells. To stain Saos-2 cells working concentrations of calcein-green at 0.5µM and EthD-1 at 2.5µM were combined into one solution and used to treat cells, and to treat NHOst cells both calcein-green and EthD-1 were both prepared at a concentration of 0.5µM. Cells were overlaid with 100µl of staining solution and left to incubate for 45 minutes at room temperature. Cells were photographed using a fluorescent microscope at 100X magnification.

Cell cytotoxicity and proliferation. Cytotoxicity was analysed using MTT viability assay (Thermo Fisher), where 5000 cells per well of both Saos-2 and NHOst cells were cultured using conditioned media containing 10mg/ml respective glass compositions, for a period of 72 hours. 10µM Etoposide was used as a positive control,

while cells grown using normal cell media served as a negative control. For the MTT assay, a 12mM stock solution of 3-(4.5-dimethylthiazol-2-yl)-2.5-diphenyltetrazolium bromide (MTT) was prepared as per manufacturer's instructions and diluted 1/10 in phenol red free media before being added to the cells, which were incubated for 4 hours at 37 ºC. Following the incubation 75µl of treatment was removed and 50µl of Dimethyl sulfoxide (DMSO) was added and left to incubate at 37 ºC for 10 minutes. Metabolically active cells reduce MTT to formazan and after formazan extraction the optical density was measured using a spectrophotometer (at 570 nm). This assay was performed in quintuplicate.

Statistical analysis.

Experiments described above were performed with at least three independent samples per data point. Data were analysed using SPSS version 21 and GraphPad Prism 6. MTT, ICP and pH results are expressed as the mean ± standard deviation. To compare cell viability between different time points and glass compositions Two-way ANOVA and Tukey's multiple comparisons test was conducted to test for significance with statistically significant values defined as $P < 0.05$. Fluorescent microscopy and Live/Dead staining was used to distinguish between viable and non-viable cells results are qualitative and clearly indicate cell cytotoxicity or lack of.

RESULTS

Glasses and hydroxyapatite formation. A series of gallium doped bioactive glasses were successfully prepared. 45S5 Bioglass was used as the control glass and gallium oxide was incorporated into the remaining bioactive glasses with increasing concentrations (1, 2 and 3% Ga_2O_3). As shown in **Figure 1(a)** the glasses were completely amorphous with no visible signs of Bragg peaks when examined using X-ray diffraction. A broad peak has previously been reported for Bioglass[10] and corresponds to the calcium silicate[27]. After placing the glasses in a simulated body fluid (salt ion solution at 37 °C) for 7 days a visible layer of amorphous calcium phosphate /apatite was observed to have formed on the glass surface. X-ray diffraction confirmed the surface layer was an amorphous calcium phosphate / poorly defined highly substituted apatite[28] (**Figure 1b**) which is consistent with results typically observed for bioactive glasses[10]. The feature ~ 26° corresponds to the 002 reflection which preferentially occurs and has been previously reported for bioactive glasses[29]. The

second feature ~ 32° whist still broad (FWHM of 1.5° is significantly narrower that the unreacted glass (FWHM 5.4°). This feature is assigned to overlapping 211, 112 and 300 reflections (Franchini *et al.*[24]). No reduction in apatite formation was observed for the gallium containing glasses compared to the 45S5 standard.

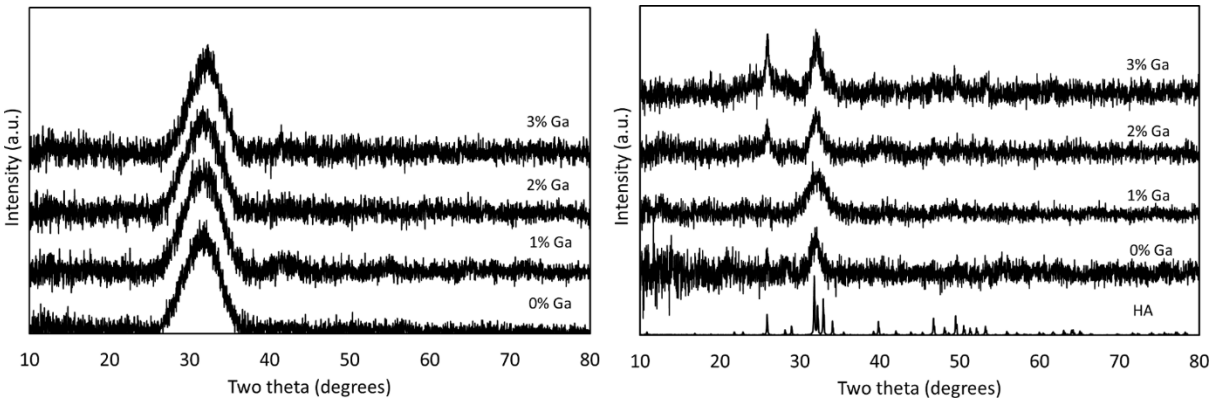

(a) (b)

Figure 1 (a) X-ray diffraction spectra of the unreacted bioactive glasses, (b) XRD spectra of bioactive glasses after exposure to simulated body fluid for 7 days and hydroxyapatite is shown for reference.

ICP analysis of dissolution products. To determine the concentration of ions released from the bioactive glasses ICP analysis was conducted. The concentration of gallium ions released in distilled water as a function of time for 10mg/ml solutions are given in **Figure 2**. A rapid release of ions was observed during the first few hours followed by a slower more gradual increase in ion concentration.

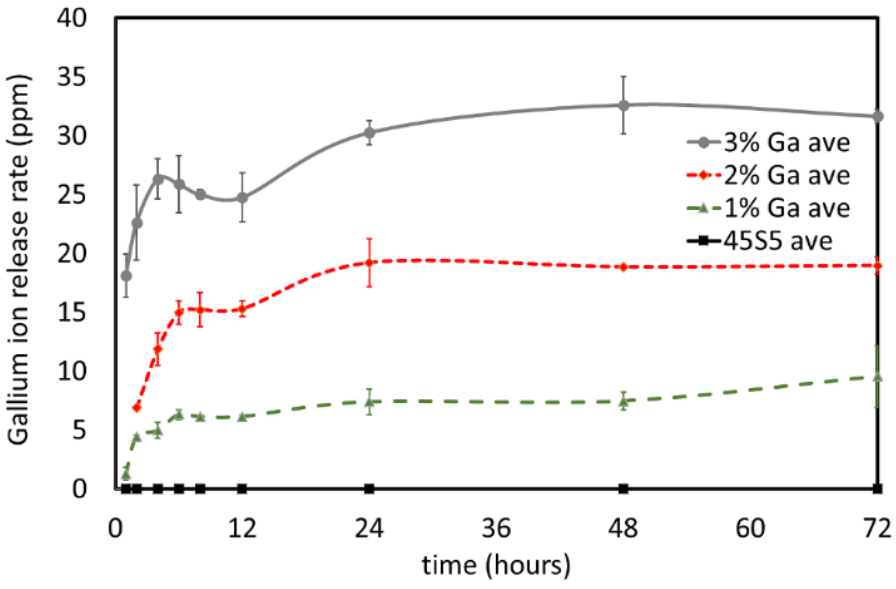

Figure 2. Release of Gallium ions from 45S5, 1, 2 and 3% Ga doped bioactive glasses.

As expected the concentration of gallium ions increases in an approximately linear trend with increasing gallium oxide content. At 24 hours the average gallium ion concentrations were 7.3, 18.8 and 30.2 ppm for the Ga1%, Ga2% and Ga3% respectively. The gallium concentration approximately stabilised after 24 hours and minimal increases in concentrations were observed at 48 and 72 hours. The release rate of Ca, P and Si is essential for upregulating gene expression[3]. The ion concentrations are not significant for altered Ca, P and Si due to the incorporation of gallium oxide into the glasses. For example, at 24 hours the concentration of Si is 65, 70, 61 and 67 ppm for 45S5, 1%, 2% and 3% respectively.

Conditioning media and pH neutralisation. During this study experiments were performed using indirect methods as direct contact measurements can cause false positive results due to the rapid increase in pH *in vitro* which is not representative of the *in vivo* environment. For example *in vitro* studies have indicated that bioglass is antimicrobial however *in vivo* studies by Xie *et al* have shown that this result is a false positive since pH in the body at the site of bioglass implantation cannot increase to the level necessary to inhibit bacterial growth[30]. Allan *et al* and Begum *et al* have also shown that following pH neutralisation bioglass-conditioned media loses it antimicrobial efficacy[31,32]. Is it also known that pH fluctuations have the same effect on cells, which is why preconditioning is sometimes required for bioactive glasses[33].

Furthermore the dissolution products will circulate more widely though the body and are therefore more like to prevent metastasis compared to direct contact with the bioactive glass. The conditioned media was prepared by adding 10mg/ml of bioactive glass to McCoy's media and incubating at 37 °C for 24 hours in a shaking incubator. As shown in **figure 3** the conditioned media shows a significant rise in pH as sodium and calcium ions rapidly leach from the glass in the surrounding media. pH readings taken directly after conditioning the media are designated as time point 0 in Figure 3. Deviations from neutral pH are known to have detrimental effects on cell viability/proliferation, furthermore it is known that the body naturally buffers pH. Therefore the conditioned media was incubated at 37 ºC in a humidified atmosphere of 5% CO_2 for up to 72 hours to buffer the pH. McCoy's media was used as a control and

it is clearly evident over the course of 72 hours the pH of the media fluctuates marginally from 7.91 at time point 0 to 7.23 at 72 hours, both readings within the physiological pH range acceptable for cell growth and maintenance. In contrast 10mg/ml of 45S5 bio-active glass significantly elevates the pH of the media and at time point 0 a reading of 10.3 was recorded and a gradual decline was observed over the course of 72 hours (1 hour, 9.4, 2 hours, 8.65, 8 hours 7.85). Conditioned media generated by the addition of 10mg/ml of 1, 2 and 3% gallium doped bioactive glass also exhibits a similar trend, as a high pH was recorded for each glass composition at time point 0 (Ga1%, pH 9.45, Ga2% pH 9.26 and Ga3% pH 9.37). At 24 hours the pH of all gallium containing conditioned media had decreased to physiologically acceptable levels where cell growth is viable (Ga1%, pH 7.77, Ga2% pH 7.81 and Ga3% pH 7.87). Beyond 24 hours negligible changes in pH were observed. Therefore in following experiments the media was conditioned for 24 hours and then placed in the incubator for 24 hours to neutralise before being used. Neutralising the pH in this way eliminated any potential cytotoxic effects of the glass conditioned media due to lethal pH.

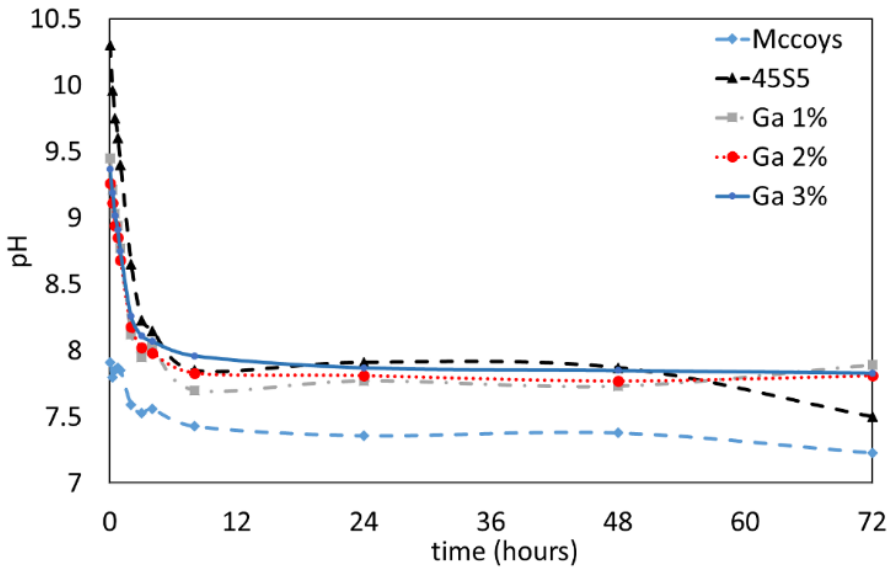

Figure 3. pH measurements of conditioned media cell treatments taken over the course of 72 hours.

Conditioned media containing respective bioactive-glass at 10mg/ml was incubated at 37°C in a humidified atmosphere of 5% CO_2/95% air. At timed intervals pH readings were recorded. McCoy's media was used a negative control.

Live/Dead Staining for cell cytotoxicity. Conditioned media containing 3% gallium oxide significantly increases osteosarcoma (tumorous) cell death relative to the 1% and 2% Ga glasses and 45S5 control as shown in **Figure 4**. A significant increase in dead cells was observed between the 45S5 control glass and the 1% and 2 % Ga glasses whilst at 3% all cells appeared dead. In contrast all the glasses including the 3% gallium remained non-toxic to primary normal human osteoblast (non-tumorous) cells (**Figure 5**).

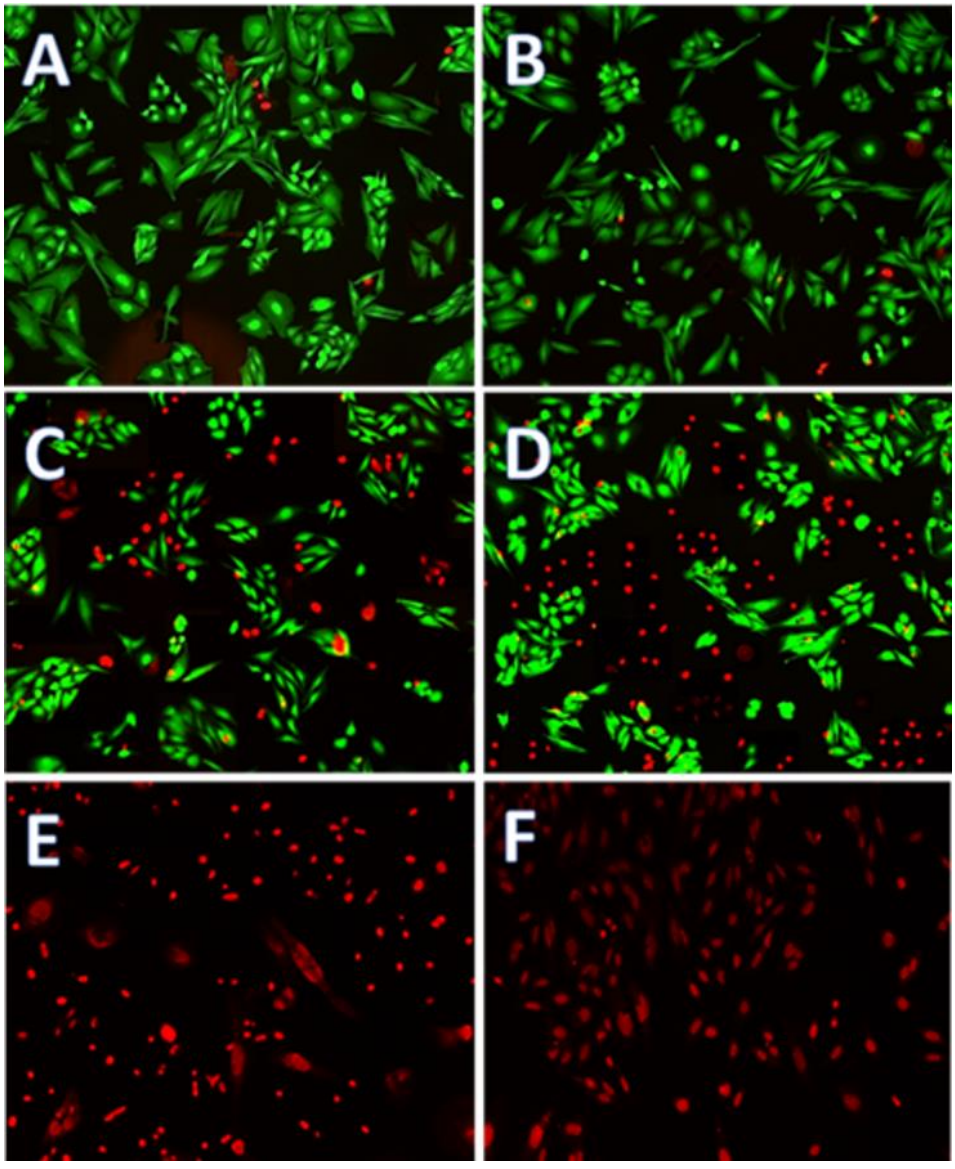

Figure 4. Fluorescence images of Live/dead staining of HTB-85 Saos-2 cells cultured for 72 hours in conditioned media containing bio-active glass after pH neutralisation. 5000 cells were seeded and left to attach for 24 hours. Following attachment cells were treated with A) Mccoy basal media, B) conditioned media

containing 45S5 bioactive glass, C) conditioned media containing 1% gallium, D) conditioned media containing 2% gallium, E) conditioned media containing 3% gallium and F) 1mM Etoposide treatment as a positive inducer of cell death. All conditioned media treatments were prepared at 10mg/ml of the respective glass. Images were taken using a fluorescent microscope at 100x magnification.

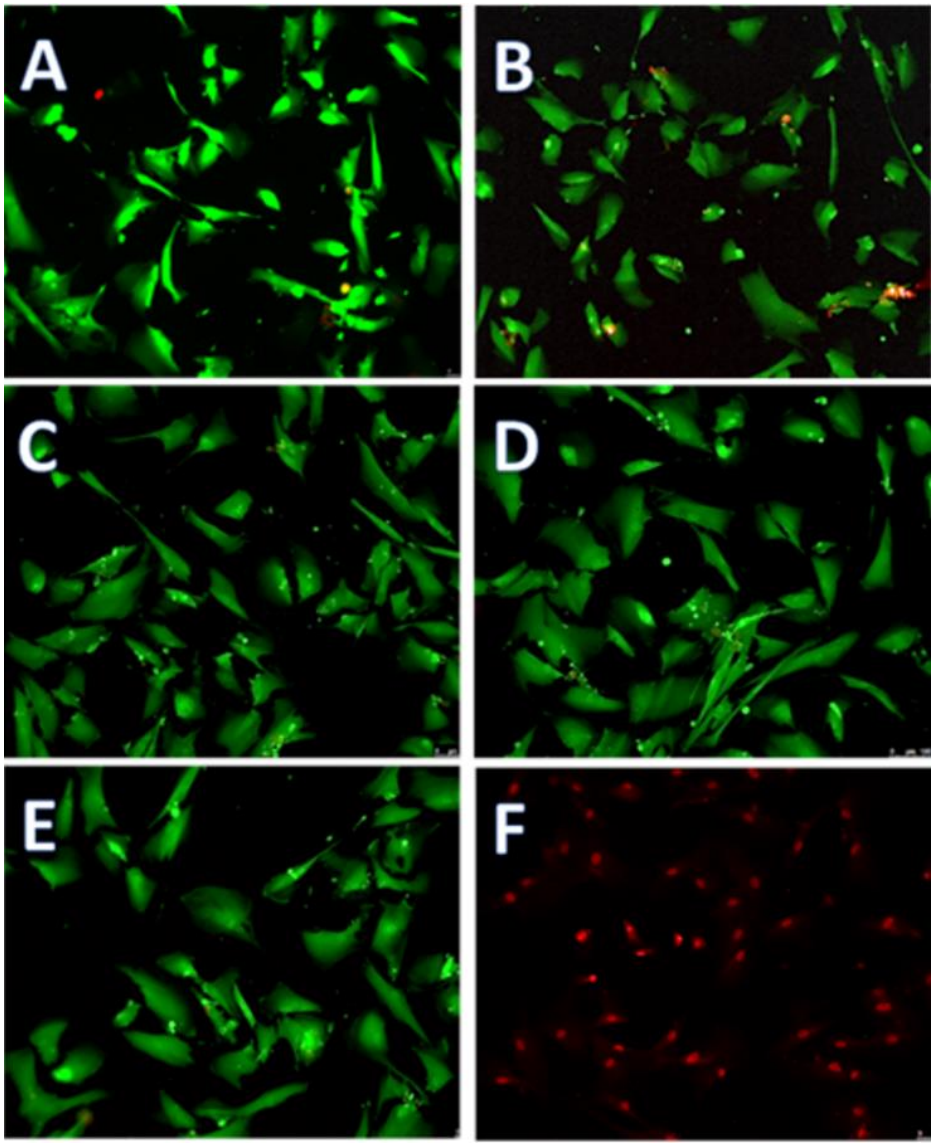

Figure 5. Fluorescence images of Live/dead staining of NHOst-Osteoblasts cultured for 72 hours in conditioned media containing bio-active glass. 5000 cells were

seeded and left to attach for 24 hours. Following attachment cells were treated with A) OBM basal media, B) conditioned media containing 45S5 bioactive glass, C) conditioned media containing 1% gallium, D) conditioned media containing 2% gallium, E) conditioned media containing 3% gallium and F) 1mM Etoposide treatment as a positive inducer of cell death. All conditioned media treatments were prepared at 10mg/ml of the respective glass. Images were taken using a fluorescent microscope at 100x magnification.

Osteosarcoma and osteoblast cell viability. The cytotoxicity of conditioned media containing 1, 2, 3% gallium at 10mg/ml was assessed using the MTT assay on both osteosarcoma and osteoblast cells. No significant reduction in Saos-2 cell viability was observed between the positive control (unconditioned media) and the gallium free control glass (45S5). However a steady but significant decrease in Saos-2 cell viability was observed with increasing gallium oxide content in a dose response manner (Ga 2% $p < 0.01$ and Ga3% $p < 0.0001$) as shown in **Figure 6**. After 72 hours in conditioned 3% Ga conditioned media Saos-2 cell viability was less than 50%. In contrast conditioned media from the glasses showed no cytotoxic effects against osteoblast cells as shown in **Figure 7**. In each experiment 10nm etoposide was used as a positive control and a known inducer of cell death ($p < 0.0001$).

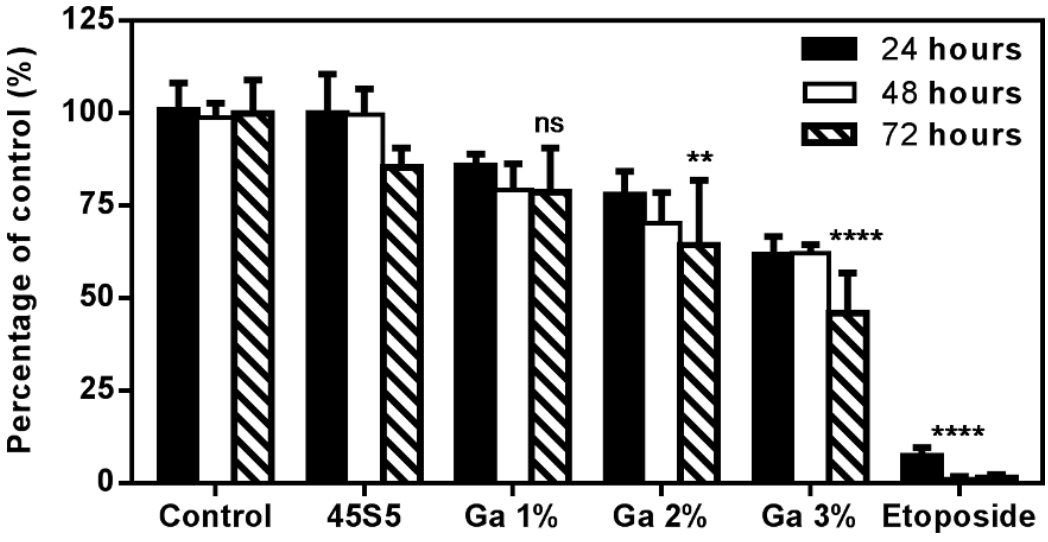

Figure 6. SOAS-2 cell viability following treatment with pH neutralised conditioned media containing 10mg/ml bio-active glass compositions over 72 hours.

SOAS-2 osteosarcoma cell viability was determined following treatment with conditioned media containing 10mg/ml 1% Gallium, 2% Gallium, 3% Gallium and

compared to 45S5 as a control. 10µM Etoposide was used a positive control (p = <0.0001). Two-way ANOVA and Tukey's multiple comparisons test was conducted to test for significance, data are presented as mean ± SD. Significance was set at p = <0.05, N = 4.

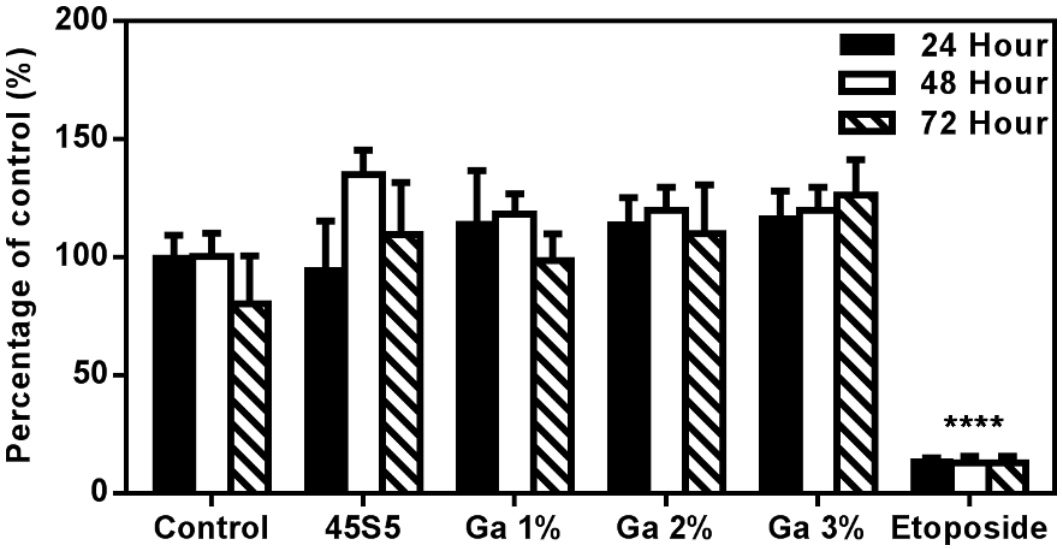

Figure 7. NHOst cell viability following treatment with conditioned media containing 10mg/ml of bio-active glass compositions over 72 hours.

NHOst osteoblast cell viability was determined following treatment with conditioned media containing 10mg/ml 1% Gallium, 2% Gallium, 3% Gallium and compared to 45S5 as a control. 10µM Etoposide was used a positive control (p = <0.0001). Two-way ANOVA and Tukey's multiple comparisons test was conducted to test for significance, data are presented as mean ± SD. Significance was set at p = <0.05, N = 4.

DISCUSSION

Orthopaedic products based on Bioglass® 45S5 have been used in a wide range of bone regeneration applications. These applications include trauma arthroplasty, spine fusion and the general filling of bone defects after cyst or tumour removal[34,35]. In essence bioactive glasses are biodegradable controlled release materials. Bioglass 45S5 provides a controlled release of Ca and P ions which precipitates into hydroxyapatite, and through the controlled release of Ca, P and Si gene expressions are upregulated. Considerable research effort has been devoted to modifying and enhancing the delivery

of ions. For example, cobalt ions have been added to bioactive glasses to enhance vascularisation[36,37] whilst silver ions have been incorporated to enhance the antimicrobial properties of bioglass[38]. To date there have been no reports of bioactive glasses being tailored specifically for bone cancer applications. Whilst there have been alternative bioactive glasses developed for treating deep seated soft tissue cancers[12,13] these materials do not work through the controlled dissolution of ions and are in fact highly insoluble as they are used to deliver controlled radiotherapy. Consequently this class of materials are unable to promote apatite formation or stimulate gene expression, in addition it is also difficult for the body to excrete these materials.

The present study has successfully incorporated gallium ions into bioactive glasses to specifically target bone cancer applications. Gallium ions have previously been incorporated into bioactive glasses for antimicrobial benefits. However the systems previously studied have been fundamentally different. For example the glasses developed by Wren and Towler were based on modifying glasses for bone cement applications which contained very high concentrations of zinc oxide[20-22]. Consequently those glasses are highly insoluble compared to the glasses developed here. The glasses developed by Franchini, Lusvardi *et al*. also found that when gallium oxide was incorporated the glasses became less soluble due to the stabilising effect of gallium. It took 30 days for glasses with 1.0 and 1.6 mol % to be fully covered in homogenous Ca-P rich layer.

The glasses presented in this study show a rapid release of gallium within an hour of immersion in SBF. It is envisaged that the release of gallium ions will be reduced by the formation of the ACP/apatite layer and that the glasses will dissolve over an extended time period provide a long term therapeutic benefit. Gallium-containing hydroxyapatite has been previously reported where the substituted apatite can accommodate up to 11% Ga ions by mass[39]. In addition gallium is known to preferentially locate in bone[40], it is therefore likely that a significant fraction of the released gallium remains localises in the ACP /apatite layers.

Here through the addition of gallium and by tailoring the silicon content to maintain the network connectivity a series of dose dependant release glasses were manufactured. Live dead staining and MTT cell viability assays both revealed a significant reduction in cell viability for tumorous Saos-2 cells in the presence of

bioactive glasses containing gallium. Glasses containing the highest concentration of gallium demonstrated the greatest reduction in sarcoma cells. Bioglass doped with 3% Ga showed a 50% reduction in viable Saos-2 cells. Gallium containing glasses were found to have no detrimental effects on the non-tumorous primary normal human osteoblast cells compared to the gallium free glass and control media. Gallium ions are known to localise in tumour cells via transferrin receptors[15]. It is noteworthy that tumour cells express a significantly higher number of transferrin receptors, relative to non-cancerous cell types. Existing literature has elucidated numerous mechanisms behind the anti-neoplastic properties of gallium; including altering the three-dimensional structure of DNA, inhibiting DNA polymerase function and dysregulating protein synthesis. Furthermore gallium has been reported to increase cell membrane permeability, thereby destabilising electric charges at the surface of the cell and inducing an increased efflux of calcium from mitochondria and initiating the preliminary steps involved in apoptosis. In addition gallium preferentially locates in metabolically active regions where new bone formation and bone remodelling occurs[40].

Whilst it is envisaged that these glasses would be used as part of a combined therapy, including drug delivery, it is interesting to compare our results directly with recently reported controlled drug release calcium phosphates developed for osteosarcoma therapy. Recently Hess et al. have assessed the efficacy of calcium phosphates doped with cisplatin, doxorubicin (DOX) and co-doped with both drugs[39]. The viability of the osteosarcoma cell line MG-63 was assessed after exposure to the controlled release calcium phosphates for up to 7 days. For samples where DOX was incorporated into the matrix only a 9% kill was reported, Samples with cisplatin beads and DOX loaded in the matrix resulted in a 19% kill of MG-63 cells. The composites co-doped with both cisplatin and DOX loaded beads exhibited the lowest cell viability of 34%[39]. The gallium doped bioactive glasses developed in this work therefore exhibit a comparable toxicity to sarcoma cells compared to calcium phosphate scaffolds loaded with anti-cancer drugs.

Whilst this study has been careful to avoid exposing cells to un-physiologically relevant pH fluctuations, which are more likely to occur *in vitro* and could potentially lead to unrepresentative results it is worth noting that pH fluctuations caused by these bioactive glasses may be potentially beneficial *in vivo*. For example, human osteosarcoma sites can be acidic in nature, the release of sodium and calcium ions from

these bioactive glasses will increase the pH and reducing the acidity. This can be potentially beneficial in two ways; firstly acidosis of intramedullary extracellular fluid can inhibit the proliferation of osteoblasts and secondly raising the pH can prevent spontaneous metastases.

CONCLUSIONS

In conclusion our data has demonstrated that gallium doped bioactive glasses can be designed to selective target bone cancer cell lines, reducing tumorous cell viability by over 50%, whilst still promoting normal human osteoblast cell viability and proliferation. Hydroxyapatite formation was observed when the glasses were placed in simulated body fluid and no reduction in formation was observed for the gallium containing glasses compared to the gallium free 45S5 bioglass control. The gallium doped bioactive glasses provide a localised controlled delivery of gallium ions at the surgical site of interest and has considerable potential clinical applications for bone cancer treatment.

ACKNOWLEDGEMENTS

The authors gratefully acknowledges Osteosarcoma UK for financial support. The authors would also like to thank the surfaces, materials and catalysis group, EBRI, Aston University and Adam F. Lee for use of XRD and ICP.

FINAL CONSIDERATIONS

The whole set of investigations described in this thesis aimed to elucidate crucial aspects of the incorporation of Niobium into the Bioglass®45S5 structure regarding bioactive properties such as osteostimulation, osteoinduction, osteoconduction, and biocompatibility. We also verified the efficacy of incorporating Gallium into biodegradable bioactive glasses to promote death of osteosarcoma cells. So far, our results showed that adding Nb_2O_5 into Bioglass®45S5 improves its bioactivity and stimulates osteogenic differentiation human Embrionic Stem Cells (hESCs) and bone-marrow- derived mesenchymal stem cells (BM- derived MSCs). In addition, the presence of Nb_2O_5 does not compromise the biocompatibility of the original glass composition.

Despite of the fact our results indicate that the tested modifications are promising for the proposed biomedical applications this study presents some limitations that require further investigations. The best approach when it comes to treating large bone defects is the use of porous three-dimensional scaffolds, so, further studies should aim to develop scaffolds made of Nb-doped bioactive glass. A complete investigation of the effects of Ga-doped glass on *in vivo* models of bone cancer should be performed to verify the efficacy in treating cancer as well as to test the biocompatibility of these glasses. Another aspect that our experiments could not clarify was the mechanism by which Nb-doped glasses enhanced bone formation in some experiments. It might have been caused by the glass dissolution products and/or by the effects of the glass surface over protein adsorption and cells adhesion and migration. More investigations should focus on the chemical and topographical characteristics of Nb- containing glass' surface in order to determine how it affects the behaviour of multipotent cells like hESCs and BM-derived MSCs.

To conclude, we believe that developing novel biomaterials for bone replacement our study will reduce the morbidity and to improve the prognostic of millions of victims of fractures. Nonetheless, the knowledge generated by the present work comes to improve the comprehension about the interaction between the synthetic bone substitutes and the injured bone tissue, clarifying the responses of the body in the presence of the Nb or Ga- doped bioactive glasses. Thus, the present study foments the literature with relevant information for clinic practise and further investigations.

References of the introduction:

1. Lieberman, D. E. *The Story of the Human Body*. (Penguin Books, 2013).

2. World Health Organization. World Health Statistics 2017 : Monitoring Health for The SDGs. *World Health Organization* (2017).

3. Loures, M. A. R. *et al.* Guidelines of the Brazilian Society of Rheumatology for the diagnosis and treatment of osteoporosis in men. *Rev. Bras. Reumatol. (English Ed.* 1–16 (2017).

4. Johnell, O. & Kanis, J. A. An estimate of the worldwide prevalence and disability associated with osteoporotic fractures. *Osteoporos. Int.* **17,** 1726–1733 (2006).

5. Svedbom, A. *et al.* Osteoporosis in the European Union: A compendium of country-specific reports. *Arch. Osteoporos.* **8,** (2013).

6. Bigham-Sadegh, A. & Oryan, A. Basic concepts regarding fracture healing and the current options and future directions in managing bone fractures. *Int. Wound J.* **12,** 238–247 (2015).

7. Hisbergues, M., Vendeville, S. & Vendeville, P. Zirconia: Established facts and perspectives for a biomaterial in dental implantology. *J. Biomed. Mater. Res. - Part B Appl. Biomater.* **88,** 519–529 (2009).

8. Hench, L. L. The story of Bioglass. 967–978 (2006).

9. Kaur, G. Bioactive glasses. Bioceramics and their Clinical Applications (Springer, 2008).

10. Bioactive glasses: Materials, properties and applications. (Woodhead Publishing Limited, 2011).

11. Bioactive Glasses : Fundamentals, Technology and Applications. (2017).

12. Hench, L. L., Polak, J. M., Xynos, I. D. & Buttery, L. D. K. Bioactive materials to control cell cycle. *Mater. Res. Innov.* **3,** 313–323 (2000).

13. Hench, L. L., Splinter, R. J., Allen, W. C. & Greenlee, T. K. Bonding mechanisms at the interface of ceramic prosthetic materials. *J. Biomed. Mater. Res.* **5,** 117–141 (1971).

14. Hench, L. L., Polak, J. M., Xynos, I. D. & Buttery, L. D. K. Bioactive materials to control cell cycle. *Mater. Res. Innov.* **3,** 313–323 (2000).

15. Jones, J. R. Acta Biomaterialia Review of bioactive glass : From Hench to hybrids. *Acta Biomater.* **9,** 4457–4486 (2013).

16. Lakhkar, N. J. *et al.* Bone formation controlled by biologically relevant inorganic ions : Role and controlled delivery from phosphate-based glasses. *Adv. Drug Deliv. Rev.* **65,** 405–420 (2013).

17. Hench, L. L. & Jones, J. R. Bioactive Glasses: Frontiers and Challenges. *Front. Bioeng. Biotechnol.* **3,** 1–12 (2015).

18. Obata, A. *et al.* Effects of niobium ions released from calcium phosphate invert glasses containing Nb2O5 on osteoblast-like cell functions. *ACS Appl. Mater. Interfaces* **4,** 5684–5690 (2012).

19. Kushwaha, M., Pan, X., Holloway, J. a & Denry, I. L. Differentiation of human mesenchymal stem cells on niobium-doped fluorapatite glass-ceramics. *Dent. Mater.* **28,** 252–60 (2012).

20. Takahashi, K. *et al.* Biomechanical Evaluation of Ti-Nb-Sn Alloy Implants with a Low Young's Modulus. *Int. J. Mol. Sci.* **16,** 5779–5788 (2015).

21. Silva, M. H. P. da, Ramirez, C. M., Granjeiro, J. M. & Rossi, A. M. In Vitro Assessment of New Niobium Phosphate Glasses and Glass Ceramics. *Key Eng. Mater.* **361–363,** 229–232 (2008).

22. Sene, F. F., Martinelli, J. R. & Gomes, L. Synthesis and characterization of niobium phosphate glasses containing barium and potassium. *J. Non. Cryst. Solids* **348,** 30–37 (2004).

23. Crovace, M. C., Souza, M. T., Chinaglia, C. R., Peitl, O. & Zanotto, E. D. Biosilicate® - A multipurpose, highly bioactive glass-ceramic. in vitro, in vivo and clinical trials. *J. Non. Cryst. Solids* **432,** 90–110 (2016).

24. Lopes, J. H., Magalhães, A., Mazali, I. O. & Bertran, C. A. Effect of Niobium Oxide on the Structure and Properties of Melt-Derived Bioactive Glasses. *J. Am. Ceram. Soc.* **97,** 3843–3852 (2014).

25. American Cancer Society. Cancer Facts & Figures 2016. *Cancer Facts Fig. 2016* 1–9 (2016).

26. Hoppe, A., Guldal, N. S. & Boccaccini, A. R. A review of the biological response to ionic dissolution products from bioactive glasses and glass-ceramics. *Biomaterials* **32,** 2757–2774 (2011).

27. Collery, P., Keppler, B., Madoulet, C. & Desoize, B. Gallium in cancer treatment. *Crit. Rev. Oncol. Hematol.* **42,** 283–296 (2002).

28. Chitambar, C. R. Medical applications and toxicities of gallium compounds. *Int. J. Environ. Res. Public Health* **7,** 2337–2361 (2010).

29. Valappil, S. P. *et al.* Antimicrobial gallium-doped phosphate-based glasses. *Adv. Funct. Mater.* **18,** 732–741 (2008).

30. Valappil, S. P. *et al.* Controlled delivery of antimicrobial gallium ions from phosphate-based glasses. *Acta Biomater.* **5,** 1198–1210 (2009).

31. Zeimaran, E. *et al.* Antibacterial properties of poly (octanediol citrate)/gallium-containing bioglass composite scaffolds. *J. Mater. Sci. Mater. Med.* **27,** 1–11 (2016).

32. Franchini, M., Lusvardi, G., Malavasi, G. & Menabue, L. Gallium-containing phospho-silicate glasses: Synthesis and in vitro bioactivity. *Materials Science and Engineering: C.* **32**, 1401-1406 (2012).

33. Lusvardi, G., Malavasi, G., Menabue, L. & Shruti, S. Gallium-containing phosphosilicate glasses: Functionalization and in-vitro bioactivity. *Materials Science and Engineering: C.* **33**, 3190-3196 (2013).

References of article 1

1 Shahgholi, M. *et al.* Mechanical characterization of glass-ceramic scaffolds at multiple characteristic lengths through nanoindentation. *J. Eur. Ceram. Soc.* **36**, 2403-2409, doi:http://dx.doi.org/10.1016/j.jeurceramsoc.2016.01.042 (2016).

2 Midha, S. *et al.* Preconditioned 70S30C bioactive glass foams promote osteogenesis in vivo. *Acta Biomater.* **9**, 9169-9182, doi:10.1016/j.actbio.2013.07.014 (2013).

3 Wang, X. S., Lu, Z. L., Jia, L. & Chen, J. X. Preparation of porous titanium materials by powder sintering process and use of space holder technique. *J Iron Steel Res Int* **24**, 97-102 (2017).

4 Altmann, B. *et al.* Cellular transcriptional response to zirconia-based implant materials. *Dent. Mater.* **33**, 241-255, doi:http://dx.doi.org/10.1016/j.dental.2016.12.005 (2017).

5 Hisbergues, M., Vendeville, S. & Vendeville, P. Zirconia: Established Facts and Perspectives for a Biomaterial in Dental Implantology. *Journal of Biomedical Materials Research Part B-Applied Biomaterials* **88b**, 519-529, doi:10.1002/jbm.b.31147 (2009).

6 Hench, L. L., Polak, J. M., Xynos, I. D. & Buttery, L. D. K. Bioactive materials to control cell cycle. *Mater. Res. Innovations* **3**, 313-323, doi:Doi 10.1007/S100190000055 (2000).

7 Hench, L. L. & Jones, J. R. Bioactive Glasses: Frontiers and Challenges. *Frontiers in Bioengineering and Biotechnology* **3**, 194, doi:10.3389/fbioe.2015.00194 (2015).

8 Hench, L. L. Genetic design of bioactive glass. *J. Eur. Ceram. Soc.* **29**, 1257-1265, doi:Doi 10.1016/J.Jeurceramsoc.2008.08.002 (2009).

9 Hench, L. L., Splinter, R. J., Allen, W. C. & Greenlee, T. K. Bonding mechanisms at the interface of ceramic prosthetic materials. *J. Biomed. Mater. Res.* **5**, 117-141 (1972).

10 Hench, L. L. Bioceramics - From concept to clinic. *J. Am. Ceram. Soc.* **74**, 1487-1510 (1991).

11 Lopes, J. H. *et al.* Hierarchical structures of β-TCP/45S5 bioglass hybrid scaffolds prepared by gelcasting. *Journal of the Mechanical Behavior of Biomedical Materials* **62**, 10-23, doi:http://dx.doi.org/10.1016/j.jmbbm.2016.04.028 (2016).

12 Zeimaran, E. *et al.* Bioactive glass reinforced elastomer composites for skeletal regeneration: A review. *Mater. Sci. Eng., C* **53**, 175-188, doi:10.1016/j.msec.2015.04.035 (2015).

13 Kaur, G. *et al.* A review of bioactive glasses: Their structure, properties, fabrication and apatite formation. *Journal of Biomedical Materials Research - Part A* **102**, 254-274, doi:10.1002/jbm.a.34690 (2016).

14 Ioannou, A. L., Kotsakis, G. A., Kumar, T., Hinrichs, J. E. & Romanos, G. Evaluation of the bone regeneration potential of bioactive glass in implant site development surgeries: a systematic review of the literature. *Clin. Oral Investig.* **19**, 181-191, doi:10.1007/s00784-014-1376-1 (2015).

15 Crovace, M. C., Souza, M. T., Chinaglia, C. R., Peitl, O. & Zanotto, E. D. Biosilicate® - A multipurpose, highly bioactive glass-ceramic. in vitro, in vivo and clinical trials. *J. Non·Cryst. Solids* **432**, 90-110, doi:10.1016/j.jnoncrysol.2015.03.022 (2016).

16 Gorustovich, A. A., Roether, J. A. & Boccaccini, A. R. Effect of Bioactive Glasses on Angiogenesis: A Review of In Vitro and In Vivo Evidences. *Tissue Eng Part B-Re* **16**, 199-207, doi:10.1089/ten.teb.2009.0416 (2010).

17 Jones, J. R. Reprint of: Review of bioactive glass: From Hench to hybrids. *Acta Biomater.* **23**, S53-S82, doi:10.1016/j.actbio.2015.07.019 (2015).

18 Sepulveda, P., Jones, J. R. & Hench, L. L. In vitro dissolution of melt-derived 45S5 and sol-gel derived 58S bioactive glasses. *J. Biomed. Mater. Res.* **61**, 301-311, doi:10.1002/jbm.10207 (2002).

19 Stoor, P., Soderling, E. & Salonen, J. I. Antibacterial effects of a bioactive glass paste on oral microorganisms. *Acta Odontol. Scand.* **56**, 161-165 (1998).

20 Lebecq, I., Desanglois, F., Leriche, A. & Follet-Houttemane, C. Compositional dependence on the in vitro bioactivity of invert or conventional bioglasses in the Si-Ca-Na-P system. *J. Biomed. Mater. Res. A* **83**, 156-168, doi:10.1002/jbm.a.31228 (2007).

21 Brink, M., Turunen, T., Happonen, R. P. & Yli-Urpo, A. Compositional dependence of bioactivity of glasses in the system Na_2O-K_2O-MgO-CaO-B2O3-P2O5-SiO2. *J. Biomed. Mater. Res.* **37**, 114-121 (1997).

22 Smith, J. M., Martin, R. A., Cuello, G. J. & Newport, R. J. Structural characterisation of hypoxia-mimicking bioactive glasses. *Journal of Materials Chemistry B* **1**, 1296-1303, doi:10.1039/C3TB00408B (2013).

23 Deliormanlı, A. M., Seda Vatansever, H., Yesil, H. & Özdal-Kurt, F. In vivo evaluation of cerium, gallium and vanadium-doped borate-based bioactive glass scaffolds using rat subcutaneous implantation model. *Ceram. Int.* **42**, 11574-11583, doi:http://doi.org/10.1016/j.ceramint.2016.04.033 (2016).

24 Fernandes, G. V. O., Alves, G. G., Linhares, A. B. R., Da Silva, M. H. P. & Granjeiro, J. M. Evaluation of cytocompatibility of bioglass-niobium granules with human primary osteoblasts: A multiparametric approach. *Key Eng. Mater.* **493-494**, 37-42 (2012).

25 Prado Da Silva, M. H., Moura Ramirez, C., Granjeiro, J. M. & Rossi, A. M. In vitro assessment of new niobium phosphate glasses and glass ceramics. *Key Eng. Mater.* **361-363 I**, 229-232 (2008).

26 Kushwaha, M., Pan, X., Holloway, J. A. & Denry, I. L. Differentiation of human mesenchymal stem cells on niobium-doped fluorapatite glass-ceramics. *Dent. Mater.* **28**, 252-260, doi:10.1016/j.dental.2011.10.010 (2012).

27 Obata, A. *et al.* Effects of niobium ions released from calcium phosphate invert glasses containing Nb2O5 on osteoblast-like cell functions. *ACS Appl Mater Interfaces* **4**, 5684-5690, doi:10.1021/am301614a (2012).

28 Sene, F. F., Martinelli, J. R. & Gomes, L. Synthesis and characterization of niobium phosphate glasses containing barium and potassium. *J. Non·Cryst. Solids* **348**, 30-37, doi:10.1016/j.jnoncrysol.2004.08.122 (2004).

29 Takahashi, K. *et al.* Biomechanical Evaluation of Ti-Nb-Sn Alloy Implants with a Low Young's Modulus. *International Journal of Molecular Sciences* **16**, 5779-5788, doi:10.3390/ijms16035779 (2015).

30 Doremus, R. H. *Glass science*. (Wiley, 1994).

31 Lopes, J. H., Magalhaes, A., Mazali, I. O. & Bertran, C. A. Effect of Niobium Oxide on the Structure and Properties of Melt-Derived Bioactive Glasses. *Journal of the American Ceramic Society* **97**, 3843-3852, doi:DOI 10.1111/jace.13222 (2014).

32 Lopes, J. H. *Biovidros derivados do 45S5: os efeitos do Nb2O5 ou da modificação da superfície com Ca2+ sobre a estrutura e bioatividade* PhD thesis, Universidade Estadual de Campinas, (2015).

33 Lopes, J. H., Mazali, I. O., Landers, R. & Bertran, C. A. Structural Investigation of the Surface of Bioglass 45S5 Enriched with Calcium Ions. *J. Am. Ceram. Soc.* **96**, 1464-1469, doi:DOI 10.1111/jace.12305 (2013).

34 Lopes, J. H. *et al.* Facile and innovative method for bioglass surface modification: Optimization studies. *Mater Sci Eng C Mater Biol Appl* **72**, 86-97, doi:10.1016/j.msec.2016.11.044 (2017).

35 Jehng, J.-M., Turek, A. M. & Wachs, I. E. Surface modified niobium oxide catalyst: synthesis, characterization, and catalysis. *Applied Catalysis A: General* **83**, 179-200, doi:http://dx.doi.org/10.1016/0926-860X(92)85034-9 (1992).

36 Peiffert, C., Nguyen-Trung, C., Palmer, D. A., Laval, J.-P. & Giffaut, E. Solubility of B-Nb2O5 and the hydrolysis of niobium(V) in aqueous solution as a

function of temperature and ionic strength. *J. Solution Chem.* **39**, 197-218, doi:10.1007/s10953-010-9495-z (2010).

37 Tilocca, A. & Cormack, A. N. Surface Signatures of Bioactivity: MD Simulations of 45S and 65S Silicate Glasses. *Langmuir* **26**, 545-551, doi:10.1021/la902548f (2010).

38 Miyazaki, T., Kim, H. M., Kokubo, T., Ohtsuki, C. & Nakamura, T. Apatite-forming ability of niobium oxide gels in a simulated body fluid. *Journal of the Ceramic Society of Japan* **109**, 929-933, doi:Doi 10.2109/Jcersj.109.1275_929 (2001).

39 Olivares-Navarrete, R., Olaya, J. J., Ramírez, C. & Rodil, S. E. Biocompatibility of Niobium Coatings. *Coatings* **1**, 72 (2011).

40 Krebsbach, P. H., Mankani, M. H., Satomura, K., Kuznetsov, S. A. & Robey, P. G. Repair of craniotomy defects using bone marrow stromal cells. *Transplantation* **66**, 1272-1278, doi:Doi 10.1097/00007890-199811270-00002 (1998).

41 Kwan, M. D., Slater, B. J., Wan, D. C. & Longaker, M. T. Cell-based therapies for skeletal regenerative medicine. *Human Molecular Genetics* **17**, R93-R98, doi:10.1093/hmg/ddn071 (2008).

42 Cancedda, R. *et al.* in *Tissue Engineering of Cartilage and Bone* 133-147 (John Wiley & Sons, Ltd, 2008).

43 De Ugarte, D. A. *et al.* Differential expression of stem cell mobilization-associated molecules on multi-lineage cells from adipose tissue and bone marrow. *Immunology Letters* **89**, 267-270, doi:10.1016/S0165-2478(03)00108-1 (2003).

44 Quarto, R., Thomas, D. & Liang, C. T. Bone Progenitor-Cell Deficits and the Age-Associated Decline in Bone Repair Capacity. *Calcified Tissue International* **56**, 123-129, doi:Doi 10.1007/Bf00296343 (1995).

45 Fenno, L. E., Ptaszek, L. M. & Cowan, C. A. Human embryonic stem cells: emerging technologies and practical applications. *Current Opinion in Genetics & Development* **18**, 324-329, doi:https://doi.org/10.1016/j.gde.2008.06.004 (2008).

46 Lakhkar, N. J. *et al.* Bone formation controlled by biologically relevant inorganic ions: Role and controlled delivery from phosphate-based glasses. *Adv. Drug Del. Rev.* **65**, 405-420, doi:http://doi.org/10.1016/j.addr.2012.05.015 (2013).

47 Xynos, I. D., Edgar, A. J., Buttery, L. D., Hench, L. L. & Polak, J. M. Ionic products of bioactive glass dissolution increase proliferation of human osteoblasts and induce insulin-like growth factor II mRNA expression and protein synthesis. *Biochem. Biophys. Res. Commun.* **276**, 461-465, doi:10.1006/bbrc.2000.3503 (2000).

48 Xynos, I. D. *et al.* Bioglass 45S5 stimulates osteoblast turnover and enhances bone formation In vitro: implications and applications for bone tissue engineering. *Calcif. Tissue Int.* **67**, 321-329 (2000).

49 Habibovic, P. & Barralet, J. E. Bioinorganics and biomaterials: bone repair. *Acta Biomater.* **7**, 3013-3026, doi:10.1016/j.actbio.2011.03.027 (2011).

50 Goltzman, D. & Hendy, G. N. The calcium-sensing receptor in bone-mechanistic and therapeutic insights. *Nature Reviews Endocrinology* **11**, 298-307, doi:10.1038/nrendo.2015.30 (2015).

51 Erkhembaatar, M. *et al.* Lysosomal Ca2+ Signaling is Essential for Osteoclastogenesis and Bone Remodeling. *J. Bone Miner. Res.* **32**, 385-396, doi:10.1002/jbmr.2986 (2017).

52 Marie, P. J. The calcium-sensing receptor in bone cells: A potential therapeutic target in osteoporosis. *Bone* **46**, 571-576, doi:10.1016/j.bone.2009.07.082.

53 Maeno, S. *et al.* The effect of calcium ion concentration on osteoblast viability, proliferation and differentiation in monolayer and 3D culture. *Biomaterials* **26**, 4847-4855, doi:http://doi.org/10.1016/j.biomaterials.2005.01.006 (2005).

54 Denry, I. L., Holloway, J. A., Nakkula, R. J. & Walters, J. D. Effect of niobium content on the microstructure and thermal properties of fluorapatite glass-ceramics. *J Biomed Mater Res B Appl Biomater* **75**, 18-24, doi:10.1002/jbm.b.30295 (2005).

55 Kaur, G. *et al.* A review of bioactive glasses: Their structure, properties, fabrication, and apatite formation. *Journal of Biomedical Materials Research Part A* **102**, 254-274, doi:10.1002/jbm.a.34690 (2014).

56 Oyane, A. *et al.* Preparation and assessment of revised simulated body fluids. *J. Biomed. Mater. Res. A* **65**, 188-195, doi:10.1002/jbm.a.10482 (2003).

57 Mathews, S., Gupta, P. K., Bhonde, R. & Totey, S. Chitosan enhances mineralization during osteoblast differentiation of human bone marrow-derived mesenchymal stem cells, by upregulating the associated genes. *Cell Prolif.* **44**, 537-549, doi:10.1111/j.1365-2184.2011.00788.x (2011).

References of article 2

[1] M. V. P., L.-C. Beata, E. N. A., J. A. C., Journal of Biomedical Materials Research Part A 2013, 101, 3349.
[2] J. R. Jones, D. S. Brauer, L. Hupa, D. C. Greenspan, Int J Appl Glass Sci 2016, 7, 423.
[3] M. Kushwaha, X. Pan, J. A. Holloway, I. L. Denry, Dental materials : official publication of the Academy of Dental Materials 2012, 28, 252.
[4] J. H. Lopes, I. O. Mazali, R. Landers, C. A. Bertran, Journal of the American Ceramic Society 2013, 96, 1464.
[5] J. H. Lopes, J. A. Magalhaes, R. F. Gouveia, C. A. Bertran, M. Motisuke, S. E. A. Camargo, E. S. Triches, J Mech Behav Biomed Mater 2016, 62, 10.
[6] J. H. Lopes, E. M. B. Fonseca, I. O. Mazali, A. Magalhaes, R. Landers, C. A. Bertran, Mater Sci Eng C Mater Biol Appl 2017, 72, 86.
[7] L. L. Hench, Journal of Materials Science-Materials in Medicine 2006, 17, 967.
[8] J. R. Jones, Acta Biomaterialia 2015, 23, S53.
[9] L. L. Hench, J. R. Jones, Frontiers in Bioengineering and Biotechnology 2015, 3, 194.
[10] L. L. Hench, J. M. Polak, I. D. Xynos, L. D. K. Buttery, Materials Research Innovations 2000, 3, 313.
[11] A. Obata, Y. Takahashi, T. Miyajima, K. Ueda, T. Narushima, T. Kasuga, ACS Appl Mater Interfaces 2012, 4, 5684.
[12] I. L. Denry, J. A. Holloway, R. J. Nakkula, J. D. Walters, Journal of biomedical materials research. Part B, Applied biomaterials 2005, 75, 18.
[13] L. Joao Henrique, B. Celso Aparecido, M. Italo Odone, Frontiers in Bioengineering and Biotechnology 2016, 4.
[14] J. H. Lopes, A. Magalhães, I. O. Mazali, C. A. Bertran, H. E. Kim, Journal of the American Ceramic Society 2014, 97, 3843.
[15] G. V. O. Fernandes, G. G. Alves, A. B. R. Linhares, M. H. P. Da Silva, J. M. Granjeiro, Key engineering materials 2012, 493-494, 37.
[16] X. Wang, X. Meng, S. Chu, X. Xiang, Z. Liu, J. Zhao, Y. Zhou, Journal of Materials Science: Materials in Medicine 2016, 27, 139.
[17] R. Ana Lúcia Roselino, H. Peter, V. Luís Geraldo, R. Luís Augusto, Biomedical Materials 2013, 8, 065005.
[18] K. Mallick, *Bone Substitute Biomaterials*, Elsevier Science, 2014.
[19] J. H. LOPES, C. A. BERTRAN, S. L. P. L. DE, I. O. MAZALI, J. A. CAMILLI, Google Patents, 2016.
[20] J. H. Lopes, in *Universidade Estadual de Campinas - Instituto de Química*, Vol. PhD, Universidade Estadual de Campinas, Caminas 2015.
[21] V. Miguez-Pacheco, D. de Ligny, J. Schmidt, R. Detsch, A. R. Boccaccini, Journal of the European Ceramic Society 2018, 38, 871.
[22] L. L. Hench, R. J. Splinter, W. C. Allen, T. K. Greenlee, Journal of biomedical materials research 1972, 5, 117.
[23] J. H. Lopes, A. Magalhaes, I. O. Mazali, C. A. Bertran, Journal of the American Ceramic Society 2014, 97, 3843.

[24] T. Minghui, C. Wenchuan, L. Jun, W. M. D., C. Linzhao, X. H. H.K., Tissue Eng Pt A 2014, 20, 1295.
[25] N. S. V. Capanema, A. A. P. Mansur, S. M. Carvalho, A. R. P. Silva, V. S. Ciminelli, H. S. Mansur, Materials 2015, 8, 4191.
[26] L. B. Mestieri, A. L. Gomes-Cornélio, E. M. Rodrigues, G. Faria, J. M. Guerreiro-Tanomaru, M. Tanomaru-Filho, Brazilian Dental Journal 2017, 28, 65.
[27] F. Diomede, A. Gugliandolo, P. Cardelli, I. Merciaro, V. Ettorre, T. Traini, R. Bedini, D. Scionti, A. Bramanti, A. Nanci, S. Caputi, A. Fontana, E. Mazzon, O. Trubiani, Stem Cell Research & Therapy 2018, 9, 104.
[28] W. Chen, J. Liu, N. Manuchehrabadi, M. D. Weir, Z. Zhu, H. H. K. Xu, Biomaterials 2013, 34, 9917.
[29] G. Krishnamurithy, M. R. Murali, M. Hamdi, A. A. Abbas, H. B. Raghavendran, T. Kamarul, Regenerative Medicine 2015, 10, 579.
[30] C. Wang, H. Meng, X. Wang, C. Zhao, J. Peng, Y. Wang, Medical Science Monitor : International Medical Journal of Experimental and Clinical Research 2016, 22, 226.
[31] G. Fernandez de Grado, L. Keller, Y. Idoux-Gillet, Q. Wagner, A.-M. Musset, N. Benkirane-Jessel, F. Bornert, D. Offner, Journal of Tissue Engineering 2018, 9, 2041731418776819.
[32] T. Shirin, B. Nima, B. Javad, Journal of Biomedical Materials Research Part A, 0.
[33] H. Matsuno, A. Yokoyama, F. Watari, M. Uo, T. Kawasaki, Biomaterials 2001, 22, 1253.
[34] Y. Bai, Y. Deng, Y. Zheng, Y. Li, R. Zhang, Y. Lv, Q. Zhao, S. Wei, Materials Science and Engineering: C 2016, 59, 565.
[35] B. Boyan, Z. Schwartz, "Modulation of osteogenesis via implant surface design", presented at *Bone Engineering*, Toronto, 2000.
[36] J. Steele, B. Dalton, "Underlying mechanisms of cellular adhesion in vitro during colonization of synthetic surfaces by bone- derived cells", presented at *Bone Engineering*, Toronto, 2000.
[37] N. J. Lakhkar, I.-H. Lee, H.-W. Kim, V. Salih, I. B. Wall, J. C. Knowles, Advanced Drug Delivery Reviews 2013, 65, 405.
[38] A. Hoppe, N. S. Guldal, A. R. Boccaccini, Biomaterials 2011, 32, 2757.
[39] S. Maeno, Y. Niki, H. Matsumoto, H. Morioka, T. Yatabe, A. Funayama, Y. Toyama, T. Taguchi, J. Tanaka, Biomaterials 2005, 26, 4847.

[40] I. D. Xynos, A. J. Edgar, L. D. K. Buttery, L. L. Hench, J. M. Polak, Journal of Biomedical Materials Research 2001, 55, 151.

References of article 3

1. Einhorn, T. A. & Gerstenfeld, L. C. Fracture healing: Mechanisms and interventions. Nat. Rev. Rheumatol. 11, 45–54 (2015).

2. Schlundt, C. et al. Clinical and Research Approaches to Treat Non-union Fracture. (2018).

3. Johnell, O. & Kanis, J. A. An estimate of the worldwide prevalence and disability associated with osteoporotic fractures. Osteoporos. Int. 17, 1726–1733 (2006).

4. Hench, L. L., Splinter, R. J., Allen, W. C. & Greenlee, T. K. Bonding mechanisms at the interface of ceramic prosthetic materials. J. Biomed. Mater. Res. 5, 117–141 (1971).

5. Hench, L. L., Polak, J. M., Xynos, I. D. & Buttery, L. D. K. Bioactive materials to control cell cycle. Mater. Res. Innov. 3, 313–323 (2000).

6. Jones, J. R. Review of bioactive glass: from Hench to hybrids. Acta Biomater. 9, 4457–4486 (2012).

7. Kowal, T. J. et al. Role of phase separation on the biological performance of 45S5. J. Mater. Sci. Mater. Med. (2017). doi:10.1007/s10856-017-5976-6

8. Bartolomé, J. F. et al. In vitro and in vivo evaluation of a new zirconia/niobium biocermet for hard tissue replacement. Biomaterials 76, 313–320 (2016).

9. Obata, A. et al. Effects of Niobium Ions Released from Calcium Phosphate Invert Glasses Containing Nb2O5 on Osteoblast-Like Cell Functions. ACS Appl. Mater. Interfaces 4, 5684–5690 (2012).

10. Kushwaha, M., Pan, X., Holloway, J. a & Denry, I. L. Differentiation of human mesenchymal stem cells on niobium-doped fluorapatite glass-ceramics. Dent. Mater. 28, 252–60 (2012).

11. Olivares-Navarrete, R., Olaya, J. J., Ramírez, C. & Rodil, S. E. Biocompatibility of Niobium Coatings. Coatings 1, 72–87 (2011).

12. Wang, C. et al. Differentiation of Bone Marrow Mesenchymal Stem Cells in Osteoblasts and Adipocytes and its Role in Treatment of Osteoporosis. Med. Sci. Monit. 22, 226–233 (2016).

13. Wang, X. et al. Osseointegration behavior of novel Ti–Nb–Zr–Ta–Si alloy for dental implants: an in vivo study. J. Mater. Sci. Mater. Med. 27, (2016).

14. Miura, K., Yamada, N., Hanada, S., Jung, T.-K. & Itoi, E. The bone tissue compatibility of a new Ti–Nb–Sn alloy with a low Young's modulus. Acta Biomater. 7, 2320–2326 (2011).

15. Takahashi, K. et al. Biomechanical Evaluation of Ti-Nb-Sn Alloy Implants with a Low Young's Modulus. Int. J. Mol. Sci. 16, 5779–5788 (2015).

16. Gabriel, S. B. et al. Characterization of a new beta titanium alloy, Ti-12Mo-3Nb, for biomedical applications. J. Alloys Compd. 536, S208–S210 (2012).

17. Lopes, J. H., Magalhães, A., Mazali, I. O. & Bertran, C. A. Effect of Niobium Oxide on the Structure and Properties of Melt-Derived Bioactive Glasses. J. Am. Ceram. Soc. 97, 3843–3852 (2014).

18. Stenlund, P. et al. Bone response to a novel Ti–Ta–Nb–Zr alloy. Acta Biomater. 20, 165–175 (2015).

19. Miyazaki, T., Kim, H.-M., Kokubo, T., Ohtsuki, C. & Nakamura, T. Apatite-Forming Ability of Niobium Oxide Gels in a Simulated Body Fluid. J. Ceram. Soc. Japan 109, 929–933 (2001).

20. Denry, I., Holloway, J., Nakkula, R. & Walters, J. Effect of niobium content on the microstructure and thermal properties of fluorapatite glass-ceramics. Appl. Biomater. 75, 18–24 (2005).

21. V, M.-P., D, D. L., J, S., R, D. & A.R, B. Development and characterization of niobium-relieasing silicate bioactive glasses for tissue engineering applications. J. Eur. Ceram. Soc. 38, 871–876 (2018).

22. Xie, Z. P. et al. In vivo study effect of particulate Bioglass® in the prevention of infection in open fracture fixation. J. Biomed. Mater. Res. - Part B Appl. Biomater. 90, 195–201 (2009).

23. Hayes, A. W. Principles and Methods of Toxicology. (Raven Press, 1994).

24. Matsuno, H., Yokoyama, A., Watari, F., Uo, M. & Kawasaki, T. Biocompatibility and osteogenesis of refractory metal implants, titanium,hafnium, niobium, tantalum and rhenium. Biomaterials 22, 1253–1262 (2001).

25. Dsouki, N. A. et al. Cytotoxic, hematologic and histologic effects of niobium pentoxide in Swiss mice. J. Mater. Sci. Mater. Med. 25, 1301–1305 (2014).

26. Zwolak, I. Vanadium carcinogenic, immunotoxic and neurotoxic effects: A review of in vitro studies. Toxicol. Mech. Methods 24, 1–12 (2014).

27. Paiva, A. V. et al. Effects of lanthanum on human lymphocytes viability and DNA strand break. Bull. Environ. Contam. Toxicol. 82, 423–427 (2009).

28. Magaye, R. & Zhao, J. Recent progress in studies of metallic nickel and nickel-based nanoparticles' genotoxicity and carcinogenicity. Environ. Toxicol. Pharmacol. 34, 644–650 (2012).

29. Einhorn, T. A. Clinically applied models of bone regeneration in tissue engineering research. Clin Orthop Relat Res 367, 59–67 (1999).

30. Spicer, P. P. et al. Evaluation of Bone Regeneration Using the Rat Critical Size Calvarial Defect. NIH Public Access 7, 1918–1929 (2013).

References of article 4

1 American Cancer Society. Cancer Facts & Figures 2016. Atlanta: American Cancer Society; 2016.

2 Hoppe, A., Gueldal, N. S. & Boccaccini, A. R. A review of the biological response to ionic dissolution products from bioactive glasses and glass-ceramics. *Biomaterials* 32, 2757-2774, doi:10.1016/j.biomaterials.2011.01.004 (2011).

3 Xynos, I. D., Edgar, A. J., Buttery, L. D. K., Hench, L. L. & Polak, J. M. Ionic products of bioactive glass dissolution increase proliferation of human osteoblasts and induce insulin-like growth factor II mRNA expression and protein synthesis. *Biochemical and Biophysical Research Communications* 276, 461-465, doi:DOI 10.1006/bbrc.2000.3503 (2000).

4 Hench, L. L., Splinter, R. J., Allen, W. C. and Greenlee, T. K. Bonding mechanisms at the interface of ceramic prosthetic materials. *Journal of Biomedical Materials Research Symposium* 5, 25, doi:DOI: 10.1002/jbm.820050611 (1971).

5 Hench, L. L. The story of Bioglass (R). *Journal of Materials Science-Materials in Medicine* 17, 967-978, doi:DOI 10.1007/s10856-006-0432-z (2006).

6 Cao, W. P. & Hench, L. L. Bioactive materials. *Ceramics International* 22, 493-507 (1996).

7 Oonishi, H. *et al.* Particulate bioglass compared with hydroxyapatite as a bone graft substitute. *Clinical Orthopaedics and Related Research*, 316-325 (1997).

8 Oonishi, H. *et al.* Quantitative comparison of bone growth behavior in granules of Bioglass (R), A-W glass-ceramic, and hydroxyapatite. *Journal of biomedical materials research* 51, 37-46 (2000).

9 FitzGerald, V. *et al.* Bioactive glass sol-gel foam scaffolds: Evolution of nanoporosity during processing and in situ monitoring of apatite layer formation using small- and wide-angle X-ray scattering. *Journal of Biomedical Materials Research Part A* 91A, 76-83, doi:Doi 10.1002/Jbm.A.32206 (2009).

10 Martin, R. A., Twyman, H., Qiu, D., Knowles, J. C. & Newport, R. J. A study of the formation of amorphous calcium phosphate and hydroxyapatite on melt quenched Bioglass(A (R)) using surface sensitive shallow angle X-ray diffraction. *Journal of Materials Science-Materials in Medicine* 20, 883-888, doi:DOI 10.1007/s10856-008-3661-5 (2009).

11 Martin, R. A. *et al.* Characterizing the hierarchical structures of bioactive sol-gel silicate glass and hybrid scaffolds for bone regeneration. *Philosophical Transactions of the Royal Society a-Mathematical Physical and Engineering Sciences* 370, 1422-1443, doi:10.1098/rsta.2011.0308 (2012).

12 Erbe, E. M. & Day, D. E. Chemical durability of Y2O3-Al2O3-SiO2 glasses for the in vivo delivery of beta radiation. *Journal of biomedical materials research* 27, 1301-1308, doi:10.1002/jbm.820271010 (1993).

13 Erbe, E. M. & Day, D. E. Properties of Sm2O3─Al2O3─SiO2 Glasses for In Vivo Applications. *Journal of the American Ceramic Society* 73, 2708-2713, doi:10.1111/j.1151-2916.1990.tb06750.x (1990).

14 Collery, P., Keppler, B., Madoulet, C. & Desoize, B. Gallium in cancer treatment. *Crit Rev Oncol Hematol* 42, 283-296 (2002).

15 Ortega, R., Suda, A. & Devès, G. Nuclear microprobe imaging of gallium nitrate in cancer cells. *Nuclear Instruments and Methods in Physics Research Section B: Beam Interactions with Materials and Atoms* 210, 364-367, doi:http://dx.doi.org/10.1016/S0168-583X(03)01052-8 (2003).

16 Chitambar, C. R. Medical Applications and Toxicities of Gallium Compounds. *International Journal of Environmental Research and Public Health* 7, 2337-2361 (2010).

17 Bockman, R. S. *et al.* A multicenter trial of low dose gallium nitrate in patients with advanced Paget's disease of bone. *The Journal of Clinical Endocrinology & Metabolism* 80, 595-602, doi:doi:10.1210/jcem.80.2.7852526 (1995).

18 Valappil, S. P. *et al.* Controlled delivery of antimicrobial gallium ions from phosphate-based glasses. *Acta Biomaterialia* 5, 1198-1210, doi:DOI 10.1016/j.actbio.2008.09.019 (2009).

19 Valappil, S. P. *et al.* Antimicrobial gallium-doped phosphate-based glasses. *Advanced Functional Materials* 18, 732-741, doi:DOI 10.1002/adfm.200700931 (2008).

20 Zeimaran, E. *et al.* Antibacterial properties of poly (octanediol citrate)/gallium-containing bioglass composite scaffolds. *Journal of Materials Science-Materials in Medicine* 27, doi:10.1007/s10856-015-5620-2 (2016).

21 Keenan, T. J. *et al.* Relating ion release and pH to in vitro cell viability for gallium-inclusive bioactive glasses. *Journal of Materials Science* 51, 1107-1120, doi:10.1007/s10853-015-9442-x (2016).

22 Wren, A. W. *et al.* Characterisation of Ga2O3-Na2O-CaO-ZnO-SiO2 bioactive glasses. *Journal of Materials Science* 48, 3999-4007, doi:10.1007/s10853-013-7211-2 (2013).

23 Lusvardi, G., Malavasi, G., Menabue, L. & Shruti, S. Gallium-containing phosphosilicate glasses: Functionalization and in-vitro bioactivity. *Materials Science and Engineering: C* 33, 3190-3196, doi:http://dx.doi.org/10.1016/j.msec.2013.03.046 (2013).

24 Franchini, M., Lusvardi, G., Malavasi, G. & Menabue, L. Gallium-containing phospho-silicate glasses: Synthesis and in vitro bioactivity. *Materials Science and Engineering: C* 32, 1401-1406, doi:http://dx.doi.org/10.1016/j.msec.2012.04.016 (2012).

25 Martin, R. A. *et al.* A structural investigation of the alkali metal site distribution within bioactive glass using neutron diffraction and multinuclear solid state NMR. *Physical Chemistry Chemical Physics* 14, 12105-12113, doi:10.1039/c2cp41725a (2012).

26 Saravanapavan, P. & Hench, L. L. Low-temperature synthesis, structure, and bioactivity of gel-derived glasses in the binary CaO-SiO2 system. *Journal of biomedical materials research* 54, 608-618 (2001).

27 Narusawa, H., Tamaki, Y. & Miyazaki, T. Development of an Experimental Phosphate-Calcium Cement with a Whisker-Like Structure. *Materials Sciences and Applications* Vol.03No.11, 5, doi:10.4236/msa.2012.311111 (2012).

28 Habraken, W. J. E. M. *et al.* Ion-association complexes unite classical and non-classical theories for the biomimetic nucleation of calcium phosphate. 4, 1507, doi:10.1038/ncomms2490

https://www.nature.com/articles/ncomms2490#supplementary-information (2013).

29 Rehman, I., Knowles, J. C. & Bonfield, W. Analysis of in vitro reaction layers formed on Bioglass (R) using thin-film X-ray diffraction and ATR-FTIR microspectroscopy. *Journal of biomedical materials research* 41, 162-166 (1998).

30 Xie, Z. P. *et al.* In Vivo Study Effect of Particulate Bioglass (R) in the Prevention of Infection in Open Fracture Fixation. *Journal of Biomedical Materials Research Part B-Applied Biomaterials* 90B, 195-201, doi:Doi 10.1002/Jbm.B.31273 (2009).

31 Allan, I., Newman, H. & Wilson, M. Antibacterial activity of particulate Bioglass (R) against supra- and subgingival bacteria. *Biomaterials* 22, 1683-1687, doi:10.1016/s0142-9612(00)00330-6 (2001).

32 Begum, S., Johnson, W. E., Worthington, T. & Martin, R. A. The influence of pH and fluid dynamics on the antibacterial efficacy of 45S5 Bioglass. *Biomedical materials (Bristol, England)* 11, 015006, doi:10.1088/1748-6041/11/1/015006 (2016).

33 Midha, S. *et al.* Preconditioned 70S30C bioactive glass foams promote osteogenesis in vivo. *Acta Biomaterialia* 9, 9169-9182, doi:10.1016/j.actbio.2013.07.014 (2013).

34 Hench, L. L. Chronology of Bioactive Glass Development and Clinical Applications. *New Journal of Glass and Ceramics* Vol.03No.02, 7, doi:10.4236/njgc.2013.32011 (2013).

35 Hench, L. L., Day, D. E., Hoeland, W. & Rheinberger, V. M. Glass and Medicine. *International Journal of Applied Glass Science* 1, 104-117, doi:10.1111/j.2041-1294.2010.00001.x (2010).

36 Hoppe, A. *et al.* Cobalt-Releasing 1393 Bioactive Glass-Derived Scaffolds for Bone Tissue Engineering Applications. *Acs Applied Materials & Interfaces* 6, 2872-2884, doi:10.1021/am405354y (2014).

37 Azevedo, M. M. *et al.* Synthesis and characterization of hypoxia-mimicking bioactive glasses for skeletal regeneration. *Journal of Materials Chemistry* 20, 8854-8864, doi:Doi 10.1039/C0jm01111h (2010).

38 Bellantone, M., Williams, H. D. & Hench, L. L. Broad-spectrum bactericidal activity of Ag2O-doped bioactive glass. *Antimicrobial Agents and Chemotherapy* 46, 1940-1945, doi:Doi 10.1128/Aac.46.6.1940-1945.2002 (2002).

39 Hess, U. *et al.* Co-delivery of cisplatin and doxorubicin from calcium phosphate beads/matrix scaffolds for osteosarcoma therapy. *Materials Science and Engineering: C* 77, 427-435, doi:http://dx.doi.org/10.1016/j.msec.2017.03.164 (2017).

40 Bockman, R. S. *et al.* Distribution of trace levels of therapeutic gallium in bone as mapped by synchrotron x-ray microscopy. *Proceedings of the National Academy of Sciences* 87, 4149-4153, doi:10.1073/pnas.87.11.4149 (1990).

APPENDICE

Certificates issued by the Committee for Ethics in Animal Use of the University of Campinas – CEUA/UNICAMP (Protocol Numbers: 3467-1 and 3467-1).

UNICAMP

CEUA/Unicamp

STATEMENT

We state for the due propose that all methods carried out during the project entitled "**Bioactivity of glass ceramics composed by niobium: an experimental study**", protocol **# 2777-1**, under the responsibility of P**rofessor Prof. Dr. José Angelo Camilli** and **PhD Student Lucas Pereira Lopes de Souza** were done in accordance with relevant guidelines and regulations.

All experimental protocols related to this project have been approved by the Committee for Ethics in Animal Use of the University of Campinas – CEUA/UNICAMP

Feel free to contact us should you have any question regarding this project (comisib@unicamp.br)

Campinas, June 29, 2018.

Prof. Dr. Wagner José Fávaro
President

Fátima Alonso
Executive Secretary

CEUA/UNICAMP
Caixa Postal 6109
13083-970 Campinas, SP – Brasil

Telefone: (19) 3521-6359
E-mail: comisib@unicamp.br
http://www.ib.unicamp.br/ceea/

UNICAMP

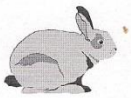

CEUA/Unicamp

STATEMENT

We state for the due propose that all methods carried out during the project entitled "**Effect Nb- containing bioactive glass on gene expression and cellular cycle of osteoblasts: an experimental in vitro and in vivo study**", protocol **# 3467-1**, under the responsibility of P**rofessor Prof. Dr. José Angelo Camilli** and **PhD Student Lucas Pereira Lopes de Souza** were done in accordance with relevant guidelines and regulations.

All experimental protocols related to this project have been approved by the Committee for Ethics in Animal Use of the University of Campinas – CEUA/UNICAMP

Feel free to contact us should you have any question regarding this project (comisib@unicamp.br)

Campinas, June 29, 2018.

Prof. Dr. Wagner José Fávaro
President

Fátima Alonso
Executive Secretary

CEUA/UNICAMP
Caixa Postal 6109
13083-970 Campinas, SP – Brasil

Telefone: (19) 3521-6359
E-mail: comisib@unicamp.br
http://www.ib.unicamp.br/ceea/

Declaração

As cópias de artigos de minha autoria ou de minha co-autoria, já publicados ou submetidos para publicação em revistas científicas ou anais de congressos sujeitos a arbitragem, que constam da minha Dissertação/Tese de Mestrado/Doutorado, intitulada **POTENCIAL TERAPÊUTICO DE VIDROS BIOATIVOS CONTENDO NIÓBIO OU GÁLIO NO TRATAMENTO DE DESORDENS ÓSSEAS: ESTUDO EXPERIMENTAL IN VITRO E IN VIVO**, não infringem os dispositivos da Lei n.° 9.610/98, nem o direito autoral de qualquer editora.

Campinas, 17/09/2018

Assinatura : _____
Nome do(a) autor(a): **Lucas Pereira Lopes de Souza**
RG n.° 463489883

Assinatura : _____
Nome do(a) orientador(a): **José Angelo Camilli**
RG n.° 104821188